NASA Contractor Report 195412

Actuator Feasibility Study for Active Control of Ducted Axial Fan Noise

John C. Simonich
United Technologies Research Center
East Hartford, Connecticut

May 1995

National Aeronautics and
Space Administration

Page intentionally left blank

TABLE OF CONTENTS

List of Figures

Summary

A feasibility study was performed to investigate actuator technology which is relevant for a particular application of active noise control for gas turbine stator vanes. This study investigated many different classes of actuators and ranked them on the order of applicability to the current application. The most difficult requirements the actuators had to meet were high frequency response (> 1 kHz), large amplitude deflections (± 0.010 inches) and a thin profile (< 0.25 inch).

Based on this assessment, piezoelectric type actuators were selected as the most appropriate actuator class for this particular application. Specifically, Rainbows (a new class of high performance piezoelectric actuators), and unimorphs (a ceramic/metal composite) appeared best suited to the requirements.

To measure performance and gain working knowledge of using such actuators, a benchtop experimental study was conducted. The performance of a variety of different actuators was examined, including high polymer films, flextensional actuators, miniature speakers, unimorphs and Rainbows. The actuator's performance was measured using optical sensors, including displacement/frequency response and phase characteristics. Physical limitations of actuator operation (for example temperature limits) were also examined.

This report includes the first known, high displacement, dynamic data obtained for Rainbow actuators. A new "hard" ceramic Rainbow actuator was designed, constructed and tested. It does not appear to be limited in operation by self heating as "soft" ceramic Rainbows are.

A peak to peak displacement at resonance of 0.013 inches was achieved with a 1.25 inch diameter, 0.015 inch thick Rainbow actuator. A 0.010 inch thick unimorph actuator with a diameter of 2 inches was able to achieve a displacement of 0.018 inches at resonance.

The study indicates that a suitable actuator for active noise control in gas turbine engines can be achieved with state of the art materials and processing.

Introduction

Rotor/stator interaction noise is a major source of fan noise in gas turbine engines. There are many possible approaches for control of noise, including suppressing temporal and spatial inflows by mixing out the wakes, increasing the axial spacing between rotors and stators and active noise control. The space between rotors and stators is chosen by designers based in part by the effect of noise. The gas turbine manufacturers need to reduce engine noise levels for both passengers and communities near airports. There is also a continual effort to reduce the size and hence the weight of gas turbines. This is a major problem in ultra high bypass ratio engines which have physically large fan chords which result in large spacings. One method of reducing the size is to bring the rotor and stator closer together. However, this increases the noise levels. Another approach which can be applied to reduce engine noise levels is active noise control. One of the current limitations of implementing an active noise control scheme in a gas turbine is the availability of an actuator which can survive in the engine environment and still produce sufficient amplitude to cancel the noise.

Active noise control in gas turbine engines is a difficult problem. The acoustic field is complex and the propagation paths are complicated. One concept for noise control is to achieve global noise reduction by canceling noise at the source. This approach involves embedding multiple actuators in the vanes.

The objective of this program was to conduct an investigation of vane surface actuation techniques for anti-sound generation in turbomachinery. This effort concentrated on evaluating the current state-of-the-art in actuation technology in order to identify feasible approaches for reducing rotor/stator interaction noise using active control/anti-sound concepts. The amplitude and size design requirements for the actuators to eliminate propagating noise components resulting from real wake/blade row interactions were identified from a theoretical and computational study recently completed at UTRC by J. Verdon and K. Kousen under Task VIII, Theoretical Analysis of Anti-Sound Actuators, of NASA Lewis Contract NAS3-25425 (ref. 1).

There were three specific objectives of the current task. The objective of the first, Evaluation of the State-of-the-Art in High Speed Actuation Technology, was to identify the best actuator approach for rotor/stator interaction noise reduction in turbomachines. The objective of the second task, Preliminary Actuator System Design, was to design an actuator system using the selected actuator technology. The objective of the third task, Preliminary Bench Test Evaluation, was to evaluate some simple characteristics of the actuator system.

Present Investigation

Objectives

The objective of the research program was to investigate actuator technology to determine whether a suitable actuator for a gas turbine active noise control application could be found. An additional objective was to appraise possible actuator candidates to experimentally further

evaluate their merit for the present application. Finally, new concepts for actuators were also investigated.

Problem Formulation and Approach

The first step in the program involved creating the specifications for the actuator. Once the specific requirements for the actuator were known, a search for candidate actuators was begun. Numerous computerized literature searches were performed. Actuator manufacturers were contacted. Scientists and engineers within UTC with actuator experience were consulted. After a review of all the candidate actuators, samples of several types of actuators were acquired for laboratory evaluation. Instrumentation was acquired and installed. Measurements of actuator amplitude were acquired and experience was gained in working with the actuators and power supplies.

Actuator Specifications

There are many possible approaches for active noise control of rotor/stator interactions in gas turbine engines. It is possible to control the noise external to the engine with speakers mounted outside the engine. It is also possible to use noise cancellation techniques that mount speakers in the engine inlet or endwalls. The approach considered for this work is to mount the anti noise actuators as close as possible to the noise source.

For rotor/stator interaction, the noise is generated near the leading edge of the vanes being struck by an impinging wake from an upstream airfoil. This concept is described as "noise control at the source" and is discussed in more detail in a paper by Kousen and Verdon (ref. 2). The concept is illustrated in Figure 1 in a two dimensional sense. The concept for a three dimensional swept vane is illustrated in Figure 2. Essentially, the concept involves embedding actuators into rotor blades or stator vanes near the source of the interaction noise. A single actuator is needed for each acoustic mode that is to be canceled. It has been shown that it is theoretically possible to completely cancel the noise of a given mode. A typical engine application would therefore consist of multiple actuators per vane. Therefore, the actuators must be very compact in order to fit into the thin cross section of the vanes. The study by Kousen and Verdon determined that the required displacements were reasonably small so that they might be achievable by state of the art actuators.

In order to evaluate candidate actuator technology, a specification for an ideal actuator was devised. This specification is shown below.

Fan Exit Guide Vane Materials	Graphite (Fiberglass) or Aluminum
Geometry	
Chord Length	4 to 9 inches
Thickness to Chord ratio	5 - 7%
	Note that the 4 inch airfoil commonly has an additional set of struts behind it. The 9 inch airfoil is for an engine without struts.
Performance	
Maximum Mach number on FEGV surface	approx 1.1 Mn
Minimum and maximum static pressure on airfoil	approx 560 - 2315 psfa
Minimum and maximum static temperature on airfoil	approx 410 - 610°R
Maximum total Pressure on airfoil	approx 2950 psfa
Maximum total temperature on airfoil	approx 655°R
Required Frequency Range for operation (desirable frequency range 500 - 10000 Hz)	500 - 8000 Hz
Required Amplitude	minimum 0.001 inches maximum 0.010 inches

Table 1 - Representative Real Engine Noise Parameters for Active Control

The actuator must be compact and thin so that it can be mounted flush with an aerodynamic surface or structure. Fan exit guide vanes are typically fabricated from aluminum or graphite composites. The chord length is generally in the range of 4 to 9 inches and the thickness to chord ratio is typically 5% to 7%. This results in a vane that is 0.2 to 0.63 inches thick at the thickest part.

High speed air, (up to a Mach number of 1.1) flows over the surface. The air temperature ranges from -50°F up to 195°F. The static pressure envelope of operation is from 3.9 to 16.1 psi.

The cross sectional area of the actuators should be on the order of 0.5 to 1 inch in diameter. Other geometries such as rectangular or square cross section up to 1 inch on a side are also considered acceptable.

The actuator must be able to generate multiple, discrete harmonic frequencies (sinusoids). The required frequency bandwidth is from 500 Hz up to 10 kHz. Actuator displacement requirements were based on the computational study by Kousen and Verdon (ref.. 1,2) for a fan rotor and fan exit guide vane similar to the Pratt and Whitney Advanced Ducted Prop (ADP). For 2-D actuators with a length of 10% of the chord, the actuator displacements needed for complete noise cancellation were determined to be on the order of 1.0×10^{-4} to 1.0×10^{-3} of a chord. For a 10 inch chord fan exit guide vane (FEGV), this means displacements on the order of 0.001 to 0.010 inches. The maximum amplitude is required at the low end of the bandwidth. Amplitude requirements decrease with increasing frequency. The voltage level used to drive the actuators is limited only by the availability of state-of-the-art amplifiers. For gas turbine applications, the actuators must also be reliable and have a long life. Depending on where they are mounted or how close they are to the leading edge of FEGVs, they must also be able to withstand foreign object damage (FOD) and bird strikes.

Review of the State of the Art in Actuator Technology

Introduction

Webster's Dictionary defines an actuator as "a mechanism for moving or controlling something indirectly instead of by hand". A cursory literature search will come up with hundreds of references to actuators (or actuator disks). Over the years, actuators have been developed for many different applications ranging in size from tenths of an inch to multiple feet and frequency responses that vary from sub Hz frequencies up to ultrasonic. Actuators have been invented for both linear and rotational motion. Due to size and bandwidth limitations, many type of actuators can be eliminated for this application. These include electrohydraulics, fluidic servoactuators, servomotors, pneumatic and hydraulic actuators. Actuator technology which could not be summarily dismissed and deserved extra attention are considered in more detail below.

Piezoelectric Materials

Basic Physical Mechanisms

Piezoelectric effect actuators are probably the oldest, most mature and developed of all of the high speed actuator technologies. When a literature search was performed on the term actuator, the number of references to the term "piezoelectric" was vastly larger than any other type. The effects were first discovered over a hundred years ago by Pierre and Jacques Curie. Piezoelectric effects have been observed in a number of natural compounds including quartz, Rochelle salt and Tourmaline, although the effects are quite small. More recently ceramic materials have been formulated which have greatly enhanced piezoelectric properties. One of the most commonly used materials is lead zirconate titanate or PZT. This is so commonly used that the acronym PZT has

become a common term for all piezoelectric ceramic materials, while in reality there are many different types.

There are actually two different physical effects which occur in these solid state motion devices, one due to piezoelectric effects and the other due to electrostrictive effects. Of the two, piezoelectric is the more common. In piezoelectric materials (also referred to as memory ceramics) the induced strain due is proportional to the applied field. In electrostrictive materials (referred to as non-memory ceramics), the strain is proportional to the square of the electric field. This effect is shown graphically in Figure 3 for typical materials. Note that the hysteresis is typically much smaller for electrostrictive than piezoelectric materials, but the displacement is also smaller. The most common electrostrictive ceramic is lead magnesium niobate or PMN.

Piezoelectricity is a property of certain materials. When an electric field is applied across one of these materials, the structure changes shape. Conversely, when a mechanical force is applied to the structure, a voltage is generated. Hence piezoelectric elements can be either sensors or actuators. Recent research has even shown that a single element can be used to concurrently sense and actuate (ref. 3).

During the manufacture of piezoelectric materials, a high voltage is applied across two faces of the element. This process is called "poling" and results in an alignment of the electrical axis of the material. Once a material has been poled, a voltage lower than the poling voltage applied along the poling axis will change the dimensions of the piezoelectric element. The element will retain this shape as long as the applied voltage is maintained. If a voltage with the same polarity as the poling voltage is applied to the element it will expand in the poling axis and contract perpendicular to the poling axis (volume is conserved). A voltage of opposite polarity causes contraction of the poling axis and an expansion perpendicular to the poling axis. This mode is called extensional and is illustrated in Figure 4.

The percentage displacement that is achieved can be predicted by the formula:

$$\frac{\Delta T}{T} = d_{33}V_E$$

where   T is the material thickness
             d_{33} is the piezoelectric constant for the material = strain / applied field
             V_E is the applied potential

The best piezoceramic materials available today have d_{33} constants of about 600×10^{-12} m/V. To prevent depolarization, typical operating limits for piezoelectric ceramic materials are around 1000 V/mm. Therefore the percentage change in thickness that can be obtained from extensional effects is about 0.06%. As an example, the maximum thickness of the FEGV that is considered here is about 0.5 in. If a piezo element were this size, the maximum displacement of the surface would be 0.0003 inches. It is apparent that the displacements achievable with extensional modes are very small indeed.

If a voltage potential is applied perpendicular to the poling axis, a shear mode is generated, and a shear deformation occurs about the axis perpendicular to both the poling axis and the electric field vector. This mode is illustrated in Figure 5. This type of small motion is often employed to amplify the motion of piezoelectrics.

When a DC voltage is applied to a piezoelectric material under static conditions, virtually no heat is generated. However, when a fluctuating voltage is applied, heat is generated inside the material in direct relation to the dissipation factor, δ. The dissipation factor describes the dielectric losses in the piezoelectric material. The accompanying temperature rise is often the limiting factor on the power handling capability of the actuator. Piezoelectric ceramics are classified into two categories depending on their dissipation factor. Materials with high dissipation factors (and high displacements and hysteresis) are called "soft" ceramics. "Hard" ceramics are characterized by low dissipation factors (and low displacements and hysteresis). The dissipation factor is related to the width of the hysteresis loop in a displacement vs voltage graph. This effect is shown in Figure 6.

Numerous applications of piezoelectric and electrostrictive actuators have been demonstrated. Uchino (ref. 4) lists 21 applications of electrostrictive actuators ranging from ultrasonic motors to piezoelectric fans to ultrasonic surgical knifes. Due to their small motion and fast response, piezoelectrics have found wide application in optics for deformable mirrors (ref. 5 , 6 , 7) and for beam steering (ref. 8). Applications include both actuator stacks as well as bimorph configurations.

Santa Maria et al (ref. 9) performed an exploratory study of the acoustic performance of piezoelectric actuators for an application for active noise control of ducted fan engines. Two different materials were tested in a wave tube: PVDF film mounted in foam and composites of PZT rods embedded in fiberglass. Of the two samples, the embedded PZT rods performed better however their acoustic output level was several orders of magnitude less than that required for active noise control in ducted engines.

Stacked Actuators

To achieve large axial displacements, disks of piezoelectric wafers are placed in stacks and wired together in parallel. Although the displacement achievable with this technique is the same as if the element were made from a single piezoelectric block of the same size, the voltage level required to achieve the displacement is much lower. In general, the thinner each individual element is, the lower the voltage that is needed to drive the stack. The classic technique for fabricating a stack is to manufacture separate wafers and assemble them by hand. Typically 70 or more layers of elements 0.020 inches thick have been made. They are driven by up to 1000 volts. For reliability reasons, the polarity of the voltage input to the stack must match the actuators. The bonds between the layers tend to fail in compression, so only positive voltages can be applied to the stack.

The typical performance of several commercially available piezo ceramic stacked actuators is shown in Figure 7. The peak displacement at the maximum voltage driving level is plotted against

7

the length of the actuator. A least squares fit was applied to the data. Most of the actuators lie nearly on the line. The average strain rate is 0.0807%. In order to achieve a displacement of 10 mils, (0.010 inches) for the current application, a 12.4 inches high stack would be required. Clearly this is not feasible.

More recently, multi-layer piezoelectric actuators have been produced using a monolithic cofired technique or a solid sintering using thick film technology (green sheet process) (ref. 10 , 11 , 12). Using this technique, mass production is possible and very thin layers (as thin as 19 μm) are possible. Actuators with as many as 360 layers have been produced. This results in operating voltage as low as 10 volts for full deflection. Sub-miniature stacked actuators as small as 9 mm long that are 1.4 by 3 mm in cross section and contain 72 layers are now mass produced commercially. Such actuators have found application in such areas as impact matrix printer heads (ref. 13).

Displacement Amplification

In order to amplify the tiny motions achievable from direct extension of piezoelectric materials, smart design has often been employed to produce devices which amplify the displacement to more usable levels. Similar to a lever arm or a block and tackle, what you gain in enhanced displacement, you lose in decreased force. This is not usually a problem since the forces generated by direct extension from piezoelectrics are quite large.

Several techniques have been successfully employed for displacement amplification. These include unimorphs, bimorphs, and flextensional actuators. These are discussed in more detail below.

Flextensional Actuators

A flextensional actuator consists of a piezoelectric stack which is coupled with a curved element. Due to their shape, these transducers are also known as barrel stave transducers. An example of a flextensional actuator is shown in Figure 8. Flextensional actuators have been designed using both concave and convex barrel staves. They have been built with both two dimensional staves and in three dimensional geometries. By applying a displacement along the major axis of an ellipse or oval, the minor axis displaces much more, by as much as a factor of 6 to 1. Flextensional actuators have found wide use in sonar (ref. 14 , 15) and are commercially available with major axes from 4 to 17 inches. This is obviously too large for the current application, however, miniaturization should be possible.

An excellent review of the history of flextensional transducers was given by Rolt (ref. 16) in 1990. The first application of the flextensional transducer was for a foghorn in 1929. It is interesting to note that it was driven by a magnetostrictive device. According to Rolt, not much more work was reported on flextensional devices until the mid-to-late 1950's when they were suggested for use as underwater transducers. Many different designs of flextensional transducers for sonar have been proposed in the past couple of decades (ref. 17). To better describe the shell geometries of flextensional devices, transducer designers have identified five different classes of flextensional transducers, Class I through Class V.

Another type of composite flextensional actuator has recently been reported (ref. 18). A cross sectional view of this actuator is shown in Figure 9. The actuator is composed of a piezo ceramic element positioned between two metal end caps. The cavities between the end caps convert and amplify the small radial displacement of the piezoelectric ceramic into a larger axial motion. The actuator has been named a "Moonie" actuator due to its half moon shape. Both piezoelectric and electrostrictive materials have been used. Displacements of 12 μm were obtained from a 13 mm diameter, 1.8 mm thick actuator. This device is different from conventional flextensional actuators in that it uses a single element instead of stacked ceramic elements and is much smaller.

Unimorphs

As was pointed out in the previous section, the relative magnitude of extensional displacement from piezoelectric materials is very small, typically on the order of a few μm. Motion amplification is often accomplished by smart design. By bonding a thin piezoceramic disk to a metal plate, it is possible to produce a device capable of much larger motion. These structures are called unimorphs. They are also referred to in the electronic industry as piezo-alarm elements or piezoelectric audio transducers or piezo buzzer elements. Typical metals used include brass, nickel and stainless steel. The composite structure also has a lower resonance frequency than the ceramic element alone. The package has a very low profile and seems well suited to gas turbine active control applications.

The operating principle is shown in Figure 10. When a voltage is applied across the thickness of the piezoceramic element, a shear force develops. The shear causes the unimorph to expand when a positive signal is applied, and to contract when a negative signal is applied. This action causes the unimorph to alternately distort concavely and convexly. When an AC signal is input to the device, the unimorph moves continuously back and forth.

Unimorphs can be mounted in three different ways: node support, edge support or center support. These mounting schemes are illustrated in Figure 11. The node is the location where no vibration takes place. Mounting at this location causes the least mechanical suppression of vibration and hence the largest amplitude. The nodal diameter is 65% of the outer diameter of the metal disk. By encasing the basic acoustic element in a resonating case, the acoustical impedance of the element and the encased air can be matched, resulting in a much larger acoustic signal at the resonant frequency. Such devices are typically used for alarms for small appliances or consumer products such as computers, smoke detectors, and toys. Typical displacements are in the range of 0.01 mil/volt and voltages are limited to about 30 volts peak to peak, or about ±0.3 mil.

Although an extensive literature search was performed to locate references on the design methodology of unimorph actuators for audio transducers, no references were located in the open literature. The information presented in this section was derived from several industrial catalogs (ref. 19 , 20 , 21).

Bimorphs

A bimorph is a structure made up of two piezoelectric strips laminated together with a common electrode. One end of the beam is typically held, resulting in a cantilevered structure. When a potential is applied, one element contracts while the other extends. This results in a bending motion. This type of actuator is illustrated in Figure 12. These can be either 2-D strips or circular disk geometries. Much larger displacements can be achieved using this technique than can be obtained using the direct extensional properties of piezoelectrics.

High Polymer Films

Piezoelectric properties have been discovered in a variety of different materials, both natural and man made. Several types of high polymer plastics have been developed for their piezoelectric properties. These include polyvinyl chloride (PVC), polyvinyl fluoride (PVF), and polyvinylidene fluoride (PVF$_2$ or PVDF). The materials are commercially available in thin sheets with thicknesses from 9 to 110 μm. Electrodes of aluminum, silver or NiCu are typically placed on both surfaces of the film. When a voltage potential is applied to the electrodes, the film elongates or contracts slightly in length, depending on the polarity of the field. A ten volt potential across a 9 μm thick film will cause it to expand or contract about 0.3 μm per centimeter of length. Due to its low profile, this material was considered as a candidate for a gas turbine active control actuator. These films have been used successfully in headphones, tweeters and loudspeakers (ref. 22 , 23 , 24).

In order to obtain reasonable surface deflections, the films must be curved so that the transverse movement of the high polymer film is converted into a pulsating motion. Several examples of high polymer film actuators are shown in Figure 13. Several patents for particular planar curved acoustic transducers have been issued (ref. 25 , 26 , 27). Micheron and Lemonon (ref. 28) developed a technique to mold a three dimensional film shape to produce a high range loudspeaker. A balloon speaker made of PVDF was patented by Radice in 1987 (ref. 29).

Other applications have also been developed using high polymer films. A low flow electronic cooling fan was developed by Toda in 1978 (ref. 30 , 31 , 32). This device uses a cantilevered, multilayer PVF$_2$ bimorph configuration which is driven at its mechanical resonance (5 Hz). The electrical to mechanical conversion efficiency of the fan was estimated to be between 25% and 50%. The bimorph structure is used to amplify the small longitudinal change in length of the film into a larger transverse motion. This utilizes the shear stress placed in the film similar to a bimetallic strip used in thermostats. Digital indicators and displays have also been proposed and tested using high polymer film elements (ref. 32). The use of corrugated PVDF bimorphs for robotics applications was investigated by Nevil and Davis in 1984 (ref. 33). Displacements of up to 40 μm (1.6 mils) were achieved statically at no load.

Rainbow Actuators

A new type of actuator based on the piezoelectric effect has recently been discovered (ref. 34 , 35). By a simple processing technique, standard piezoelectric or electrostrictive ceramic wafers

(PZT, PLZT, PSZT or PBZT) can be transformed into high displacement actuators. The process consists of chemically reducing one surface of the wafer with carbon (graphite) in an oxidizing atmosphere at elevated temperature. This reduces the lead oxide in the wafer to its metallic state. The resulting actuator contains an integral electrode as part of the conductive metal oxide structure. The Rainbow is a monolithic structure. The processing places an internal compressive stress bias on the ceramic element which strengthens the element. The actuator produced was named Rainbow for Reduced And Internally Biased Oxide Wafers.

To date Rainbow actuators have only been produced from thin circular disks. Photographs of two different size Rainbow wafers are shown in Figure 14 and Figure 15. Other geometries such as two dimensional strips may be produced from circular shapes by scoring the surface and breaking. During the processing, the flat disks are transformed into dome or saddle structures. This structure is partly responsible for the high electromechanical displacement and the enhanced load bearing capability of Rainbows. They are available commercially in 1.25 and 2.0 inch diameters and thickness ranging from 0.008 to 0.030 inches. Under static conditions, displacements as high as 1 mm has been achieved from a single element. As with many other actuators, Rainbows can be stacked to achieve even larger total displacements.

Rainbow actuators appear to command a unique niche among solid state actuators in stress/strain space. A comparison of load carrying capacity versus displacement for various piezoelectric effect actuators is shown in Figure 16. Strain is defined in the normal definition as the change in displacement normalized by the thickness of the element. Piezoelectric ceramics excited directly have very small displacements but can handle very large loads. Flextensional devices amplify the small extensional displacements but give up some load carrying capacity. Unimorph and bimorph configurations yield higher displacements still but give up a large amount of load carrying capacity. Rainbows extend both the strain and the stress capabilities of bimorph actuators by factors of up to 10 and 100 times respectively. Strains as high as 500% have been reported for very thin Rainbow actuators.

The maximum achievable displacement increases inversely with thickness. There is a practical limit to how thin the wafers can be manufactured as wafers below about 0.010 inch in thickness are very weak and easy to break.

Being a new technology, the only application data available is from the inventor and the actuator company which owns the patent. Applications demonstrated by the inventor include a pump, a mechanical parts shaker and a speaker. Many of the properties of Rainbows such as linearity, hysteresis, lifetime, frequency response, and mechanical efficiency were largely unknown at the start of this study.

Piezoelectric Actuator Feasibility Study

As part of this research program, a small portion was sub-contracted to Hersh Acoustical Engineering, a female owned business, for a study of the feasibility of using piezoelectric actuators for the current gas turbine application. The text of the final report is included in Appendix A. The results of the study are summarized below.

The goal of the study was to review piezoelectric actuator technology, assess the potential to generate the sound power signature required and recommend the best piezoelectric technology to meet the actuator goals. In the study, eleven articles were reviewed and summarized. Based on the use of a single slab of piezoelectric material, it was confirmed that the required displacement goals could not be met with present state-of-the-art, commercially available piezoceramic materials and have the actuator fit inside the required space. Alternative configurations suggested include a piezo stack, and a bimorph similar to a tweeter driver for high frequencies (3 - 20 kHz).

Electrodynamics

Electrodynamics refers to the magnetic force generated on a current carrying conductor. Conventional loud speakers are designed using this phenomenon. The speaker diaphragm is driven by a voice coil which fluctuates in response to the current supplied from the amplifier. In a typical moving coil loudspeaker driver, a hollow, self supporting cylindrical coil is attached to a cup-shaped, low mass, moving element. A permanent magnetic circuit is used to direct the flux through the coil. The flux produced by the magnets is a constant and the driving current (the desired acoustic signal) creates a flux that alternately aids and opposes the permanent magnetic field. The coil responds to the current amplitude and the speaker cone is vibrated.

The thickness of miniature loudspeakers has decreased significantly over the past few years as speaker designers have changed from AlNiCo and ferrite magnets to rare-earth magnets (ref. 36). With the use of rare-earth magnets, the total loudspeaker weight can be reduced to only 13% of the weight of loudspeakers made from ferrite magnets. Equally dramatic profile reductions are also achieved. The power capacity and frequency response are not altered. Miniature speakers with a diameter of 20 mm (0.78 in) and thickness of 4.0 mm (0.157 in) and a power rating of 0.1 watt are commercially available.

Electrodynamic actuators have also been developed using rare-earth permanent magnet materials for use in active vibration control (ref. 37 , 38). These so called electrodynamic linear actuators produce a force proportional to the input current. In general these devices are much too large for the current application.

Electrostatics

An electrostatic force is generated when a voltage is applied between two conductive plates. The force is attractive when the voltages are of opposite sign and repulsive when the voltages are of the same sign. Loudspeakers have been proposed using this technology in the past, (ref. 39) however, compared to voice coil based speakers, much higher voltage levels are required. Electrostatics have been used successfully in micro mechanical systems as discussed below.

A new type of transducer material which employs the electrostatic effect was recently developed by Kirjavainen (ref. 40) in Finland. This material is a foamized plastic called electro-thermomechanical film or ETMF. The film is typically 20 μm thick with small flat gas bubbles embedded in it. The bubbles make up about half of the volume. Electrodes of aluminum foil are

attached to the upper and lower surfaces of the film. Due to the configuration of the bubbles, the film has a high breakdown voltage in electrostatic applications. Multi-layers can be used when large displacements are needed. Typical plastics used are polyethylene, polypropylene and Teflon. Representative displacements are about 5% of the thickness of the film when a potential of 1 kV is applied. Demonstrated applications for the film have included both tweeters and loudspeakers (ref. 41 , 42).

Shape Memory Actuators

One type of "smart material" being used for actuators is the so called shape memory metals or ceramics. A shape memory alloy is described as a material which undergoes a reversible phase transformation. Below a transformation temperature, the material is weak and easily deformed without permanent damage. Above a certain temperature, the deformation disappears and the material returns to its original shape. Actuators made from shape memory metals typically rely on Joulean electric heating to raise the temperature, and radiation or convective cooling to lower the temperature. Changes in length on the order of a few percent are possible. Bandwidth is typically on the order of fractions of a Hz. With high enough current, actuation on heating can be achieved in a few milliseconds. The cooling process typically takes orders of magnitude longer.

Shape memory metals are available commercially as fine diameter wires. The wires are typically constructed of alloys of nickel-titanium (NITINOL) since they have a high electrical resistivity suitable for heat generation. Actuators fabricated using shape memory metals typically utilize helical coils or springs fabricated of shape memory metal (ref. 43 , 44) although actuators using linear lengths of shape memory metal **have** also been reported (ref. 45).

Recently actuators made from shape memory ceramics have also been reported (ref. 46 , 47). In this case the actuators were formed from single and multiple layers of ceramic material. A latching relay was demonstrated by Oh (ref. 46) and a mechanical clamper was constructed by Furuta (ref. 47).

Due to the low bandwidth of shape memory materials, they are not a good candidate for a gas turbine active control actuator.

Micro Mechanical Actuators

Actuators can be classified by the physical phenomenon which causes the movement or by general geometric shape or by function. One geometric class of actuators is called micro mechanical actuators or micro-electromechanical systems (MEMS). These actuators are characterized by their extremely small size. Various physical processes have been employed to form micro mechanical actuators including piezoelectric, electrostatic, and thermoelectric effects. One common feature is that they are typically constructed using microelectronic fabrication techniques. An excellent review article for aerospace applications of MEMS devices was given by Scott (ref. 48).

Several researchers have conceived and demonstrated micro mechanical actuators based on piezoelectric effects. One of the most promising for the current application was presented by Xu et al (ref. 49). They designed an actuator disk consisting of a piezo-ceramic element sandwiched between two metal endplates with crescent shaped cavities on the interior surfaces. The crescent shaped elements (also known as Moonies due to the half moon shape) gives the element an amplification effect. When a strain is applied along the longitudinal axis of the piezo ceramic, the displacement of the surface perpendicular to that axis is amplified by a factor of four to six. Displacements of up to 20 μm (0.79 mils) were reported for a 11 mm (0.43 in) diameter, 1.6 mm (0.063 in) thick actuator. The bandwidth of the actuator was not reported but resonant frequencies above 6 kHz were noted. For higher displacements, it is suggested that single actuators be stacked to form a composite, although no such device was tested.

Other devices with less relevance to the current application have also been presented in the literature. This includes a linear displacement microactuator based on a meander line or folded path geometry (ref. 50). This actuator had an estimated displacement of 2.3 μm (0.09 mils). No devices were actually tested. Smits and Choi (ref. 51) built and tested a micro mechanical bimorph actuator 3 mm (0.12 in) long and achieved a displacement of 1.2 mm (47 mils) at the end of the bimorph. A miniature linear actuator for bio-medical applications named a cybernetic actuator was developed by Ikuta et al (ref. 52). It consisted of a piezoelectric device coupled with an electromagnetic clamp and was moved using a controlled friction impact drive. The overall size was 20 mm (0.79 in) and the cross section was 5 by 5 mm (0.2 by 0.2 in). The device was demonstrated for frequencies up to 27 kHz. Brei and Blechschmidt (ref. 53) designed a microactuator using a semicircular bimorph of high polymer film. The semicircular shape appeared to increase the force capability of the bimorph without greatly sacrificing deflection capability compared to a straight bimorph.

Most micro mechanical actuators appear to be based on electrostatic principles. It is well known that if a charge is placed across two conductive plates an attractive or repulsive force will develop depending on whether the electrodes are of opposite sign or the same. In the small scale world, electrostatic actuators have an advantage over other types of actuation. As the size of an electrostatic actuator is reduced, its force to volume ratio increases.

Several examples of electrostatic microactuators have been published in the literature. A six degree of freedom micro manipulator was designed and tested by Fukuda et al (ref. 54). The displacement was 3.15 μm. The complete actuator fit into an 8 mm cube. A microvalve actuator for rarefied gas flow control was presented by Sato and Shikida (ref. 55). In this configuration, an S-shaped film moves back and forth between a pair of electrodes. The actuator package in this concept is on the order of 3 mm high by 12 mm wide. Propagation speeds up to 4.0 m/s were observed with an applied potential of 150V. Another actuator for a micromechanical valve was demonstrated by Branebjerg and Gravesen (ref. 56). Their device consisted of a silicon membrane bonded to a glass plate with gold electrode. It had a displacement of 18 μm (0.71 mils). A type of linear motor called a stacked, variable capacitance motor with active slider (SVCMA) was developed by Niino et al (ref. 57). This actuator was 120 by 110 by 5 mm in overall size and generated 21 N of force along the longitudinal axis. An electrostatically driven, pneumatic

14

actuator consisting of two sealed, air-filled, concentric chambers was designed by Gabriel et al (ref. 58). The outer diameter was 200 - 750 μm. No performance data was presented.

A thermoelectric effect micro actuator for fluid jet deflection using the Coanda effect was demonstrated by Doring et al (ref. 59). The actuator consisted of a bimetalic strip of silicon and aluminum, 1 mm wide and 1 mm long. The time constant was reported to be 1 ms. For the high flow rate associated with the device, large cooling rates were available and hence the responsiveness of the device was acceptable.

While micro mechanical actuators show great promise as robotics tools in the future, the displacements are limited to the microscopic scale. By assembling many small actuators (microactuators) together it is possible to obtain an ordinary sized actuator (macroactuator). Currently research is ongoing to develop the fundamental building blocks. Many of the references described above deal only with the concept and fabrication processes and do not give performance data. Future work should see the development of multi-element actuators. Most of the literature describing these devices is from university researchers. Another deterrent to using these devices for the current application is that no devices are commercially available.

Photostrictive Materials

Photostrictive actuators are materials which move in response to light. The effect is a superposition of a photovoltaic and a piezoelectric effect. Large photostriction occurs in certain PLZT ceramics when irradiated with light. One benefit of these devices is that no lead wires need to be attached to the actuator. A photo driven relay and micro walking machine were developed and demonstrated by Uchino (ref. 60). The response of the relay was one to two seconds. The walking machine moved 50 μm in five minutes.

Magnetostrictive Materials

Magnetostrictive materials are materials which change size in response to magnetic fields. The effect has been known for over 100 years. Most materials however do not exhibit large effects. A highly reactive material was discovered in 1978. The material is a rare-earth, grain-oriented alloy of terbium, dysprosium and iron. It is known under the trade name Terfenol-D. It offers strains 40 times greater than previous magnetostrictive materials and better performance than piezoelectric ceramic materials by an order of magnitude. It exhibits excellent frequency response and has a high energy density. A review of the properties of Terfenol as it relates to its use in high speed actuators is given by Goodfriend (ref. 61). A hybrid actuator using Terfenol and PZT for use in industrial robotics applications was reported by Akuta (ref. 62). The use of Terfenol as a high speed actuator has been demonstrated in deformable mirrors (ref. 63, 64). Actuators for active vibration control systems have also been demonstrated by several researchers (ref. 65, 66). A hybrid magnetostrictive/hydraulic actuator was developed by Bushko and Goldie in 1991 (ref. 67). Its large size precludes its use in the present study. Actuators made from magnetostrictive materials are commercially available in piston type geometries.

15

At first examination, it would appear that this would be a favorable candidate for a surface mounted actuator. However, there are several features of Terfenol which limit its usefulness for stator noise generation devices. Since magnetostrictive materials only respond to magnetic fields, any actuator must also include an electric coil to generate this field. This adds size and weight to the total package. For maximum performance from magnetostrictive materials, mechanical prestressing is also necessary. This is turn implies a large, sturdy structure to hold the actuator, making miniaturization difficult. To date, Terfenol-D is only available in long, cylindrical shapes best suited for linear, piston type actuation.

Polymer Actuators

One type of actuator which is still in it's early developmental stage is polymer or gel actuators. An excellent review of these actuators is provided by Rossi et al (ref. 68). These types of actuators have been proposed for use in robotics as a replacement for muscles. Several classes of polymeric gels have been demonstrated to produce reversible contraction and expansion under both chemical and electrical stimuli. While high mechanical power densities have been achieved for chemical inputs (by alternately placing the gel in one chemical and then in another), electrically driven systems have much lower performance. The limiting factor for these devices for fan noise active control is their inherent low frequency response. Typical time constants are on the order of a few tenths of a second for chemically driven systems but one or two orders of magnitude longer for electrically stimulated devices.

Actuator Selection

A review of the properties of the different actuator technologies was performed. The characteristics of each actuator technology were rated relative to the following criteria for the current application: frequency response, size, linearity and dynamic range. Table 2 summarizes these characteristics for the actuator classes identified above. Other types of actuators were not ranked in this table since they were inherently too large or too slow to be applicable. This list includes but is not limited to: thermoelectric, electromechanical, hydraulic, pneumatic, servomotors, fluidic servoactuators and electrohydraulics. Based on this summary, many types of actuators had to be discarded due to their low frequency response: photostrictive, polymer gels, and shape memory materials. Magnetostrictive materials, while having excellent responsiveness, require the addition of extra material to produce the required magnetic field and their basic shape is not conducive to the current geometry. They were also not considered further.

The technologies which were selected for further experimental evaluation were: piezoelectrics, electrostrictives and electrodynamics. While they were not ruled out, electrostatic foams may be viable, but no commercial supplier could be found and the technology is still largely undeveloped.

Actuator Technology	Frequency Response	Size (thin profile)	Linearity	Dynamic Range	Comments
piezoelectric	high	small	poor	good	PZT, PVDF high voltage
electrostrictive	high	small	good	good	PMN, high voltage
magnetostrictive	high	medium	good	excellent	requires magnetic field and pre-load, low voltage
electrostatic	high	small	fair	good	high voltage
electrodynamic	high	medium	fair	good	voice coil
shape memory	low	small	poor	good	requires cooling
polymer gels	low	medium	?	good	chemical response
photostrictive	low	small	?	good	undeveloped

Table 2 - Comparison of Actuator Properties

Actuator Concepts

During the course of this study, a number of actuator concepts were formulated. After review, some of the concepts were judged to be possible candidates, others were discarded. The following is a description of some of those concepts.

Extensional Airfoil

One of the simplest concepts one can imagine for this application is shown in Figure 17. The idea behind this concept is to build an entire stator vane of piezo ceramic material. The vane surface would be made up of strips of piezoelectric stacks mounted to a metal spar. Each stack could be actuated independently. For a two dimensional airfoil, the actuator could be two dimensional strips, but for an actual three dimensional stator vane, patches of strips could be pasted across the span.

The problem with this technique is that with current piezoelectric materials, it is not possible to achieve the required displacement with the geometrical constraints of the thickness of the vanes. As pointed out in the section describing the properties of piezoelectric materials, the amount of increase in thickness that is possible with pure extensional motion is limited to about 0.06% for the best materials today. Even if the entire thickness of the stator, (about 0.5 inch maximum)

17

were made of piezoelectric material, the most the surface would grow would be 0.3 mil. This is about an order of magnitude less than required. The responsiveness of engineered piezo materials has increased by an order of magnitude in the last decade (ref. 69). It appears likely that with improved material selection and processing techniques, this trend will continue. Therefore it is possible that in the next decade or two, this concept may prove feasible.

Tunable Unimorph

This actuator is based on an established and well known unimorph piezo ceramic construction, composed of a sandwich of piezo ceramic and brass. High displacements are obtained when these devices are operated at the resonance frequency of the composite package. Displacements at resonance are as much as ten times larger than those at off resonance.

The unique feature of this concept involves the ability to change the natural resonance frequency of the unimorph by applying tension or compression to the unimorph by the use of a second piezo ceramic element. Applying tension raises the resonant frequency of the plate above its natural frequency while compression lowers the frequency. The ability to "tune" the actuator is important since the blade passage frequencies will change with engine operating point. By "tuning" the actuator to the required frequency, the maximum displacement can be obtained from the unimorph actuator over a broad range of frequencies.

Figure 18 shows a sketch of the components of the actuator. The top half of the actuator is a conventional unimorph actuator. The active element in the upper half of the actuator is piezo ceramic element #1 which is driven by an AC voltage at the required noise cancellation frequency (typically several kHz). In order to achieve the maximum displacement output, the upper brass surface is placed in either tension or compression to alter the natural frequency of the upper plate. The driving force to apply this tensile force is provided by the second piezo ceramic element, #2, which is driven by an applied DC voltage.

Feasibility studies were undertaken to evaluate the concept. The displacement at resonance for a typical unimorph configuration was calculated. Displacements up to 10 thousandths of an inch are theoretically achievable using this concept. The required diameter for an actuator to be tuned at approximately twice the blade passage frequency for a typical gas turbine engine is on the order of 1 inch. (Twice BPF was used as a worst case since Kousen and Verdon (ref. 1) showed that amplitude requirements decreased with harmonic number.) The change in resonance frequency of a circular plate under tension and compression was investigated. Using realistic voltage limits to drive the compression member, it appeared that it may be possible to vary the tuned frequency down by as much as a factor of three under compression and up by as much as 50% in tension from the unstressed natural frequency.

It also possible to change the natural frequency of a conventional single element unimorph by applying a DC offset sine wave to drive it. The DC component is used to stress the brass member while the AC part drives the device at resonance. This approach is simpler than the device described above but may not yield as high a performance. This actuator concept was constructed and tested. The results are presented below.

Miniature Flextensional Actuator

As discussed in the piezoelectric materials section above, flextensional actuators are a means of amplifying the micro-scale extensional effects in piezoelectric materials into macro motions. Commercially available flextensional actuators used in underwater sonar applications were much too large to be embedded into a fan exit guide vane. For this reason, a miniature flextensional actuator was designed.

A sketch of the miniature flextensional actuator mounted in a stator vane is shown in Figure 19. The actuator is in the shape of an ellipse with a 0.4 inch minor axis and a 1 inch major axis. The actuator is shown placed in a cavity in the vane in the cross sectional view. The other view shows the actuator from the top. In this example, the span of the actuator is also 1 inch. Two miniature piezoelectric stacks are used to activate the actuator. Based on a commercially available 0.7 inch long piezoelectric stack and a 6X multiplying effect of the ellipse, the 0.00059 inch extensional displacement of the stack should translate into a 0.0035 in displacement at the surface.

One of the advantages of this concept is that the actuator should be relatively robust to foreign object damage. A disadvantage is that the cavity in the vane (or multiple cavities) will have an effect on the structural integrity of the vane.

This actuator concept was built and tested. Details of the fabrication and the experimental results are included below.

Terfenol Moonie Actuator

A concept for a flextensional device using a magnetostrictive material was also considered. A sketch of the concept is shown in Figure 20. This concept uses half of an ellipse as the flextensional member. Magnetostrictive materials require two features which make them more difficult to use than piezoelectric materials. For one, they require a device to produce a magnetic field and secondly, the Terfenol rod must be kept in tension. Both of these features require additional material, which makes compact packaging difficult. In this concept the flextensional member is used to keep the Terfenol rod in compression. An end cap is bonded to the upper surface of the domed shape flextensional member. This cap extends across the cavity in the vane and serves to act as a rigid piston. In this way a larger volume displacement is achieved than if the flextensional member acts alone since the maximum displacement from the elliptical member occurs in the center. The effect of adding an additional mass to the actuator may be detrimental.

This concept was not pursued in the current study since miniature Terfenol actuators were not available commercially as standard items.

Hybrid Actuator

Conventional electromechanical actuators can achieve relatively high displacements but only up to several hundred Hz. On the other hand, piezoelectric type actuators can achieve high

frequencies, but with displacements in the microinches. The hybrid device described below has the potential to achieve both high speed actuation and high amplitudes simultaneously.

The high frequency, large amplitude actuator is a hybrid device. It combines the high frequency characteristics of a piezoelectric actuator with hydraulic amplification. A sketch of the device is shown in Figure 21. One of the modes of operation of a piezoelectric material is that its thickness changes in response to electric potential. The lower area of the actuator consists of several layers of piezoelectric material. When a voltage is applied to the material, it expands in thickness. The inner reservoir of the actuator contains an incompressible fluid. When a potential is applied to the piezoelectric element, fluid is displaced. This displacement can only occur in the area of the upper actuator surface. By continuity of mass, a small displacement over the large surface area of the piezoelectric will cause a correspondingly large displacement over the small displacement area of the actuator surface.

$$V = AD = ad$$

where V is the volume of the reservoir
A is the area of the piezoelectric element
D is the displacement of the piezoelectric element
a is the area of the actuator surface
d is the displacement of the actuator surface

The displacement of the actuator surface is directly proportional to the ratio of the areas:

$$d = D\frac{A}{a}$$

As large a displacement as necessary can be achieved by making the ratio of piezoelectric area to actuator surface area as large as necessary.

For a static condition, the pressure acting on both the piezoelectric surface and the actuator surface will be equal:

$$p = \frac{f}{a} = \frac{F}{A}$$

where F is the force acting on the piezoelectric element
f is the force acting on the actuator surface.

The force acting on the actuator is therefore:

$$f = F\frac{a}{A}$$

20

There is therefore a reduction in force at the actuator compared to the piezo element. This does not present a problem since the piezoelectric elements typically have large forces and small displacements.

As drawn in Figure 21, the concept will not work. This is because the piezoelectric element conserves volume when it is activated. When it increases in thickness, it decreases in diameter. Two actuator concepts which are feasible are shown in Figure 22 and Figure 23. Figure 22 shows an exploded view of a hybrid concept which makes use of a piezoelectric stack and a diaphragm to keep the stack separated from the hydraulic fluid. The thin metal tape at the top of the actuator is the actual displacement surface. Figure 23 uses a unimorph actuator as the driving member. Again, the displacement surface is a thin metalized tape over an opening in the case.

These actuator concepts were not pursued since it appeared that other less complicated techniques were available to accomplish the same displacements.

Composite Rainbow Actuator

A composite Rainbow actuator consists of a Rainbow wafer bonded to a brass disk. This is similar to the unimorph configuration where a piezoceramic disk is bonded to a brass disk, changing the resonance frequency of the piezo and increasing the surface displacement. A conducting epoxy was used to bond the Rainbow to the brass.

Two prototype composite Rainbow actuators were fabricated and tested. They were constructed by bonding a 0.015 inch thick, 1.25 in diameter piezoelectric wafer to a 2 inch diameter brass disk. Two different brass thicknesses were used, 0.004 and 0.007 inches. The composite Rainbow actuators were similar to unimorph actuators which are used as computer buzzers, except the buzzers make use of conventional piezoelectric ceramics.

Hard Ceramic Rainbow Actuator

Temperature limitations were encountered with soft ceramic Rainbow actuators due to the high dissipation associated with the soft ceramics used for the commercial Rainbow actuators. Better results may be obtained by using low dissipation, hard ceramics. Since Rainbow actuators fabricated from hard ceramics were not available from the only known source of Rainbow actuators, a hard ceramic actuator, 1.25 inch diameter, 0.015 inch thick, was fabricated in house.

Experimental Assessment Program

Introduction

An experimental program was undertaken to evaluate the actuator technologies selected above as being the most viable for the current active noise control application. The goal of this phase of the program was to further access candidate actuators, to obtain measurements of actuator performance, to obtain practical experience with the actuators and gain a working knowledge of problems and difficulties associated in working with the technology. In this regard, selected actuators from each technology were purchased whenever possible. Some actuators were not

21

available commercially in the form we wanted to use them. In this case, custom fabrication was used. Amplifiers were purchased or fabricated to drive the devices. The sound and displacement characteristics of the actuators were tested under static conditions (i.e. without flow).

Mounting Scheme for Rainbow Actuators

The mounting of Rainbow actuators was not a trivial matter. The first attempts to measure the displacement of the actuators by simply supplying voltage to the leads of an unconstrained actuator, resulted in the actuator vibrating all around the benchtop. It was therefore not possible to perform displacement measurements. The next approach was to rigidly mount the Rainbow in a circular cavity with a rigid cover plate. This mount was too stiff, since it limited the displacement of the actuator and caused the ceramic to crack. Our next attempt was to mount the Rainbow with a rubber O ring between the actuator and the mount. This too resulted in failure of the actuator due to cracking during activation.

The final successful mount design used an RTV rubber sealant to mount the actuator to a Plexiglas holder which had a hole slightly smaller than the OD of the Rainbow actuator. A photograph of a Rainbow actuator mounted to a Plexiglas plate is shown in Figure 24. This assembly was then mounted to a fixture which included a shop air impingement cooling scheme, which is shown in Figure 25.

Miniature Flextensional Actuator Fabrication

Flextensional actuators for sonar use are commercially available, however, the smallest ones are at least an order of magnitude larger than would fit inside a fan exit guide vane. Therefore, the concept was evaluated by fabricating a miniature flextensional actuator. A concept for a miniaturized version of a flextensional actuator was formulated. An advantage of this design is the robustness of the actuator which should enable it to withstand foreign object strikes in an engine. One of the concerns regarding these devices is the overall thickness of the "moonie" package, on the order of 0.4 inches. In order to be mounted flush with the inlet guide vane surface, a hole in the vane would be required. The effect this hole would have on the structural integrity of the inlet guide vane is uncertain.

The flextensional concept (also known as the "moonie" or barrel stave concept) is a way of amplifying the small displacement of an actuator. In one version, the device is an ellipse with an actuator placed on the major axis. When the actuator along the major axis contracts, the minor axis expands by as much as six times that of the major axis. A miniature piezoelectric stack is available commercially. The 0.08 by 0.12 by 0.7 inch rectangular shaped block has a displacement of 0.00059 inches along its length when activated. When combined with the 6X multiplying effect of a "moonie", the surface displacement would be 0.0035 inches, which is in the range of displacement necessary for active noise reduction.

To fabricate the shell for the miniature flextensional actuator, an elliptical shaped jig fixture was designed and numerically machined to shape a piece of thin walled aluminum tubing into the elliptical form required for the displacement amplification effect. A hydraulic press was used to form the thin walled aluminum tubing into the elliptical form required for the displacement

amplification effect. End caps were fabricated to mount the miniature piezoceramic stack in the elliptical shaped actuator. The shell was pre-stressed prior to the insertion of the stack so that the stack would never be in tension, which is a reliability problem with stacked actuators.

A photograph of the jig used to fabricate the actuator, the piezoelectric stack and the completed actuator assembly is shown in Figure 26. Per the piezo stack vendors specifications, voltage to the piezo stack must always be positive (in order to avoid tensional operation). The actuators must then be driven with a DC offset sine wave, which necessitates the use of a DC amplifier.

Instrumentation

The primary measure of performance of the actuators was the surface displacement, which was measured by a non-contact measurement system described below. Additional instrumentation was used to monitor the health of the actuators and to further analyze the results. A schematic diagram of the instrumentation setup is shown in Figure 27. A photograph of the experimental arrangement is shown in Figure 28.

The flowrate of cooling air for the actuator was measured with a variable area meter (float meter) with a full scale range of 3.562 SCFM. The temperature of the actuators was monitored by soldering a thermocouple directly to the actuator surface. A digital panel meter accurate to ±1°F was used to display the temperature.

A swept sine wave generator was used to send a signal to the amplifier. The true RMS voltage and the power consumption of the actuator was measured with a digital power meter. The displacement of the actuator was measured with the non-contact displacement instrument. A low pass filter/amplifier unit was used to precondition the signal to the spectrum analyzer. The low pass filter setting was 10 kHz. This helped to improve the signal to noise ratio. An oscilloscope probe with a 100 to 1 voltage attenuation was used to reduce the high voltage levels used to drive the actuators into a low enough range for input into the oscilloscope and the spectrum analyzer. The spectrum analyzer was used as the primary data acquisition instrument. It was used to obtain transfer functions between the input signal to the amplifier and the resulting displacement signal from the actuator, and the frequency response of the actuator to swept sine waves. Data was transferred from the spectrum analyzer to a laboratory PC via IEEE-488 bus transfer for further analysis.

Amplifiers

The actuators tested required driving voltages ranging from tens of volts up to many hundreds of volts. In addition, the larger the actuator, the larger the current requirements. Initially, a variety of audio amplifiers were employed to drive the various actuators. Each amplifier had its own characteristics, but in general audio amplifiers are limited to something less than 100 volts peak output. This limit depends on the impedance of the actuator. Audio amplifiers are typically used to drive speakers with impedances from 4 to 16 ohms. The impedance of piezoceramic actuators are typically orders of magnitude larger.

Direct driving with audio amplifiers was successful for some of the actuators, for example, the miniature speakers. Other actuators such as the PVDF films required many hundreds of volts to obtain any substantial output. For this reason, a high voltage DC amplifier (±750 volts, 50 mA) built specifically for powering piezoelectric materials was purchased. This worked well for the PVDF application but proved not to be powerful enough for driving piezoelectric stacks or Rainbow actuators. Several other audio amplifiers were also used with limited success including 20 watt and 100 watt PA amplifiers. Neither of these had sufficient current to drive the Rainbow actuators.

One approach which is used to obtain high power output amplifiers for piezoelectric actuators is to couple an audio amplifier (or power amplifier) with a step up transformer. This technique is used commercially by manufacturers of vibration test equipment such as piezoelectric shakers. The transformer or network must be matched to the impedance of the load. In general, this technique only supplies an AC signal to the load. In some applications of piezoelectrics, such as stacked actuators where only positive voltages can be applied to the actuator, an additional DC voltage must be tied to the AC signal to keep the voltage positive.

An alternative technique which is more general and does not require separate control for the AC and the DC amplification factor is to use a high power DC amplifier. Based on a design for a DC amplifier for a piezoelectric inchworm controller (ref. 70), a high power DC amplifier was built in house. This design is quite simple, however, it does requires a high voltage power supply to power it. The results obtained with it were acceptable only for low frequencies and currents.

The final amplifier used for most of the study was a commercial 200 watt, high voltage op amp. This amplifier had an output limit of ±200 volts at a maximum current of 1 amp. The -3 dB bandwidth was specified as DC to 4 kHz in the voltage mode. A second identical op amp was obtained late in the program. The two amplifiers were used in a serial master/slave arrangement. This arrangement permitted the amplifiers to produce an output of ±400 volts at a maximum current of 1 amp.

The current requirements for an amplifier to drive a piezoelectric element is given by:

$$I = \frac{V}{X_c}$$

where   V is the voltage
                      X_c is the reactance

The reactance is a function of the driving frequency and the capacitance:

$$X_c = \frac{1}{\omega c}$$

where ω is the frequency in radians/sec
                      c is the capacitance in farads

The capacitance of two samples of Rainbow actuators were measured at frequencies from 1 kHz to 10 kHz using a capacitance measurement instrument. The capacitance did not vary much above 3 kHz. A 1.25 inch diameter, 20 mil thick piezoelectric Rainbow had a capacitance of 15.5 nF at 2 kHz. A 25 mil electrostrictive Rainbow wafer measured 45.5 nF at 2 kHz. A chart showing the current and power requirements to drive an electrostrictive Rainbow at 450 volts (the maximum voltage used by the inventor) is given in Figure 29 and Figure 30. The current requirement rises linearly with frequency up to almost 1.3 amps at 10 kHz. The power requirements rise exponentially as the frequency increases up to 47 watts at 10 kHz.

Displacement Measurements

A variety of different techniques are available for measuring surface displacements. The standard technique used to measure the very tiny motions achievable with conventional direct extensional piezoelectrics is linear variable differential transformers or LVDTs. These devices are extremely sensitive and highly responsive. However they require direct contact with the measurement surface and have a moving element which contains mass. For a light structure such as speaker cones, unimorphs or Rainbows, contact with the vibrating surface will cause interference. A nonintrusive measurement technique which doesn't influence the object it is measuring is preferred.

There are a number of different techniques for non-contact measurement. These include laser vibrometers, microwave and fiber optic intensity probes. The laser vibrometers are expensive but have an advantage of being able to be used remotely from the surface. They can be separated by distances up to 10 or 20 feet from the measurement point. They are also able to make point measurements. Commercial units which scan a beam over an entire surface are also available. Non-contact displacement sensors based on microwave technique have limited frequency response and sensitivity for the current application.

The technique chosen for the current study was the fiber optic intensity probe. The probe consists of two sets of optical fibers bundled together, one for transmitting light and the other for receiving. The displacement measurement is based on the interaction between the field of illumination of the transmitting fibers and the field of view of the receiving fibers. The sensitivity of these devices is very high, as is the frequency response. However, to work properly, the device must be mounted very close to the vibrating surface. Also, the probes average the reading over an area about 1.5 to 2 times the probe diameter. Each probe has a limited distance range over which it will operate. To accurately cover a large range of displacements, several different probes may be required. In addition, the output of the device is non-linear. The output is dependent on the surface reflectivity and must be calibrated for each different surface. To avoid the problem associated with different response due to different surface reflectivity, in this study the surface of each actuator studied was coated with the same silver paint.

Two fiber optic probes were purchased. The smaller diameter (1/32 in) covered a displacement range of up to 6 mils. The larger diameter probe, (1/8 in), was suited for displacements up to 25 mils. In order to position and calibrate the sensors, a manual X-Y traverse was assembled. A photograph of the probe in the traverse is shown in Figure 31. The vertical traverse contained

two stages, a coarse and a fine stage. The fine stage permitted setting increments as small as 0.1 µm (0.00393 mils). The horizontal traverse was used to position the probe in the center of the actuator and also for off axis displacement measurements.

A typical displacement vs output voltage curve for the small and the large probes is shown in Figure 32 and Figure 33 respectively. The output is non-linear with displacement. The shape of the curves are similar. When the probe is touching the surface, there is no output signal. As the probe is pulled away from the surface, the output increases until the optical peak is reached. The probe is most sensitive in this region. Beyond the optical peak the voltage decreases. For our purposes, the absolute distance of the probe from the surface (the standoff distance) is unimportant. We only care about the AC component of displacement. A straight line is fit to the data in the relatively linear region beyond the optical peak. For the small diameter probe, a least squares fit was made to the data between 7 and 17 mils. For the large diameter probe, 10 to 40 mils was used for the fit. Amplitude data was then only acquired over these regions. It is clear that the smaller probe is much more sensitive to changes in displacement but has a smaller operating range than the larger diameter probe.

The effect of standoff distance on the AC displacement measurement was also checked. A 30 volt peak to peak, 1 kHz sine wave was input into a unimorph actuator. The standoff distance was then varied and the apparent output level was measured. Figure 34 shows a plot of the peak to peak output signal from the non-contact sensor as a function of the probe's DC voltage, which is related to the distance of the probe from the surface. If the instrument were perfect, the AC output level would be constant with DC voltage. The voltage reaches a peak at about 3.6 volts. Therefore, this value was used to position the standoff distance for the probe for subsequent measurements, since this is the region where the measured AC output is least sensitive to changes in standoff distance.

Actuator Performance Results

High Polymer Films

One of the most compact sound sources available was the high polymer or PVDF films. Preliminary experiments were performed to gain experience with the devices and to measure the acoustic output characteristics. The material is available commercially in a variety of different sizes and shapes. Strips 40mm by 15 mm (1.57 by 0.59 in) and 28 µm thick were selected as appropriate to the size requirements of the current application (ATOCHEM part number DT1-028K). A photograph of these actuators is shown in Figure 35.

Preliminary sound pressure measurements were made in a non-anechoic environment with a 0.5 inch microphone located 5 inches from the actuator. A sine wave generator and an amplifier were used to drive the film at several frequencies from 500 Hz up to 10 kHz. The output level was too low to measure below 2 kHz and was only about 50 dB between 2 and 5 kHz. The output was around 80 dB between 6 and 10 kHz.

Later in the program, attempts were made to measure the surface displacement of a PVDF film mounted on a piece of foam rubber. The surface displacement was too low to measure using the

most sensitive non contact measurement probe. It is possible to increase the output of PVDF films by using multiple layers. Attempts to produce a five layer actuator were not successful. In light of the poor performance of the single layer PVDF film, no further work was done with high polymer films.

Miniature Speakers

The performance characteristics of two different miniature speakers were evaluated. Both used rare earth samarium cobalt magnets. The first one had a metal frame and was 1.01 inches in diameter with a frame depth of 0.193 inches (InterVox part number S125RL). The second speaker had a plastic frame and was 0.78 inches in diameter with a frame height of 0.157 inches (Intervox part number SR800RMF). Both were rated for 0.1 watt of power. A photograph of the speakers is shown in Figure 36.

Both speakers were tested at their maximum rated power of 0.1 watt. The displacement characteristics of the plastic and the metal frame speakers vs frequency are shown in Figure 37 and Figure 38 respectively. Both speakers exhibit a resonance near 500 Hz and the output above or below that is much smaller. The metal frame speaker had a peak to peak displacement of 12 mils while the plastic frame speaker had a peak displacement of less than 10 mils.

The phase relationship between the input signal to the speaker and the resulting output displacement was also measured for the plastic speaker. This result is shown in Figure 39. For four different input power levels (0.025, 0.05, 0.075 and 0.10 watts) the phase response versus frequency was independent of input power level. The phase increased rapidly from 100 to 600 Hz and then was reasonably flat (at 165°) over a range from 600 to 2100 Hz before falling and rising again. The flat region occurred above the resonance frequency (500 Hz) for this actuator.

Flextensional Actuator

The displacement of the miniature flextensional actuator was measured over a range of frequencies. The stacked actuator was driven with a ± 50 volt sine wave which was DC offset by 50 volts. This prevented the piezoelectric stack from experiencing a negative polarity which causes compressive failures in the bonds between the stack's layers. The displacement characteristics are shown in Figure 40. The maximum peak to peak displacement was found to be 0.0022 inches at 2200 Hz. Since the stack actuator is capable of extending by 0.00059 inches, this indicates an amplification factor of 3.7. This is somewhat less than the 6X that has been demonstrated in commercial units. The frequency response of this actuator was the most flat of any actuators tested. It was nearly uniform in the range from 200 to 1500 Hz.

The shift in phase between the input voltage to the actuator and the displacement of the actuator was also measured and is shown in Figure 41. The phase shift was very uniform with frequency over the flat frequency response region of the actuator (200 -1500 Hz). The phase changed from 16° at 160 Hz to 118° at 2000 Hz near the end of the flat frequency response. The total harmonic distortion (THD) is shown in Figure 42. It was also excellent, averaging less than 0.5% over the range from 100 to 2000 Hz.

Unimorph

Two different types of unimorph actuators were tested. One is a basic acoustic element which consists of a 41 mm diameter brass disk 0.4 mm thick, with a thin ceramic disk, 0.24 mm thick bonded to one side (muRata Erie part number 7BB-41-2AO). These types of actuators are manufactured by a number of different Japanese companies for electronic applications. They all appear to have the same basic geometry and voltages limitations.

The second was a piezo element designed for a telephone application as a microphone and speaker/tone ringer (muRata Erie part number VSB41D25-07ARO). These will be referred to as the basic unimorph and the telephone unimorph.

Basic Unimorph

The non-contact displacement system was used to measure amplitude displacements of two different configurations of the basic unimorph actuator. One was mounted at the edges and the other was mounted at the nodal diameter. It is suggested by the manufacturer that mounting the unimorph at the node causes the least suppression of vibration and hence allowing the greatest amplitude. A photograph of the basic unimorph package is shown in Figure 43.

A 30 volt peak-to-peak sine wave at selected frequencies from 500 Hz up to 10 kHz was input into the unimorphs. A plot of the peak to peak surface displacement vs frequency is shown in Figure 44. The peak-to-peak displacements of the actuators at non-resonant conditions were in the range of 0.0001 inch, which is at least an order of magnitude less than required. As expected, the devices exhibited a much higher response at their structural resonance. The node mounted configuration had a peak-to-peak displacement of 0.0013 inch at a resonant frequency of 2.9 kHz, while the edge mounted device had about a 0.6 mil displacement at 1.6 kHz. These data were acquired at the manufacture's recommended maximum voltage driving level. Higher output can probably be obtained using higher voltage levels for selected high quality samples.

The total harmonic distortion for the basic unimorph is shown in Figure 45. Although there is considerable scatter in the data, the total harmonic distortion of the surface fluctuations was typically less than 1% over the frequency band of interest.

Telephone Unimorph

A photograph of the telephone unimorph is shown in Figure 46. The characteristic which makes this actuator different from the basic unimorph is the thickness of the brass substrate. For this application, the brass element is only 0.0035 inches thick, compared to typical thicknesses of 0.008 to 0.010 inches. The ceramic element is 0.0065 inches thick. This results in a very flexible diaphragm.

The manufacturer recommends a maximum operating voltage of 30 volts peak to peak. These devices have been tested at levels several times this recommended level with no adverse effects noted, even after many days of continuous use at elevated voltages. Endurance testing was performed on the unimorph actuator at levels three times those recommended by the

manufacturer. A 2.5 kHz signal at 90 volts peak to peak was input to the unimorph and it was cycled for a week continuously without failure. Cooling air was supplied to keep the devices from overheating. Since these devices are not typically actively cooled during use, this may be why the manufacturers specify the 30 volt limit. Failure was observed in some specimens when the voltage was raised to 150 volts peak to peak, resulting in arcing and cracking in the ceramic.

The displacement characteristics of the telephone unimorph as a function of frequency was determined for several voltage levels from 20 volts peak to peak up to 120 volts peak to peak. The results are shown in Figure 47. Two resonant peaks in the spectrum are noted at around 1 kHz and 3 kHz. The maximum displacement achieved at 120 volts peak to peak was 18 mils at 1 kHz and 14 mils at 3 kHz. This same displacement information is shown plotted in a different format in Figure 48. In this plot, the displacement of the actuator surface is plotted against peak to peak voltage for several selected frequencies. In this way the linearity (or non-linearity) of the actuator can be deduced. This plot shows that except near the 3 kHz resonance, the displacement of the actuator is quite linear with voltage.

The phase between the input signal to the actuator and the surface displacement as a function of frequency is shown in Figure 49. Data was acquired for four different driving voltage levels: 30, 60, 90 and 120 volts peak to peak. In general, the phase increases with frequency up to about 1500 Hz before dropping off to a minima at 2200 Hz and then rising again. The largest variation in phase occurs for the lowest voltage case (30 volts peak to peak). Each voltage level produces a different phase relationship with frequency, although the data seems to collapse at frequencies above 2600 Hz.

Tunable Unimorph

As was shown in the previous section, unimorph actuators typically have resonances where the output of the actuator is much higher than it is elsewhere in the spectrum. The ideal actuator would have a flat frequency response over a wide bandwidth. However, to obtain very high displacement levels it may be necessary to use the high displacement provided at resonance. To make this technique useful for a gas turbine engine, the actuator must be able to follow changes in the operating frequency of the engine. Hence the actuator must be able to change its resonance.

Two different techniques were used to determine whether or not the unimorph actuators could be remotely tuned. In the first method, two unimorph actuators were bonded together. A DC voltage was placed across one actuator to put the other element in tension or compression to change its natural frequency and hence its resonance. The other element was driven with an AC signal. The second technique used a single actuator and was driven with a DC offset sine wave. The DC part of the signal was used to self induce a stress on the element.

The displacement vs frequency characteristics of the first concept is shown in Figure 50. An AC signal of 30 volts peak to peak was input to one of the unimorphs while a DC voltage varying from -50 to +50 volts was supplied to the other unimorph of the pair. The shifting of the resonance peak is clearly visible. The resonant frequency is plotted against the offset voltage in Figure 51. By applying a ±50 volt DC signal to one unimorph, the resonant frequency changes

29

by about ±2.8%. Depending on the application, this may be enough to tune the peak displacement to the required cancellation frequency. It is interesting to note that only a single resonance was noted in the frequency range measured compared to two resonances observed with a single telephone unimorph. This is probably caused by shifting the first resonance to a higher frequency by stiffening the actuator by the act of doubling of the thickness.

The second concept of supplying a DC offset sine wave to a single unimorph is demonstrated in Figure 52. The actuator was driven with a 90 volt AC signal which was DC offset from -90 to +90 volts. The shift in the two resonant peaks is apparent. The resonant frequency for both the first and the second resonance is shown plotted vs offset voltage in Figure 53. The effect of both positive and negative offset voltages is to lower the resonant frequency.

A phenomenon was noted when running the unimorphs at these high voltages levels. The performance of the actuators could be greatly improved or worsened by alternately applying large positive and negative offset voltages. This phenomenon appears to be related to repoling of the soft piezoelectric ceramics. The literature indicates that all piezoelectric materials suffer from an aging process after poling. This aging process is virtually negligible for hard ceramic materials, but can be substantial in soft ceramics. The aging process is a logarithmic function of time and the material exhibits typical decays of 1% to 6% per decade of time, i.e. 1 to 10 days, 10 to 100 days, etc. Soft materials can show deterioration of their piezoelectric response over periods of time as small as a few days. However, the loss can be regenerated by applying high voltage at room temperature for a short time.

This effect is demonstrated in Figure 54. This plot shows the displacement from a unimorph actuator as a function of time as a result of a slowly varying DC offset voltage. The displacement is the solid line and the dashed line shows the DC offset voltage. A 90 V peak to peak AC sine wave at 500 Hz was supplied to the unimorph and the DC offset voltage was varied from -80 to +100 volts. The unimorph displacement starts at 3 mils when the DC offset is -80 volts. The displacement drops to near zero when the DC offset reaches +30 volts. As the offset continues to rise, the displacement reaches a peak and levels off, even as the DC offset is decreased. The displacement again drops to near zero as the DC offset voltage falls to -10 volts. There is an apparent hysteresis effect on displacement from the offset voltage. This may be due to the continuous poling and repoling process which may be occurring when these high voltage levels are applied to the actuator.

Rainbow Actuators

Rainbow Actuator Testing

The majority of the bench testing was performed for Rainbow actuators. This was done for several reasons. First of all, they seemed promising for use as a gas turbine active noise control actuator since they had the potential for large displacements and were of the right size and shape. Secondly, since they are a new technology, little was known about their performance characteristics, especially dynamic performance.

Three different types of Rainbow actuators were tested. Two types are available commercially from Aura Ceramics. These are a soft piezoelectric Rainbow (C3900) and a soft electrostrictive Rainbow (PLZT). Two different diameters (1.25 and 2 inches) and several thicknesses (0.008, 0.015, 0.030 inches) were tested. Due to difficulties with self heating, a third type of actuator, a hard piezo ceramic Rainbow was fabricated in house and tested. Test results for these actuators are detailed below.

Displacement Characteristics

One of the most important measures of performance of any actuator is its frequency response. The frequency response of the Rainbow actuators was measured by applying a swept sine wave at constant input voltage amplitude across the frequency range of interest. Due to the limitations of the sweep function generator that was employed, sweeps were generally made between 200 and 3700 Hz.

Electrostrictive Rainbows

Displacement measurements were acquired for two types of electrostrictive Rainbow actuators, one with a 0.015 inch thickness and the other with a 0.030 inch thickness. Both were 1.25 inches in diameter. The displacement for the actuator vs frequency is shown in Figure 55. The actuator response is shown plotted for several input voltage levels from 50 to 150 volts peak to peak. A 100 volt DC offset was used. Since the displacement is proportional to the square of the electric field for electrostrictive materials, this meant that the actuator would never be subjected to a negative voltage. Four resonant peaks are visible roughly equally spaced at 600, 1600, 2400 and 3200 Hz. A maximum peak to peak displacement of 4.5 mils was obtained at the first resonance.

Another way of looking at this data is shown in Figure 56. In this figure, the output displacement is shown plotted vs voltage for various frequencies. The linearity of the actuator is very good. Even with air cooling, voltage levels were limited to 150 volts peak to peak due to self heating.

A test was also performed of a 1.25 inch diameter, 0.030 inch thick electrostrictive Rainbow actuator. These results are shown in Figure 57. The peak achieved displacement was only 0.6 mil at the highest voltage available from the power supply and self heating was becoming a problem at the higher frequencies. As expected, the resonance frequency is much higher than the thinner Rainbow due to the shift in natural frequency with thickness of the circular plate of ceramic material.

Soft Piezoelectric Rainbows

Displacement measurements for a 1.25 inch diameter, 0.008 inch thick soft piezoelectric Rainbow actuator are shown in Figure 58 and Figure 59. The former figure shows the displacement vs frequency characteristics while the latter shows the displacement vs voltage attributes. Data was acquired over a range of AC voltage amplitudes from 100 to 225 volts. A DC offset voltage of 88 volts was chosen to prevent depoling or reverse poling of the material based on the manufacture's recommendations. A maximum peak to peak displacement of 11

mils was obtained at the resonance frequency of 1300 Hz. The linearity of the actuator is again seen to be quite good.

Figure 60 and Figure 61 show the displacement vs frequency results for a 1.25 inch diameter, 0.015 inch thick, soft piezoelectric Rainbow actuator. Input voltage levels to the actuator were varied from 100 to 350 volts peak to peak. A 25 volt DC offset voltage was chosen to prevent depoling. Again, a single resonance was noted in the frequency range measured, from 200 to 3700 Hz. The maximum peak to peak displacement of 13 mils occurred at 2200 Hz. Except for points near resonance, the linearity of the displacement vs voltage is quite good.

For Rainbow actuators with thicknesses above 0.015 inch, the maximum achievable displacement was reduced. Results for a 1.25 inch diameter, 0.030 inch thick, soft Rainbow actuator are shown in Figure 62 and Figure 63. The peak displacement achieved was only 3.3 mils at 3100 Hz and 400 volts. No DC offset was used for this actuator. The linearity of the displacement vs voltage was again very good. The frequency of the resonance again was higher than that seen for the thinner actuators.

Displacement measurements were obtained for one sample of a 2 inch diameter, 0.015 inch thickness Rainbow. The displacement vs frequency characteristics are shown in Figure 64. Measurements were acquired at voltages from 100 to 300 volts peak to peak. No DC offset was used. A maximum peak to peak displacement of 13 mils was obtained at the resonance frequency of 1200 Hz. The actuator exhibited the rather strange characteristic that the peak displacement was the same for 200 and 300 volts. This may have been due to an amplifier limitation rather than an actuator characteristic. Due to the large diameter, these actuators were not further evaluated since they did not appear to be feasible for the desired gas turbine application.

Hard Piezoelectric Rainbows

The displacement vs frequency characteristics of a Rainbow actuator made from a hard ceramic material is shown in Figure 65. The displacement as a function of voltage for various frequencies is shown in Figure 66. The actuator was 1.25 inches in diameter and was 0.015 inches thick. Since hard ceramic materials typically have lower dissipation losses compared to soft materials, this actuator could be driven to much higher voltage levels than the soft Rainbow actuators without over heating. Displacement measurements were obtained from 200 to 800 volts peak to peak. The maximum peak to peak displacement of 10 mils was achieved at a resonance frequency of about 1200 Hz. This actuator exhibited two resonances in the range of frequencies of interest, the second was at about 2200 Hz. Compared to the soft Rainbow actuators, this actuator had a much flatter frequency response.

The output displacement observed for the highest voltage level did not appear as smooth as the lower voltage settings. This also shows up in the otherwise good linearity of the actuator on the displacement vs voltage curves in Figure 66. This may have been caused by amplifier limitations since this was the upper voltage limit of the staged master/slave op amps.

Composite Rainbow Actuators

Displacement tests were performed for two composite Rainbow samples. Both had a 0.015 inch thick, 1.25 in diameter piezoelectric wafer bonded to a 2 inch diameter brass disk. Two different brass thicknesses were used, 0.004 and 0.007 inches. The displacement results are shown in Figure 67. Compared to the baseline Rainbow, the first resonance frequency was lowered, as was expected. The resonance frequency changed from about 1400 Hz for the Rainbow alone to about 500 Hz for the composite. Unfortunately, the displacements were also lower. At the first resonance, the displacement was 2.75 mils peak to peak for a 200 V peak to peak excitation for the 7 mil thick brass composite and only about 1 mil for the 4 mil thick brass composite actuator. The displacements were higher at the second resonance peaks for both samples. Data was only obtained at frequencies up to about 3700 Hz due to temperature and cooling limitations. At this frequency, the displacement for the 7 mil thick composite was over 4 mils and still rising with frequency.

Traverse Displacement

Displacement measurements reported above have been made in the center of the actuator since this is the location of maximum movement. For use as a noise actuator, a better measure of performance might be the total unsteady volume displacement from the actuator. Since the actuators are mounted at the ends, the displacement must go to zero at that point. The computational rotor/stator active noise cancellation studies by Kousen and Verdon (ref. 1,2) have assumed a rigid two dimensional piston. In order to better determine the effective volume displacement of the Rainbow actuators, a traverse was made of the peak to peak displacement of the actuator across the radius.

Measurements were obtained at 1 mm increments for 31 points across the 1.25 inch diameter of a 0.015 inch thick, piezoelectric Rainbow actuator. Results are shown in Figure 68. Measurements were obtained at three frequencies: 500 Hz, 1.5 kHz and 3 kHz. The curve of displacement vs radial position was in the form of a symmetrical Gausian curve, with the peak displacement occurring at the center. A second much smaller maxima occurred at the 0.8 radius position.

The area weighted average displacement was determined by integrating the displacement vs distance data. For a round disk actuator, the effective displacement varied from 27% of the peak displacement at 3000 Hz to 43% at 500 Hz. It may be possible to increase the volume displacement by mounting a rigid plate at the peak displacement point on the top of the Rainbow actuator dome.

The phase difference between the input signal to the actuator and the achieved displacement is needed to determine whether or not the entire actuator surface is moving together. Phase results for the same actuator are shown in Figure 69. The phase was relatively constant across 60% to 70% of the central portion of the diameter. As expected, the phase shift was different for the different frequency cases. Beyond 60% or 70% radius, the phase shift changed smoothly for the lower frequency cases, and rather abruptly for the 3 kHz case. This indicates that at least the

33

entire inner portion of the actuator is moving in unison and therefore should be effectively displacing a large volume of fluid.

Phase Between Input Voltage and Displacement

The purpose of this test was to determine the phase shift between the input signal and the output displacement as a function of frequency and input voltage level. For the test, the phase was measured as the signal from a sine wave generator was swept from 100 to 3700 Hz. A spectrum analyzer was used to measured the phase difference between the two signals.

The phase was measured for two different types of Rainbow actuators, electrostrictive and piezoelectric. The results are shown in Figure 70 and Figure 71 respectively. Multiple driving voltage levels were tested for each actuator.

The phase characteristics for these actuators were complicated. While the phase vs frequency curves for each input level were similar in shape, the phase did change with the input voltage level. The two different types of Rainbow actuators had similar phase characteristic curve shape. The phase generally increases with increasing frequency from 30° at 200 Hz up to 170° at 3700 Hz. Two local maxima were observed, one at 500 Hz and the second at about 1600 Hz. Different input voltage levels again were seen to produce different phase characteristics, although at a somewhat smaller degree of difference than the unimorph.

Harmonic Distortion

An important characteristic of any noise generator is its ability to clearly reproduce sound without distortion. One measure of the distortion level is the total harmonic distortion (THD). To obtain a measure of the harmonic distortion, pure sine wave signals at various discrete frequencies were input to the different actuators and the harmonic distortion of the output displacement was measured.

An indication of the purity of signal reproduction can also be obtained by examining the spectral content of a displacement signature. The displacement spectrum for a 1.25 inch diameter, 0.015 inch thick, piezoelectric Rainbow actuator is shown in Figure 72 and Figure 73 for two different input signal levels (100 and 200 volts peak to peak). Four different plots are shown in each figure, corresponding to four different sine waves which were input (500 Hz, 1 kHz, 2 kHz, and 3 kHz). In each case, harmonics of the driving frequency are apparent in the spectrum. However, those harmonics levels are typically 15 to 20 dB down from the fundamental tone.

The total harmonic distortion is a measure of the relative energy in the harmonics of a fundamental compared to the energy in the fundamental. The total harmonic distortion was measured for one sample of electrostrictive Rainbow and for three different sizes of piezoelectric actuators.

The total harmonic distortion of a 1.25 inch diameter, 0.015 inch thick, electrostrictive Rainbow actuator as a function of frequency is shown in Figure 74. The total harmonic distortion of the input to the actuator (the amplifier output) is also shown to confirm that the amplifier was not

contributing to the actuator distortion. The THD of the amplifier are much lower than those produced by the actuator. The highest THD of about 13% occurred at about 900 Hz. In general the THD levels were quite low, generally under 4%.

The total harmonic distortion for the 0.008, 0.015 and 0.030 inch thick piezoelectric Rainbow actuators are shown in Figure 75, Figure 76 and Figure 77 respectively. The diameter was 1.25 inches for all three samples. In general, the THD levels were quite low, in the range of two to three percent. However, there were frequency ranges where the levels were higher. These appeared to occur not at the primary resonance but at much smaller resonances in the displacement spectra. The amplifier did not contribute to the THD for the two thinnest actuators. It did contribute for the 0.030 inch thick actuator at frequencies above 3 kHz where the power draw is the most severe.

Operating Limitations Due to Self Heating

The maximum steady state operating levels of the Rainbow actuators are limited by temperature rise due to the high internal dissipation factors of the soft ceramics used. In order to determine that operating limit, measurements of the power consumed by the actuators vs frequency and input voltage were acquired. This was done by selecting a frequency, and slowly increasing the input voltage until a specified power level (as indicated by a power meter) was reached. A 1.25 inch diameter, 0.015 inch thick piezoelectric actuator was used. For this test, the maximum temperature of the actuators was limited to 100°F.

Contours of equal power are shown plotted as a function of peak to peak voltage and frequency in Figure 78. With the amount of cooling available with our shop air impingement cooling scheme, 3.1 SCFM, a limit of 4 watts was found to be the maximum power limit. The input voltage needed to achieve this power limit was found to decrease with increasing input frequency.

Conclusions

1. Through the use of current state of the art actuator technology it appears possible to build an actuator which can meet the requirements for a gas turbine active noise control scheme. These requirements include high frequency response (> 1 kHz), large amplitude deflections (± 0.010 inches) and a thin profile (< 0.25 inch).

2. For this application, piezoelectric effect actuators are best suited. Rainbow actuators and unimorph actuators have the greatest possibility of success in meeting these goals. These technologies were selected after a thorough literature review and analysis of the state of the art actuator body of knowledge.

3. Bench top static experiments measured a peak to peak displacement at resonance of 0.013 inches with a 1.25 inch diameter, 0.015 inch thick Rainbow actuator. A 0.010 inch thick unimorph actuator with a diameter of 2 inches was able to achieve a displacement of 0.018 inches at resonance.

4. The long term endurance capability of both Rainbow and unimorph actuators appears to be favorable. These results are based on preliminary cyclic testing over a relatively short period of time.

5. All actuators tested with the exception of the flextensional actuator have resonance frequencies where output displacements are high. Hard ceramic Rainbow actuators had flatter frequency response than soft Rainbows. Schemes were demonstrated which tune the resonance of actuators to enable the maximum displacement to be obtained over a range of frequencies. This is important since the blade passage frequency changes with engine operating point.

6. Temperature rise due to self heating of high dissipation materials may be a limiting factor in soft piezoelectric ceramics. Thicker disks and electrostrictive materials have more severe limitations than thin disks and piezoelectric material. Rainbow actuators made from hard ceramic materials do not seem to be limited by this mechanism.

7. Proper mounting is crucial for reliable actuator operation. A soft mounting scheme which allows the actuators to have some edge movement is preferable to a hard, constrained mount.

8. The dynamic displacement of Rainbow actuators is inversely proportional to their thickness. However, there is a practical lower thickness limit of about 0.010 inches based on durability, fabrication and strength issues.

9. High voltage/high current amplifiers are required for high displacement operation of Rainbow actuators. The actuators do not consume a large amount of power, but the high capacitance of the actuators requires a high current capacity at high frequency.

10. The maximum displacement of Rainbow actuators occurs at the center of the dome. The surface of the actuator moves in phase, resulting in an effective unsteady volume displacement for noise generation.

Appendix A - Final Report - Piezoelectric Actuator Feasibility Study

1. INTRODUCTION

The objectives of this purchase order are to (1) review open literature relevant to piezoelectric actuator technology, (2) assess the potential of piezoelectric actuator technology to generate the sound power signature required in the application of UTRC's proprietary rotor-stator interaction device and (3) recommend the piezoelectric technology considered to have the "best" potential to comply with the requirements defined in Table I below.

Table I. Piezoelectric Target Operating Goals

Description	Minimum/Maximum Operating Range
Static Temperature	410 - 610 °F
Static Pressure	4 - 16 psi
Desired Frequency Range	500 - 10,000 Hz
Required Frequency Range	500 - 8,000 Hz

2. SUMMARY OF LITERATURE REVIEW

A total of eleven articles were reviewed. A brief summary of the important findings of each article is described below.

Ref . 1.   **Multilayer Actuator Design**
Carlson, Trolier, Safari, Newnham and Cross
I.E.E.E. Proceedings 1986
CH2358-0/86/0000-0641

This article contains a brief description of multilayer actuator design criteria, failure modes and fruitful methods of analytical attack. It is common knowledge in the piezoactuator community that "multi-layer actuators" describes a piezotransducer that is constructed in layers that have the following properties:

a.   There are "N" layers where N is typically greater than 100.

b.   They are very thin with a thickness equal to or less than 0.005-inches.

c.   They are stacked face-to-face so that all layer motions are additive.

d.   They are electrically driven in parallel (i.e., 25 volts applied to a stack means each

layer has 25 volts).

     e.   They are assembled one-on-top-of-the-other along with the electrodes while the piezoceramic is still in a putty-like state pressed together and kiln-fired all as one piece.

When manufactured in this fashion, the actuator holds the promise of economy in scale.

Ref 2   **Fatigue Effects in High Strain Actuators**
     Cross and Jiang
     J. of Intell. Mater. Syst. and Struct.
     Vol. 3, Oct. 1992

It is common knowledge that many piezoceramic transducers have exhibited what practically amounts to an infinite operating life. Further, they are often deliberately designed to have low strain. This paper contains a thorough discussion of failure modes observed in ceramic transducers which are strained to their operating limit. The following failure modes were identified:

a.   Electrode separation from ceramic surfaces.

b.   Crack propagation originating from pores that are "fired"during manufacture.

c.   Crack propagation originating between grains that are characteristic of ceramics capable of high strain.

The authors discuss experimentally validated ceramic preparation methods to remedy the above shortcomings.

Ref. 3   **A New Piezoelectric Driver Enhances Horn Performance**
     Jonathan R. Bost
     Journal of the Audio Engineering Society
     Vol. 28, Number 4, April, 1980.

Ref. 4   **A New Type of Tweeter Horn Employing a Piezoelectric Driver**
     Jonathan R. Bost
     Journal of the Audio Engineering Society
     Vol. 23, December, 1975.

These articles describe two steps in the evolution of the piezoelectric "tweeter" speaker which is commercially available. The articles include descriptions of how to construct the tweeter as well as the underlying principles of its operation.

This style of piezo transducer is a complex one, consisting of a piezo flexure element, a conical elastic diaphragm, and a tuned acoustic horn all coupled together. When properly designed, manufactured and driven, such transducers are capable of 40 KHz bandwidth with +/-5 dB. Graphical results are presented.

Ref. 5   **The Effectiveness of A Piezoelectric Bimorph to Perform Mechanical Work Under Various Constant Loading Conditions**
Jan G. Smits
Ferroelectrics
Vol. 119, 1991

Ref. 6   **The Effectiveness of a Piezoelectric Bimorph to Perform Mechanical Work Against Various Spring-Type Loads**
Jan G. Smits
Ferroelectrics
Vol. 120, 1991

A companion set of articles. Perhaps the only full and correct mathematical treatment of piezoceramic flexure elements converting electrical energy into specific types of mechanical energy *other than damping*. The body of both papers contain considerable formal matrix mathematics which is required to adequately treat the full energy transformation problem for an elastic solid. The introductions contain excellent summaries of experimental work regarding designing piezo transducers to do work on various loads.

Conclusion of both articles state mathematical constraints applicable to piezo transducers for maximizing efficiency under various loads. The bibliographies are exceptional.

Ref. 7   **A High Speed Impact Actuator Using Multilayer Piezoelectric Ceramics**
Chang and Wang
Sensors and Actuators
Vol 24, 1990

This article contains a large amount of experimental detail concerning operation of actual multi-layer piezoceramic stacks under high drive conditions. Energy output, power consumption, and self heating are discussed as relevant to high speed printers. An impact repetition rate of 2.8 KHz was demonstrated.

The achieved repetition rate and energy conversion conclusions are relevant to the present subject, however the physical principles utilized to create a ballistic mass launch are not applicable to sinusoidal sound sources.

Ref. 8   High Speed Electro-Hydraulic Servovalves Using Electrostrictive Ceramic
          Actuators
          Ouchi, Nakano, Uchino, Endoh, and Kufumoto

This paper describes an interesting set of experiments with two different piezo-hydraulic valves. Both Piezo flexors and piezo stacks were employed as the first stage in a hydraulic serve amplifier. The bandwidth range tested varied from 0 to 2 KHz. The paper contained large amounts of plotted data.

In theory, a servovalve of this type could be used as an acoustic source, however the inclusion of liquid and the attendant difficulties make it inconsistent with the stated requirements.

Ref. 9   Piezoelectric and Electrostrictive Sensors and Actuators for Adaptive
          Structures and Smart Material
          Cross
          Presented at Annual Meeting of Amer. Soc. of Mech. Eng.
          San Francisco, CA December 10-15, 1989

These two introductory articles treat the broad concept of using piezo materials as actuators and sensors. It contained a brief, informative introduction to piezoelectric stacks and stack applications (see page 13)

Ref. 10   High Speed Magnetic Actuator
          Helinski
          IBM Technical Disclosure Bulletin
          Vol 24, No. 10 March 1982

Ref. 11   Servo Controlled Foil Bearing Actuator
          Wang
          IBM Technical Disclosure Bulletin
          Vol. 27, No. 1B June 1984

Both articles are irrelevant to the present subject and contain no information of interest.

3. BROADBAND PIEZOELECTRIC TRANSDUCERS

3.1 Requirements

Piston motion:	0.001- 0.010 inches
Piston force:	Motion delivered into a load
Piston bandwidth:	500 - 10,000 Hz
Pressure environment:	4 -16 psi
Temperature environment:	410 - 610 °F

3.2 Basic Configuration

Figure 1 shows a simple sound transducer consisting of a single slab of piezo ceramic attached to a rigid backplane, radiating out into a half-space. When a DC voltage is applied to the leads, the free face of the slab moves a distance Δx defined by the expression

$$\Delta x = V*d_{33} \tag{1}$$

where Δx is the motion of the slab face, V is the applied electrical potential (in volts) and d_{33} is the piezoelectric charge coefficient for the material (in meters/volt).

Each piezoceramic transducer has a limit to the magnitude of Voltage V which can be applied. This limiting voltage (V_{max}) is defined by the expression

$$V_{max} = E_{max}*L \tag{2}$$

where E_{max} is the (normally empirically determined) limiting electric field (volts/meter) and L is the thickness of the slab. The *direction* of the motion of the slab face depends on the *sign* of the applied voltage. When an "ac" voltage is applied, the slab behaves as a broadband transducer, with uniform displacement over the frequency band defined below

$$0 < f < \frac{c}{4*L} \tag{3}$$

Here f is the operating frequency (Hz), c is the speed of sound in the piezoceramic ($\approx 3,600$ meters/sec)and L is the thickness of the ceramic slab (meters). For sinusoidal voltage inputs within the frequency band defined by Eq. (3), the face of the piezoceramic behaves just like a piston moving with a peak amplitude equal to Δx defined by Eq. (1). In this region, the frequency response is perfectly flat.

4. DESIGN CONSIDERATIONS

4.1 Piezoceramic Material Selection

The temperature requirement defined in Table I eliminates all but a few materials. The usual rule-of-thumb for transducer materials is that the operation temperature should be less than or equal to one-half of the Curie temperature measured in degrees Centigrade (the origin of this rule-of-thumb is not known). Table II below summary some of the available commercial piezocramics.

Table II. Summary of Commercial Piezoceramics

Material	Manufacturer	Piezo Charge Coeff.	Curie Point	Max. Operating Temp.
		d_{33} x 10^{-12} m/V	T_c - °C	T_{max} - °C
PZT 5A	Vernitron	374	365	344
#4 LM	Stavely	160	400	376
Quartz	not required	2.3	576	534
LiNbO$_3$	not known	6	1250	1141

Substituting the above charge coefficients (d_{33}) for the selected materials into Eq. (1) reveals a drastic drop in achievable motion with increasing temperature hardiness. Although the materials identified in Table II is not complete, it does, however, correctly identify the sensitive trade-off between available motion and operating temperature.

4.2 Piezoceramic Motion

As an example, the performance of a 1-inch thick slab (i.e. L = 0.0254m) of PZT 5A material will be estimated. The maximum limiting electric field for this material E_{max} = 4.72 x 10^5 V/m. The maximum voltage allowed for this slab is estimated using Eq. (2) to be

$$V_{max} = E_{max} * L = 4.72 * 10^5 \, V/m * 0.0254 \, m = 11,988 \, V \tag{4}$$

The motion of the slab face for Vmax follows from Eq. (1) to be

$$\Delta x_{max} = V_{max} * d_{33} = (11,988 \, V) * (374 * 10^{-12} \, m/V) = 4.484 * 10^{-6} \, m = 0.1765 mil \qquad (5)$$

4.3 Piston Forces

In general, the ambient air pressure requirements of 4 to 16 psi (see Table I) will have an negligible effect on the operation of any slab type of piezo transducer because the internal stresses created by the electric field in a piezoelectric ceramic are typically several thousand psi.

The dynamic pressures on the face of the slab is of course dependent on the geometry of the transducer (e.g. circular or square cross section) and on the drive frequency. For piezoceramic transducers operating into an air load, the effects of dynamic pressure forces occurring during acoustic broadcast are normally neglected.

5. PRELIMINARY FEASIBILITY ANALYSIS

It is instructive to make a quick sketch of an actuator satisfying as many of the requirements defined in Table I as possible.

5.1 Piezoceramic Size

Referring to Section 4.2 above, it is clear that in order to achieve even 1-mil peak-to-peak displacement (0.5 mil peak) on the piston face with the most motion "friendly" piezoceramic identified in Table II (PZT-5A), the slab thickness (L) must approach 2-inches.

Utilizing Eq. (3), it also becomes clear that transducers made from the more exotic #4 LM (a Lead Metaniobate material made by Stavely and having a $d_{33} = 160 \times 10^{-12}$ m/V) would approach a thickness of 4-inches. The other two materials identified in Table II would require thicknesses of over 100-inches to achieve the required 1-mil peak-to-peak motion.

Regarding transducer size, a plausible estimate of a manufacturable high temperature transducer suitable for mounting in arrays would be 2-inches in diameter. Thus the transducer is 2-inches thick and has a diameter of 2-inches. If constructed from solid ceramic (typical density of piezoceramics is 7.5 g/cc - see Appendix A), its mass will be 0.772 kg (about 1.7 lb).

5.2 Electrical Drive

The electrical energy requirements to drive piezoceramic transducers are of obvious importance. The transducer appears simply as a capacitor in its designated broadband operating zone below the first resonance. Consider a simple solid block of diameter 2-inches and thickness 2-inches. Its capacitance is defined by the expression

Here A is the total cross sectional area of the transducer (m^2), ε_o is the dielectric permitivity of

$$C = A * \epsilon_o * K_{33}/L \qquad (6)$$

free space (= 8.86×10^{-12} Farads/m), K_{33} is the relative dielectric constant of the piezo material (=1700 for PZT 5A - see Appendix A) and L is the thickness of the slab. Substituting these values into Eq. (6) yields C = 0.6 nanoFarads.

The drive voltage for a single based slab is 24,000 volts zero-to-peak (i.e., 24,000 volts will maintain E_{max} across L = 2-inch thickness, just as 12,000 volts will maintain E_{max} across L = 1-inch - see Eq. 2). The drive amplifier power requirements for a sinusoisdal signal at 500 Hz will be 1.08×10^3 volt-amps. At a frequency of 10,000 Hz, the amp power requirements are 21.7×10^3 volt-amps.

Note: The power actually consumed by the transducer will be vastly lower than the volt-amp rating of the amplifier itself. There is however no way of getting around supplying the required current to the transducer at the required peak voltage, and power losses in the amplifier, measured in watts, will be close to the volt-amps delivered to the capacitive load.

5.3 Dynamic Pressure on Transducer Face

The near field pressure created by a 2-inch diameter piston displaced 1-mil peak-to-peak will be approximately 0.3 psi at 500 Hz and 120 psi at 10,000 Hz (see Appendix B for full calculation). As previously mentioned, the internal stresses created by the piezoelectric effect in the ceramic are nominally several thousand psi, and therefore the effect of the dynamic pressure on the motion of the face of the slab can be safely neglected.

6. FEASIBILITY OF PIEZOCERAMIC SOUND SOURCES

6.1 Variations on the Instructive Design

It seems clear that the example transducer described above, while having some merits (e.g., reasonable output at its high frequency end), would really have to be much lighter and lower in power consumption to be feasible with respect to turbofan engine applications.. The discussion below considers further schemes to improve its feasibility.

6.1.1 Weight Reduction

The transducer can be made lighter by "hollowing out" its center axis portion, while still requiring it to support a "piston" structure (see Figure 2). This leaves an annulus with perhaps 0.37-inch thick walls, still 2-inches high. Its weight would then be reduced to about 0.45 kg which is approximately one-half of its original weight. Its weight however would still be sufficiently high to retain sufficient rigidity to support the design concept sketched in Figure. 2.

6.1.2 Volt-Amp Requirement Reduction

The design change described in Section 6.1.1 above will also reduce the volt-amp requirement by a factor of 0.6. We believe that a factor of two reduction is within the realm of possibility.

6.1.3. High Voltage Requirement Reduction

Within limits, the design voltage requirement can be traded against the required amperes requirement. This can be achieved by stacking, say, 10 annuli each 2-inches in OD, 1.25-inches in ID and 0.2-inches thick. (An arrangement commonly referred to as a PIEZO STACK). The voltage required would then be reduced by a factor of about 10 reducing the 24,000 V requirement of Section 5.2 to about 2,400 V.

It is tempting to consider further extension of this scheme by making a stack of 100 layers, requiring only 240 volts. If this is attempted, the stack would almost certainly have to be fabricated as a single integral unit in order to be made economically. Quite a lot of research is being done on this subject at present (see Reference 1), primarily addressed toward vibration control and other mechanical servo applications under 500 Hz. Piezo stacks which have been fabricated as one integral unit have internal electrodes that exhibit failure modes related to electric field edge effects within the transducer (see Reference 2). An additional difficulty with applying the 100 layer variety of stack to the 1 KHz acoustic transducer is that significant and sometimes destructive self-heating occurs in the transducer.

At present, 100 layer stacks should not be considered a viable path. This design would be most practical at 2,400 V.

6.2 Alternative Configurations

Piezoceramic is very stiff and air is very compliant. The reasoning of Section 6.1 is aimed at reducing the volume of ceramic which addresses the air load on the piston in order to produce a better, less wasteful match. Is there some other avenue toward this goal? In the audio industry, piezoceramics have been successfully matched to air for high frequencies only (3,000 Hz to 20,000 Hz - see Reference 3). This is achieved by use of a bimorph piezo structure which acts in flexure rather than expansion. A flexure element as thin as a dime and as large as a silver dollar can drive a paper cone quite effectively, creating 120 dB output. It's possible that this approach might work, however the following points must be noted:

1. The efficacy of the design depends on some stiffness-to-weight properties of paper which would be difficult to reproduce with materials that would withstand the Table I identified required temperatures.

2. The design requires an extremely high strength epoxy butt joint between the piezo and the cone. This would be difficult to achieve with the required temperatures.

3. The cone is actually a large diaphragm that will withstand destructive forces when exposed to the pressure environment identified in Table I provided that it is well sealed.

4. The low frequency end of the spectrum 500 - 3000 Hz will have to be treated via some other transducer design scheme.

MOUNTING PLANE,
an INFINITE, RIGID
BAFFLE

SURFACE MOTION +/- x (peak)

PIEZOCERAMIC
SLAB, with SURFACE
AREA "A"

SOUND OUTPUT

AC

GENERALIZED PIEZO ACTUATOR
MOUNTED TO A RIGID PLANE

Fig. 1

MOUNTING PLANE, an INFINITE, RIGID BAFFLE

PIEZOCERAMIC SLAB, with SURFACE AREA "A"

PISTON, with AREA LARGER than "A" ATTACHED RIGIDLY TO PIEZOCERAMIC

PISTON MOTION +/- x (peak)

SOUND OUTPUT

AC
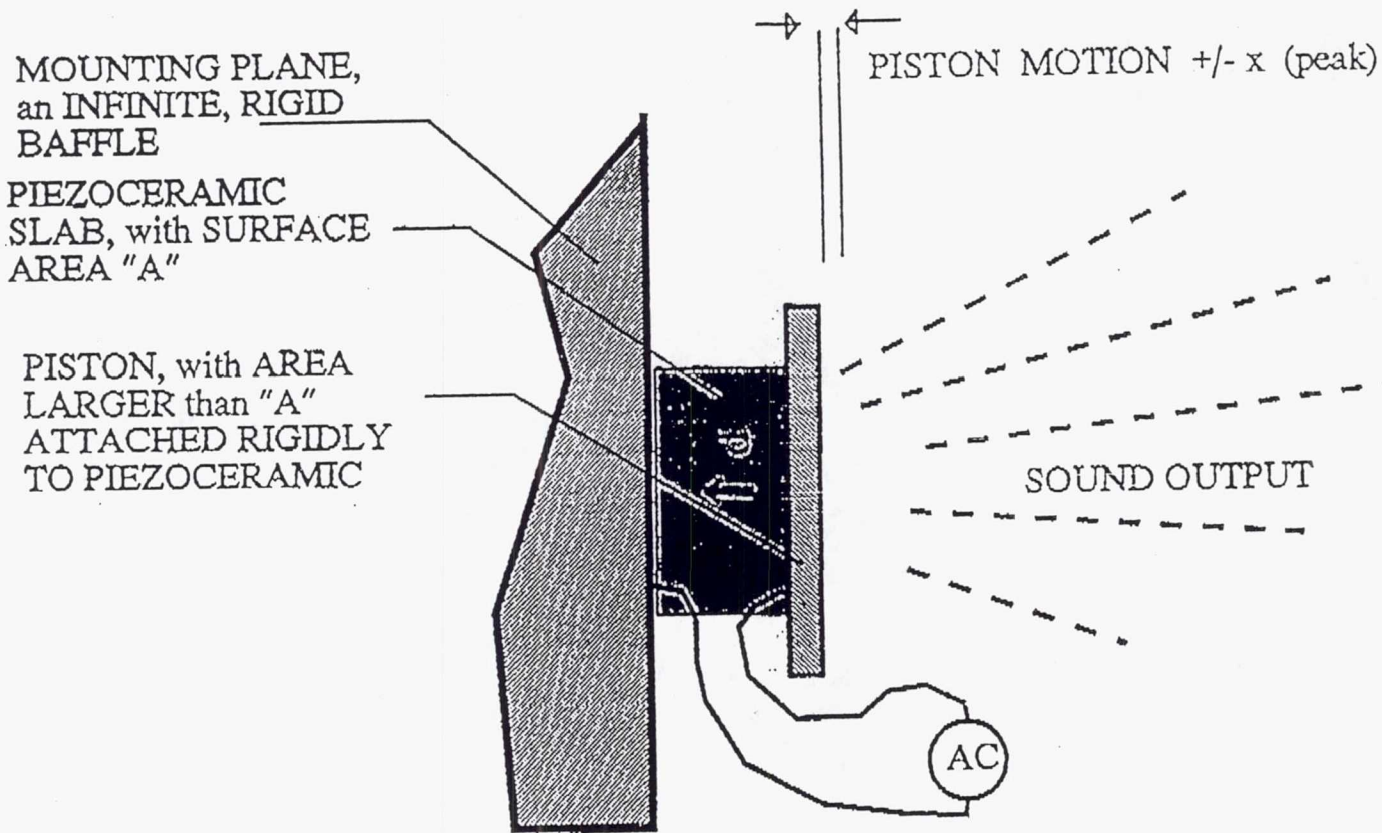
GENERALIZED PIEZO ACTUATOR MOUNTED TO A RIGID PLANE, WITH A LARGE AREA PISTON ATTACHED

Fig. 2

Piezoelectric Ceramics—Typical Room Temperature Data (Low Signal)

		Ceramic B	PZT-4	PZT-5A	PZT-5H	PZT-8
At one kcps *	$\epsilon_{33}^T/\epsilon_0$	1200	1300	1700	3400	1000
	$\epsilon_{33}^S/\epsilon_0$	910	635	830	1470	600
	$\epsilon_{11}^T/\epsilon_0$	1300	1475	1730	3130	1290
	$\epsilon_{11}^S/\epsilon_0$	1000	730	916	1700	900
	$\tan \delta$	0.006	0.004	0.02	0.02	0.004
	k_p	−.33	−.58	−.60	−.65	-.51
	k_{31}	−.194	−.334	−.344	−.388	.30
	k_{33}	.48	.70	.705	.752	.64
	k_{15}	.48	.71	.685	.675	.55
	k_t	.384	.513	.486	.505	.48
	k_{13}	.491	.715	.715	.754	.63
	d_{31}	−58	−123	−171	−274	-.97
	d_{33}	149	289	374	593	225
	d_{15}	242	496	584	741	330
	d_h	33	43	32	45	.31
	g_{31}	−5.5	−11.1	−11.4	−9.11	-10.9
	g_{33}	14.1	26.1	24.8	19.7	25.4
	g_{15}	21.0	39.4	38.2	26.8	28.9
	s_{11}^E	8.6	12.3	16.4	16.5	11.5
	s_{33}^E	9.1	15.5	18.8	20.7	13.5
	s_{44}^E	22.2	39.0	47.5	43.5	31.9
	s_{12}^E	−2.6	−4.05	−5.74	−4.78	-3.7
	s_{13}^E	−2.7	−5.31	−7.22	−8.45	-4.8
	s_{11}^D	8.3	10.9	14.4	14.05	10.1
	s_{33}^D	7.0	7.90	9.45	8.99	8.5
	s_{44}^D	17.1	19.3	25.2	23.7	22.6
	s_{12}^D	−2.9	−5.42	−7.71	−7.27	-4.5
	s_{13}^D	−1.9	−2.10	−2.98	−3.05	-2.5
	Q_M	400	500	75	65	1000
	N_1	2290	1650	1400	1420	1700
	N_{3t}	2740	2000	1890	2000	2070
	N_{3a}	2530	2060	1845	1930	2000
	ρ	5.55	7.5	7.75	7.5	7.6
	Curie Point	115°C	328°C	365°C	193°C	300° C

*For PZT-5A the dielectric constants decrease about 2.4%/decade of frequency to at least 20 mcps and increase 2.4%/decade of frequency below 1 kcps to at least 1 cps.
For PZT-4 the dielectric constants decrease about 1.0%/decade of frequency to at least 1 mcps and increases 1.0%/decade of frequency below 1 kcps to at least 1 cps.

TREATMENT OF 'ON AXIS' PRESSURE DISTRIBUTION
for SIMPLE PISTON IN A BAFFLE

$f := 10000 \cdot sec^{-1}$ DRIVE FREQUENCY

$a := .0254 \cdot m$ RADIUS of PISTON

$Xo := .5 \cdot 10^{-3} \cdot in$ PEAK DISPLACEMENT of PISTON

$Uo := 2 \cdot \pi \cdot f \cdot Xo$ VELOCITY of PISTON FACE (peak)

$Uo = 0.798 \cdot length \cdot time$

$rho := 1000 \cdot kg \cdot m^{-3}$ DENSITY of ACOUSTIC MEDIUM

$c := 1435 \cdot m \cdot sec^{-1}$ SOUND VELOCITY of ACOUSTIC MEDIUM

$\lambda := \dfrac{c}{f}$ $\lambda = 0.144 \cdot m$

$k := 2 \cdot \dfrac{\pi}{\lambda}$

$ka := k \cdot a$ $ka = 1.112$

$i := 0 ..20$

$x_i := i \cdot \dfrac{a}{10}$

$Pinf := 2^{-.5} \cdot rho \cdot c \cdot Uo$ RMS pressure due to infinite plate moving Xo, f

$$P_i := 2^{.5} \cdot rho \cdot c \cdot Uo \cdot sin\left[\frac{k}{2} \cdot \left[\left[x_i^2 + a^2\right]^{.5} - x_i\right]\right]$$ RMS PRESSURE on AXIS of finite circular disk radiator
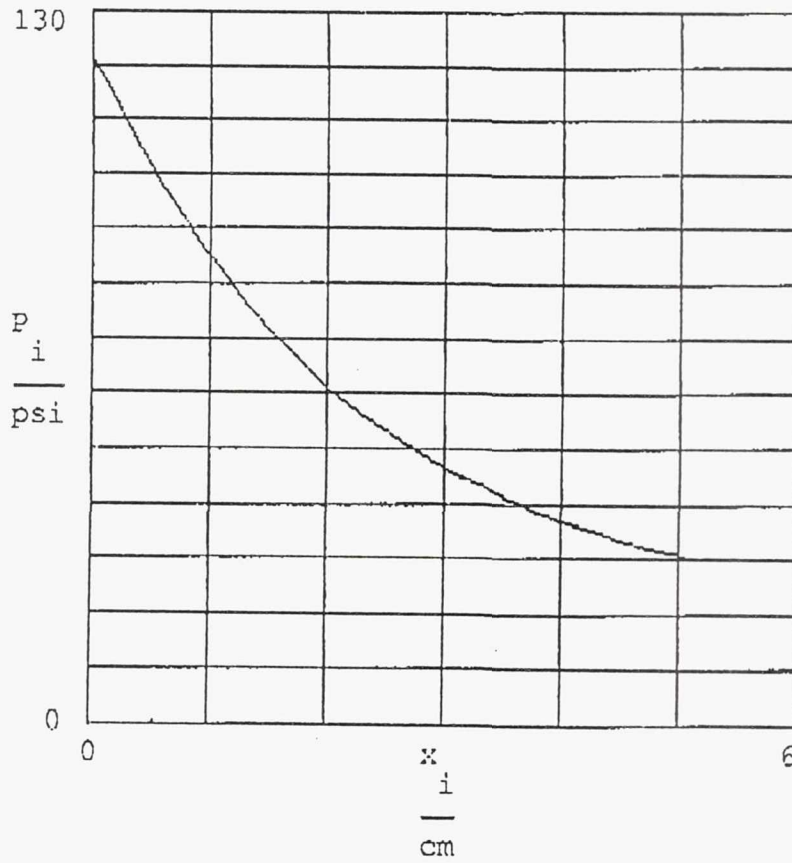
For a 2 inch diameter transducer operated at 10 kHz:

P_i , peak acoustic pressure on axis at distance x_i from face.

UNITS and CONVENTIONS USED IN CALCULATIONS

FUNDAMENTAL UNITS

$j := (-1)^{.5}$ used for complex number representation

$m \equiv 1L$ $\qquad\qquad$ $kg \equiv 1M$ $\qquad\qquad$ $sec \equiv 1T$ $\qquad$ $coul \equiv 1Q$

DERIVED UNITS

LENGTH

$in \equiv .0254 \cdot m$ $\qquad\qquad$ $cm \equiv .01 \cdot m$

$mil \equiv .0254 \cdot 10^{-3} \cdot m$ $\qquad$ $mm \equiv .001 \cdot m$

MASS

$g \equiv .001 \cdot kg$

VOLUME

$cc \equiv 10^{-6} \cdot m^{3}$

FORCE

$N \equiv kg \cdot \dfrac{m}{sec^{2}}$ $\qquad$ $gf \equiv .00988 \cdot N$ $\qquad$ $lbf \equiv 4.48 \cdot N$

PRESSURE

$psi \equiv 7.037 \cdot 10^{3} \cdot \dfrac{N}{m^{2}}$

POWER

$watt \equiv \dfrac{N \cdot m}{sec}$

ELECTRIC CURRENT

$amp \equiv \dfrac{coul}{sec}$

ELECTRIC POTENTIAL

$V \equiv \dfrac{watt}{amp}$

ADDENDUM

AN EXPLORATION OF THE CONCEPT OF USING A BROAD BAND PIEZO TRANSDUCER FOR NOISE CANCELLATION IN AIR

1.   Static Temperature

The operating temperature range shown in Table I is corrected as follows:

°R	°C	°F
410	-45.37	-49.67
610	65.74	150.33

This temperature range implies that the ceramic which we used in our numerical example, rather than being marginal regarding survival and/or use at the extremes of the specification, is excellent.

PZT-5A, the mateial used in the example, has a motion output which is relatively temperature independent. Its variation over this particular temperature range will be within a 20% band.

We re-iterate that there are piezoceramics which have piezoelectric coefficients which appear better on paper than PZT-5A, however, none which we have examined was capable of any more motion or work output *in the high electric field limit*.

2.   Practicality

No response. What is available envelope?

3.   State of the Art for Piezoelectric Actuation

Piezoelectric actuation is an extremely fragmented application area. State of the art is therefore meaningful only in the context of specific application areas such as acoustics, ink-jet printing, atomization, optical path modulation, machine tool vibration compensation, etc. State of the art actuators for each of these areas is completely different.

4.   Unpublished Actuator Approaches

We know of nothing which has not been reported on at least once in the open literature. There is no "magic" high motion ceramic which works over the desired temperature range.

5.   Vendors

No response.

6. Regarding Appendix 2

See attached.

7. Driving Equations for Bimorph

See attached formula for motion and first resonance of simple beam mounted rectangular bimorph. The surface of the bimorph deforms into a near-perfect circular curvature, approximating a section of a cylinder wall.

The displacement of the center of the bimorph will be constant from 0 HZ up to the beginning of the first resonance region, where it will rise sharply to approximately 10 times the value in the formula.

8. Alternative Configurations

In view of the true temperature operation requirment, our previous objections to the "tweeter" approach can be somewhat relaxed.

It is still true that the "achilles heel"or that approach is a glue bond with very small surface area which must endure high normal, angular, and shear stresses both in tension and compression. This is a high demand for any bond. At the moderate Rankine tempratures in the requirement this approach is in principle worth trying. Our other objections to the approach still hold however.

A lower acoustic output, but *much* more sturdy approach, would be a simple beam mounted bimorph. As a transducer it is light and "as mounted" would occupy a depth no more than 1/4-inch. (See item 7, Driving equations for bimorph).

9. Recommendations

We would summarize and recommend as follows:

1. Plain plane piezo slab.

   > Very poor for this application due to acoustic impedance mismatch between ceramic and air. Transducer is too heavy for what it does. No further action.

2. Piezo slab (or tube) with a large area piston attached.

Possible good performer, but still over 2-inches deep. Still has a pretty "bad" acoustic impedance mismatch, but is superior to plane slab. No further action.

3.   Tweeter.

Good performer for weight, materials related engineering problems to solve. Recommended action:

a. Examine existing designs for any crucial material properties. Determine if waterproof materials can be subsituted for paper cone.

b.   Determine the theoretical diameter of required piezo disk for frequency range in specification. Is it too large for anyone to manufacture?

c. Determine whether some other method can be used for critical joint OTHER than epoxy bond.

4.   Simple beam bimorph.

Will not have as high an ouput as tweeter. Recommended action:

a. Calculate acoustic output relative to plane slab based on circular curvature deformation.

b. Estimate surface area required a resultant amplitude. Does it fit?

c.   Determine weather proofing schemes.

Comments Regarding Appendix 2

The purpose of Appendix 2 was to support our assertion that the piezo slab would not be impeded by the *dynamic* forces arising from creating the desired sound waves.

The stated formula regards an upper bound pressure occurring near the face of the piston "on axis". In general, the pressure drops off at locations near the perimeter of the disk, but not at all frequency regimes for a given disk. We implied that one could take the π in the formula, multiply it by the surface area of the piston and have a valid upper bound, however, this is not the case.

On second thought, an exact expression for the *force* exerted on the piston (the true quantity of interest here) as a function of frequency is more readily available than an upper bound.

We refer you to the textbook Acoustics by L.L. Beranek, Chapter 5, p. 118 for a treatment of a planar circular piston in an infinite baffle.

The expressions there pertain to the complex mechanical impedance Z for the entire rigid piston as seen by the driving force.

The force magnitude F on the piston may be obtained by the following expression:

$$F = V*Z$$

where V is a real number velocity value (obtained from the sinusoidal motion of the piston) and Z is a complex impedance value.

Attached is a copy of the relevant section.

Observe that the piezo slab is quite stiff by comparison to both its static and dynamic load.

INPUT VOLTAGE "V"

SINGLE LAYER t

L

ΔX, DISPLACEMENT

P
P
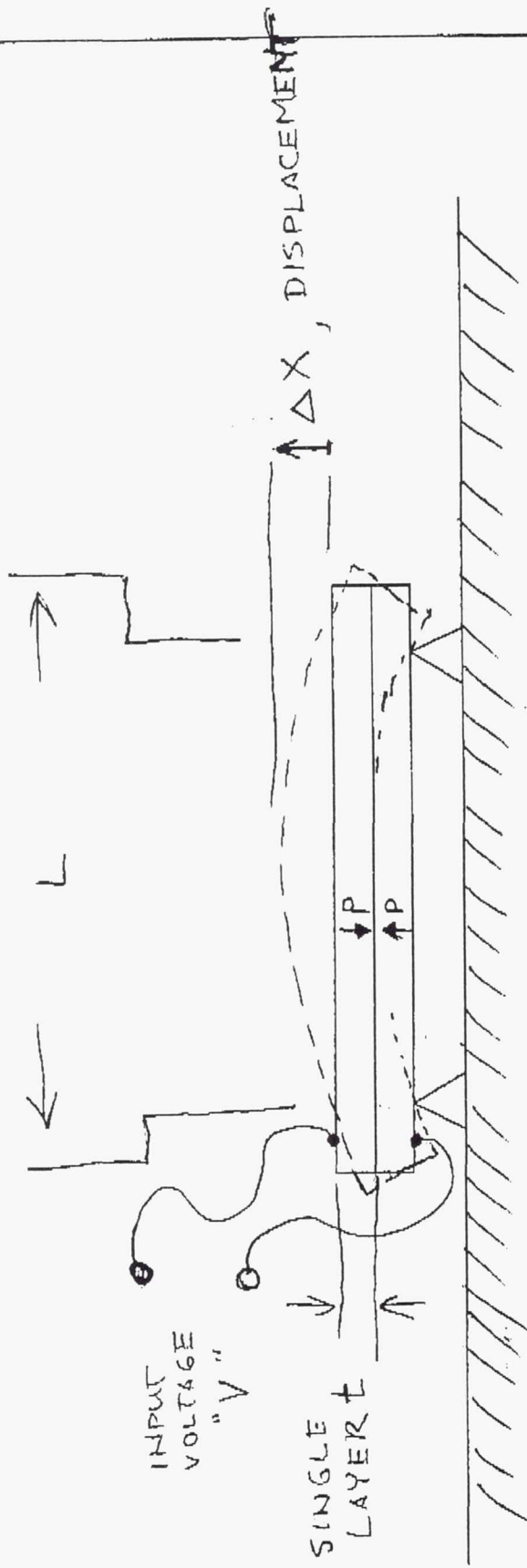
RECTANGULAR BIMORPH
SIMPLE BEAM MOUNT
QUASI STATIC MOTION

$$\Delta X = \frac{3}{16} V d_{31} \frac{L^2}{t^2}$$
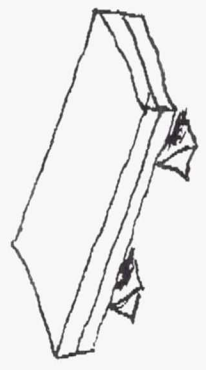
ΔX = DISPLACEMENT AT CENTER.

V = APPLIED VOLTAGE, (PEAK)

d_{31} = PIEZO COEFFICIENT

L = DISTANCE BETWEEN SIMPLE BEAM MOUNTS

t = SINGLE PIEZO LAYER LAYER THICKNESS

P↑ DENOTES POLARIZATION DIRECTION
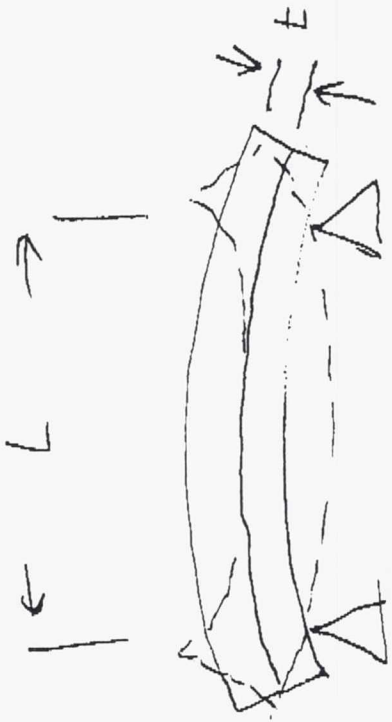
RECTANGULAR BIMORPH

SIMPLE BEAM MOUNT

RESONANT FREQUENCY ESTIMATE

FIRST (LOWEST) RESONANCE $\cong$ $.95 \left(\dfrac{\rho}{Y}\right)^{-\frac{1}{2}} \dfrac{t}{L^2}$

$= .95 \sqrt{\dfrac{Y}{\rho}} \dfrac{t}{L^2}$

$Y =$ YOUNG'S MODULUS
$\rho =$ DENSITY
$t =$ SINGLE LAYER THICKNESS

References

1 Kousen, K. A. and J. M. Verdon, "Active Control of Wake/Blade-Row Interaction Noise," NASA CR-4556, December 1993.

2 Kousen, K. A. and J. M. Verdon, "Active Control of Wake/Blade-Row Interaction Noise," AIAA Paper No. 93-4351, October 1993.

3 Dosch, J. J., D. J. Inman, and E. Garcia, "Measurement of Strain and Stress in a Piezoelectric Actuator for Collocated Control," ADPA/AIAA/ASME/SPIE Conf. on Active Materials and Adaptive Structures - Session 11, pp. 195-198, 1992.

4 Uchino, K., "Electrostrictive Actuators: Materials and Applications," **Ceramic Bulletin**, Vol. 65, No. 4, pp. 647-652, 1986.

5 Aldrich, R. E., J. H. Everson, and N. P. Albertinetti, "High Bandwidth, Fine Resolution Deformable Mirror Design," AFWL-TR-70-5, March 1980.

6 Ikeda, O. and T. Sato, "Comparison of Deformability Between Multilayered Deformable Mirrors with a Monomorph or a Bimorph Actuator," **Applied Optics**, Vol. 25, No. 24, pp. 4591-4597, December 15, 1986.

7 Swift, C. D., J. W. Bergum, E. S. Bliss, F. A. House, M. A. Libkind, J. T. Salmon, and C. L. Weinzapel, "Zonal Deformable Mirror for Laser Wavefront," SPIE 1991 International Symposium on Optical Applied Science and Engineering, San Diego, CA., July 21-26, 1991.

8 Ono, T., "Optical Beam Deflector Using a Piezoelectric Bimorph Actuator," **Sensors and Actuators**, A21-A23, pp. 726-728, 1990.

9 Santa Maria, O. L., E. M. Thurlow, and M. G. Jones, "Exploratory Study of the Acoustic Performance of Piezoelectric Actuators," ADPA/AIAA/ASME/SPIE Conf. on Active Materials and Adaptive Structures, pp. 529-534, 1992.

10 Takahashi, S., "Development of New Piezoelectric Ceramic Actuators," **New Materials & New Processes**, Vol. 3, pp. 63-68, 1985.

11 Lubitz, K. and H. Hellebrand, "Properties of PZT Multilayer Actuators," Proceedings of the 7th International Symposium on the Applications of Ferroelectrics, pp. 509-512, June 6-8, 1990.

12 Murakawa, K., K. Terao, T. Izaki, Y. Ariake, and M. Masuda, "Piezoelectric Actuators," The Sumitomo Search, No. 47, pp. 141-144, October 1991.

13 Chang, S. H. and H. Wang, "A High Speed Impact Actuator Using Multilayer Piezoelectric Ceramics," **Sensors and Actuators A**, Vol. 24, pp. 239-244, 1990.

14 Royster, L. H., "Flextensional Underwater Acoustics Transducer," **J. Acoust. Soc. Am.**, Vol. 45, No. 3, pp. 671-682, March 1969.

15 Brigham, G., and B. Glass, "Present Status in Flextensional Transducer Technology," **J. Acoust. Soc. Am.**, Vol. 68, No. 4, pp. 1046-1052, October 1980.

16 Rolt, K. D., "History of the Flextensional Electroacoustic Transducer,", **J. Acoust. Soc. Am.**, Vol. 87, No. 3, pp. 1340-1349, March 1990.

17 Pagliarini, J. A. and R. P. White, "A Small, Wide-Band, Low-Frequency, High-Power Sound Source Utilizing the Flextensional Transducer Concept,", Oceans 78, The Ocean Challenge, Washington, D. C., pp. 333-338, Sept. 1978.

18 Xu, Q. C., K. Onitsuka, S. Yoshikawa, Q. C. Xu, R. E. Newnham and K. Uchino, "Metal-Ceramic Composite Actuators," ADPA/AIAA/ASME/SPIE Conf. on Active Materials and Adaptive Structures, pp. 143-148, 1992.

19 "Piezo-Alarms and Ultrasonic Microphones," Catalog No. P-01-C, Murata Erie North America, 1992.

20 "Piezoelectric Audio Tone Transducers," NTK Technical Ceramics Division, NGK Spark Plug Co. Ltd.

21 "Guide to Modern Piezoelectric Ceramics," Electro Ceramics Division, Morgan Matroc Inc, Bedford, Ohio, July 1991.

22 Tamura, M. T. Yamaguchi, T. Oyaba, and T. Yoshimi, "Electroacoustic Transducers with Piezoelectric High Polymer Films," **Audio Eng. Soc. J.**, Vol. 23, pp. 21-26, 1975.

23 Tamura, M., K. Ogasawara, and T. Yoshimi, "Piezoelectricity in Uniaxially Stretched Poly (Vinylidene Fluoride) Films and Its Applications," **Ferroelectrics**, Vol. 10, pp. 125-127, 1976.

24 Klapholz, J., "High Polymer Piezo Film in Electroacoustical Transducer Applications," 79th Convention of the Audio Engineering Society, New York, N.Y., October 12-16, 1985.

25 Yamauro, I. and M. Tamura, "High Molecular Weight, Thin Film Piezoelectric Transducers," U.S. Patent 3,832,580, August 27, 1974.

26 Tibbetts, G. C., "Transducer Having Piezoelectric Film Arranged with Alternating Curvatures," U.S. Patent 4,056,742, November 1, 1977.

27 Taylor, A. L., "Method of Making Piezoelectric Polymeric Acoustic Transducer," U.S. Patent 4,322,877, April 6, 1982.

28 Micheron, F., and C. Lemonon, "Moulded Piezoelectric Transducers Using Polar Polymers," **J. Acoust. Soc. Am.**, Vol. 64, Series 6, pp. 1720-1721, December 1978.

29 Radice, P. F., "Piezoelectric Polymeric Film Balloon Speaker," U. S. Patent 4,638,207, January 20, 1987.

30 Toda, M., "Theory of Air Flow Generation by a Resonant Type PVF_2 Bimorph Cantilever Vibrator," **Ferroelectrics**, Vol. 22, pp. 911-918, 1979.

31 Toda, M., "High Field Dielectric Loss of PVF_2 and the Electromechanical Conversion Efficiency of a PVF_2 Fan," **Ferroelectrics**, Vol. 22, pp. 919-923, 1979.

32 Toda, M., S. Osaka, and E. O. Johnson, "A New Electromotional Device," **RCA Engineer**, Volume 25-1, pp. 24-27, June/July 1979.

33 Nevil, G. E., Jr. and A. F. Davis, "The Potential of Corrugated PVDF Bimorphs for Actuation and Sensing," MS84-491, First World Conference on Robotics Research, Bethlehem, PA, August 14-16, 1984.

34 "New Piezoelectrics Provide Dramatic Performance Gains," **R&D Magazine**, pp. 17-18, October 1993.

35 Haertling, G. H., "Rainbow Ceramics - A New Type of Ultra-High Displacement Actuator," **American Ceramic Society Bulletin**, Vol. 73, Num. 1, pp. 93-96, January 1994.

36 Ratnam, D., "The Incredible Shrinking Speaker," **Machine Design**, pp. 63-66, June 20, 1991.

37 Buck, M., F. T. van Namen, and R. Weisman, "Electrodynamic Linear Motors for Active Vibration and Noise Control," 2nd Conf. on Recent Advances in Active Control of Sound and Vibration, Blacksburg, VA, pp. S53-S65, April 28-30, 1993.

38 Bartosh, B., "New Magnetic Circuit Design Yields High Force, Long Stroke Linear Actuators," **Power Conversion and Intelligent Motion**, October 1991.

39 Sakamoto, N., T. Gotoh, N. Atoji, and T. Aoi, "Frequency Response Considerations for an Electrostatic Horn Tweeter Using Electret Elements," **Audio Eng. Soc. J.**, Vol. 24, pp. 368-372, 1976.

40 Kirjavainen, K., "Electromechanical Film and Procedure for Manufacturing Same," U.S. Patent 4,654,546, March 31, 1987.

41 Backman, J., "Audio Applications of Electrothermomechanical Film (ETMF)," **J. Audio Eng. Soc.**, Vol. 38, No. 5, May 1990.

42 Backman, J. and M. Karjalainen, "Audio and Ultrasonic Transducers Based on Electrothermomechanical Film (ETMF)," 1990 International Conference on Acoustics, Speech and Signal Processing, Albuquerque, N.M., Vol. 2, pp. 1173-1176, April 1990.

43 Yaeger, J. R., "A Practical Shape-Memory Electromechanical Actuator," **Mech. Eng**, Vol. 106, pp. 51-55, July 1984.

44 Baz, A., K. Iman and J. McCoy, "The dynamic and thermal characteristics of shape memory actuators," **SPIE**, Vol. 1170, Fiber Optic Smart Structures and Skins II, pp. 271-293, 1989.

45 Neukomm, P. A., H. P. Bornhauser, T. Hochull, R. Paravicini, and G. Schwarz, "Characteristics of Thin-wire Shape Memory Actuators," **Sensors and Actuators**, Vol. A21-A23, pp 247-252, 1990.

46 Oh, K. -Y., A. Furuta, and K. Uchino, "Development and Application of Shape Memory Ceramic Actuators," 1990 IEEE 7th Int. Sym. on Applications of Ferroelectrics, pp. 525-527, June 1990.

47 Furuta, A., K. -Y. Oh, and K. Uchino, "Mechanical Clamper Using Shape Memory Ceramics," 1990 IEEE 7th Int. Sym. on Applications of Ferroelectrics, pp. 528-529, June 1990.

48 Scott, W. B., "Micro-Machines Hold Promise for Aerospace," **Avia. Week & Space Tech.**, pp. 36-39, March 1, 1993.

49 Xu, Q. C., A. Dogan, J. Tressler, S. Yoshikawa and R. E. Newnham, "Ceramic-Metal Composite Actuator," 1991 Ultrasonics Symposium, pp. 923-928, 1991.

50 Robbins, W. P., D. L. Polla, T. Tamagawa, D. E. Glumac and W. Tjhen, " Design of linear-motion microactuators using piezoelectric thin films," **J. Micromech. Microeng.**, Vol. 1, pp. 247-252, 1991.

51 Smits, J. G. and W. Choi, "Very Large Deflection with Quadratic Voltage Dependence of ZnO on Si_3N_4 Bimorph," **IEEE Trans. On Ultra., Ferro. And Freq. Control**, Vol. 39, No. 2, pp. 302-304, March 1992.

52 Ikuta, K., S. Aritomi, and T. Kabashima, "Tiny Silent Linear Cybernetic Actuator Driven by Piezoelectric Device with Electromagnetic Clamp," Presented at Micro Electro Mechanical Systems '92, Travemunde (Germany), pp. 232-237, February 4-7, 1992.

53 Brei, D. E. and J. Blechschmidt, "Design and Static Modeling of a Semicircular Polymeric Piezoelectric Microactuator," **J. of Microelectromechanical Systems**, Vol. 1, No. 3, pp. 106-115, September 1992.

54 Kukuda, T. M. Fujiyoshi, K. Kosuge, and F. Arai, "Electrostatic Micro/Nano Manipulator with 6 D.O.F.," **Micromechanical Sensors, Actuators, and Systems**, Vol. 32, pp. 197-202, 1991.

55 Sato, K. and M. Shikida, " Electrostatic Film Actuator with a Large Vertical Displacement," Presented at Micro Electro Mechanical Systems '92, Travemunde (Germany), pp. 1-5, February 4-7, 1992.

56 Branebjerg J. and P. Gravesen, "A New Electrostatic Actuator Providing Improved Stroke Length and Force," Presented at Micro Electro Mechanical Systems '92, Travemunde (Germany), pp. 6-11, February 4-7, 1992.

57 Niino, T., S. Egawa, N. Nishiguchi, and T. Higuchi, "Development of An Electrostatic Actuator Exceeding 10N Propulsive Force," Presented at Micro Electro Mechanical Systems '92, Travemunde (Germany), pp. 122-127, February 4-7, 1992.

58 Gabriel, K. J., O. Tabata, K. Shimoka, S. Sugiyama, and H. Fujita, "Surface-Normal Electrostatic/Pneumatic Actuator," Presented at Micro Electro Mechanical Systems '92, Travemunde (Germany), pp. 128-132, February 4-7, 1992.

59 Doring, C. T. Grauer, J. Marek, M. S. Mettner, H.-P. Trah, and M. Willmann, "Micromachined Thermoelectrically Driven Cantilever Structures for Fluid Jet Deflection," Presented at Micro Electro Mechanical Systems '92, Travemunde (Germany), pp. 12-18, February 4-7, 1992.

60 Uchino, K. " Photostrictive Actuator," 1990 Ultrasonics Symposium, pp. 721-723, 1990.

61 Goodfriend, M., "Material Breakthrough Spurs Actuator Design", **Machine Design**, pp. 147-150, March 21, 1991.

62 Akuta, T., "An Application of Giant Magnetostrictive Material to High Power Actuators", Paper No. 18A0107, Proceedings of the 10th International Workshop on Rare-Earth Magnets and Their Applications, Kyoto, Japan, May 16-19, 1989.

63 Glomb, W. L., "Advanced Magnetostrictive Actuator Development", Air Force Weapons Laboratory Report AFWL-TR-84-145, January 1986.

64 Aksinin, V. I., V. V. Appollonov, S. A. Chetkin, and S. V. Muravev, "New High-Precision Displacement Devices Based on Magnetostriction for Adaptive Optical Elements," Actuator 90, Proceedings of the 2nd International Technology-Transfer Congress, Bremen, Germany, p. 236, June 21-22, 1990.

65 Flatau, A. B., D. L. Hall, and J. M. Schlesselman, "Magnetostrictive Active Vibration Control Systems," AIAA Paper 92-0490, January 1992.

66 Goodfriend, M. J., and K. M. Shoop, "Adaptive Characteristics of the Magnetostrictive Alloy, Terfenol-D, for Active Vibration Control," **J. of Intell. Mater. Syst. and Struct.**, Vol. 3, pp. 245-254, April 1992.

67 Bushko, D. A. and J. H. Goldie, "High Performance Magnetostrictive Actuators," **IEEE AES Systems Magazine**, pp. 21-25, November 1991.

68 Rossi, D. De, Suzuki, M., Osada, Y. and Morasso, P., "Pseudomuscular Gel Actuators for Advanced Robotics," **J. of Intell. Mater. Syst. and Struct.**, Vol. 3, pp. 75-95, January 1992.

69 Kynar Piezo Film Technical Manual, Pennwalt Corporation, p. 19, 1987.

70 Chen, X., B. Cousins, M. McEllistrem, and R. J. Hamers, "High-performance, Low-Noise Digital Controller for Inchworm Piezoelectric Translators," **Rev. Sci. Instrum.**, Vol. 63, Num. 10, pp. 4308-4313, October 1992.

71 Galvagni, J. and D. DuPre, "Electrostrictive Actuators, Precision Electromechanical Components," AVX Technical Information, Report AVX-DEA-8902.5-K, 1989.

72 The Piezo Book, Burleigh Instruments, Inc., June 1992.

73 Active Noise & Vibration Control, EDO Corp., Acoustics Division.

74 Piezo-Alarms and Ultrasonic Microphones, muRata Erie Catalog No. P-01-C, 1992.

75 Taylor, A. L., "Method of Making Piezoelectric Polymeric Acoustic Transducer," U. S. Patent 4,322,877, April 1982.

76 Tibbetts, G. C., "Transducer Having Piezoelectric Film Arranged with Alternating Curvatures," U. S. Patent 4,056,742, November 1977.

77 Yamamuro, I. and M. Tamura, "High Molecular Weight, Thin Film Piezoelectric Transducers," U. S. Patent 3,832,580, August 1974.
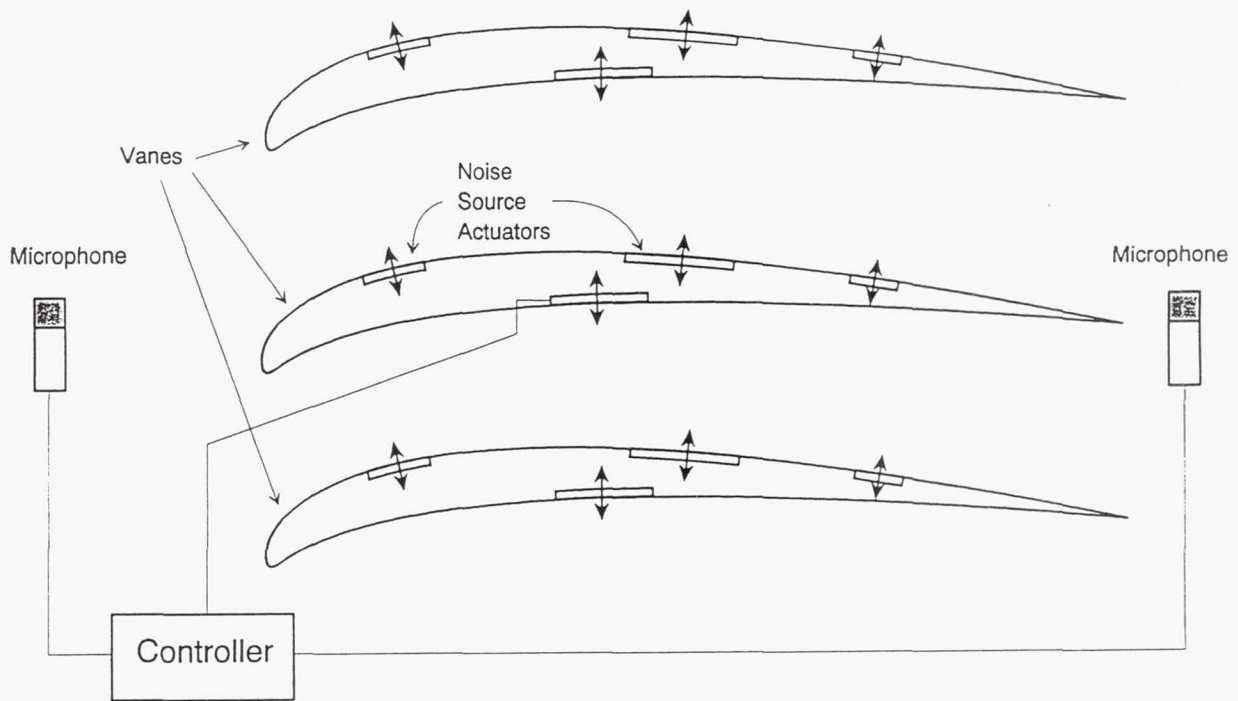
Figure 1 - Active Controlled Vane
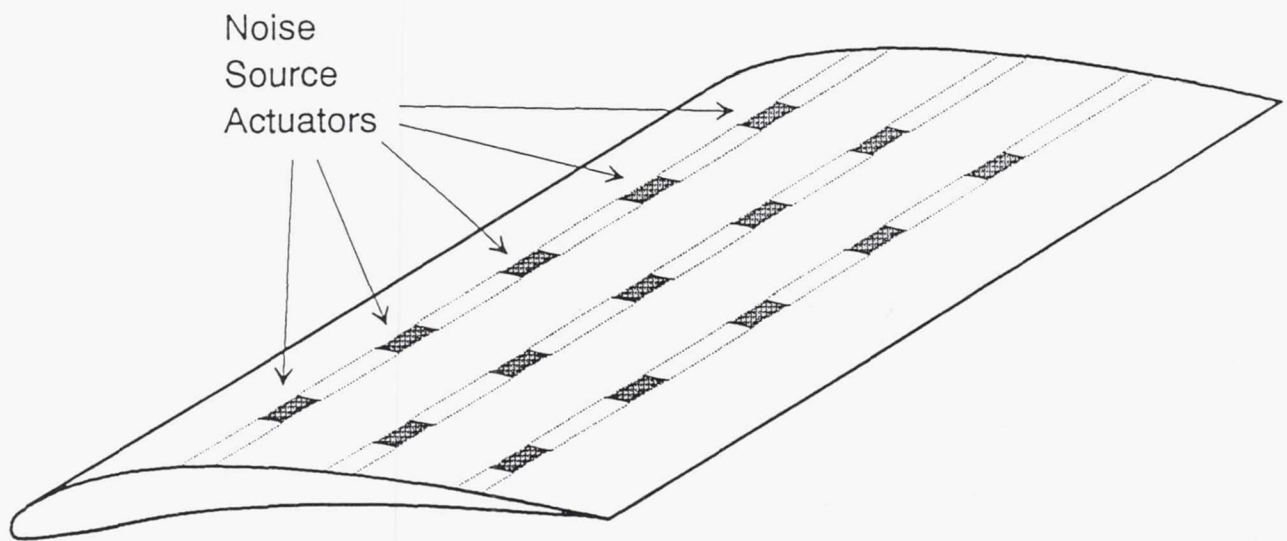
Figure 2 - Actuated Swept Vane
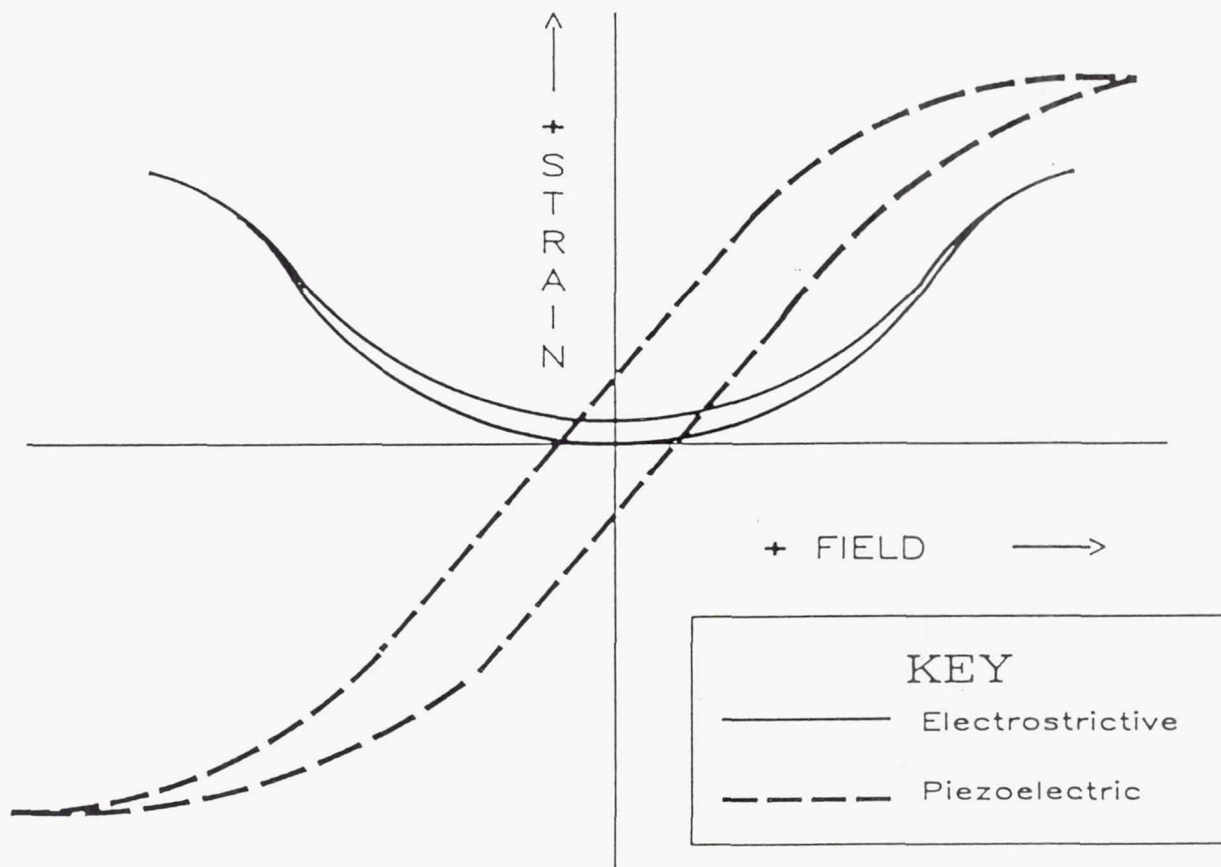
Figure 3 - Strain Behavior of Piezoelectric and Electrostrictive Materials[71]

Resultant Displacement

+33 mode:
Electric field E pointing in the same
direction as p, resultant motion (y)
observed along the 3 axis also.

-33 mode:
Electric field opposing polarization
field, resultant motion (y) observed
along the 3 axis also
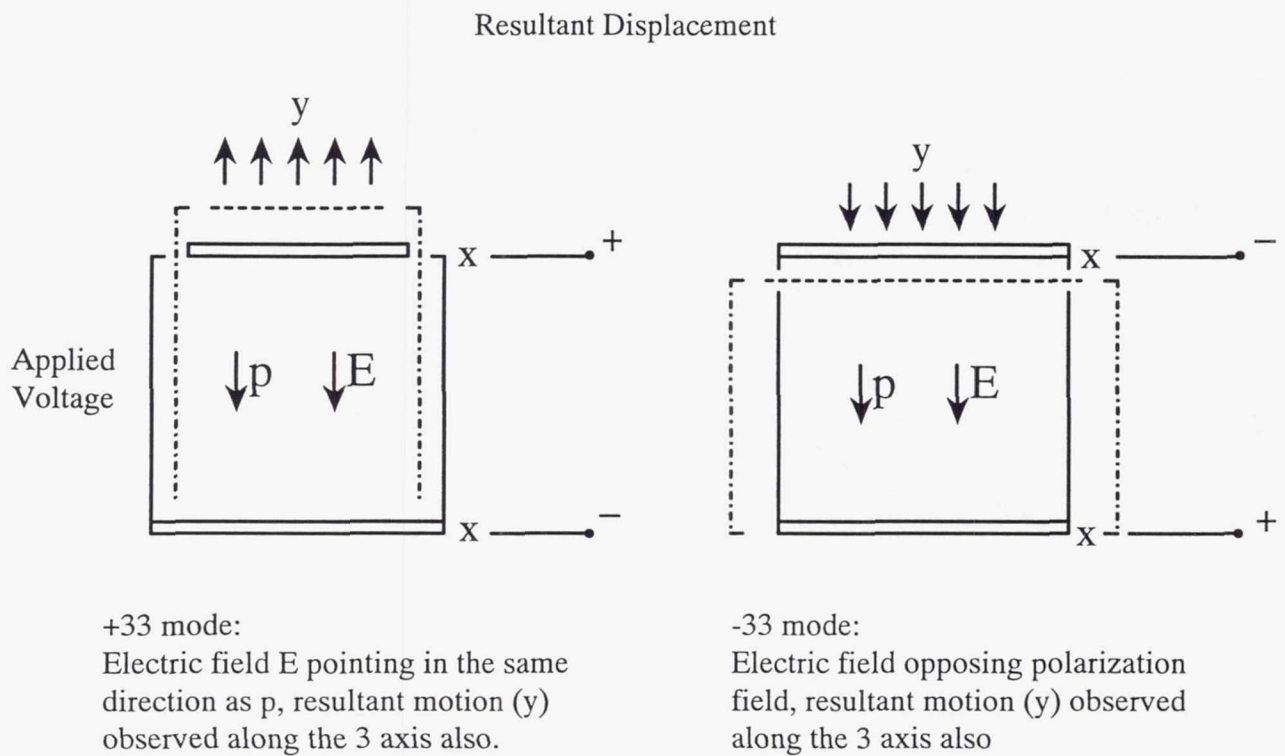
Figure 4 - Piezoelectric Deformation Due to Potential Applied Along Poling Axis

70
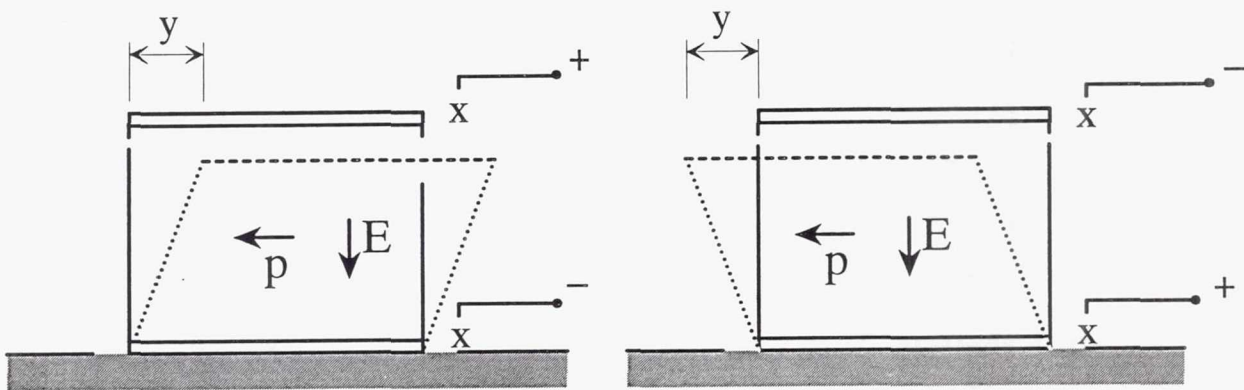
Electric field applied perpendicular to polarization vector, a shear deformation about the axis perpendicular to both p and E. The "d15" coefficient relates the applied field to linear displacement along the polarization axis.

Figure 5 - Piezoelectric Deformation Due to Potential Applied Perpendicular to Poling Axis
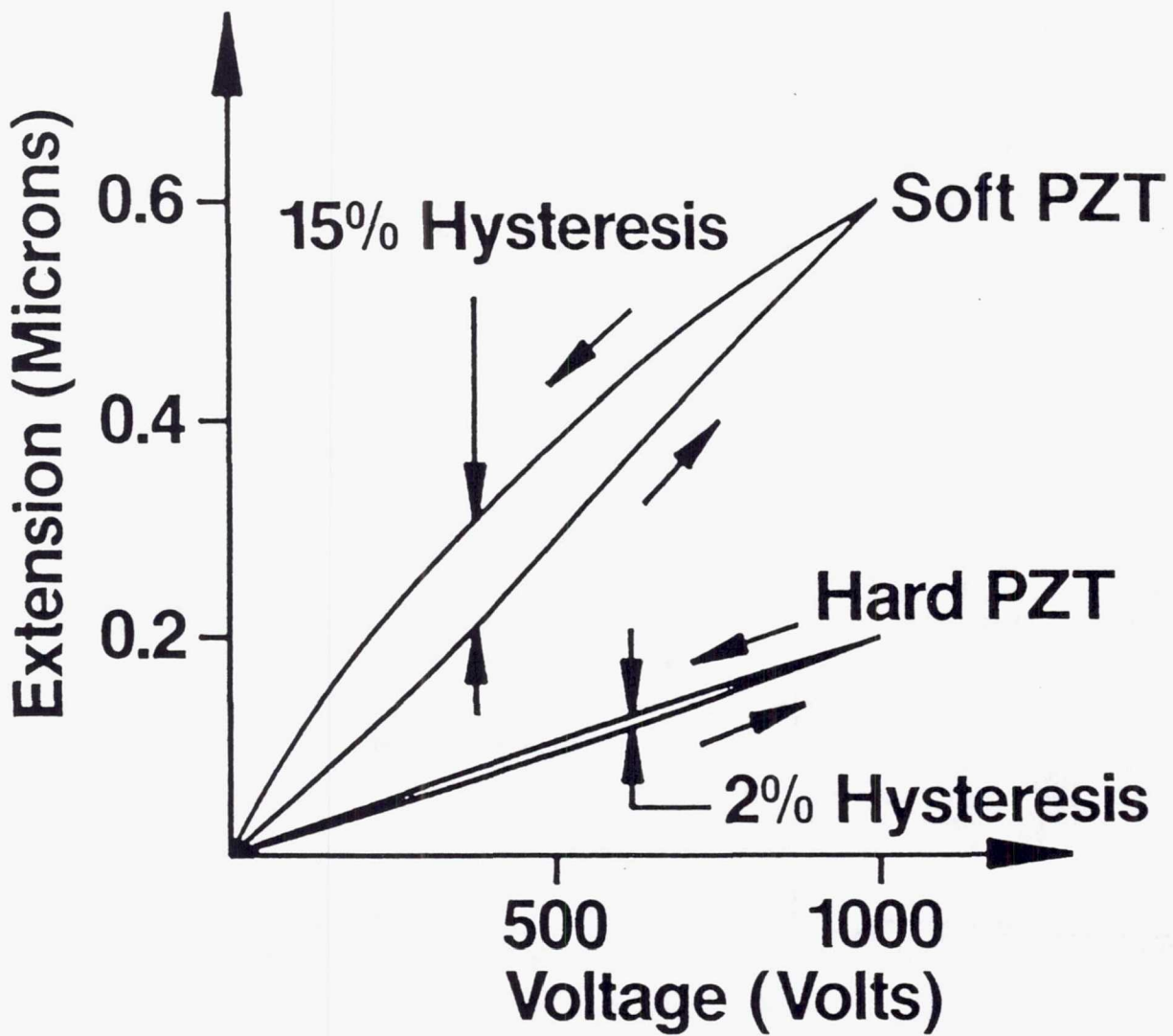
Figure 6 - PZT Hysteresis Curves[72]
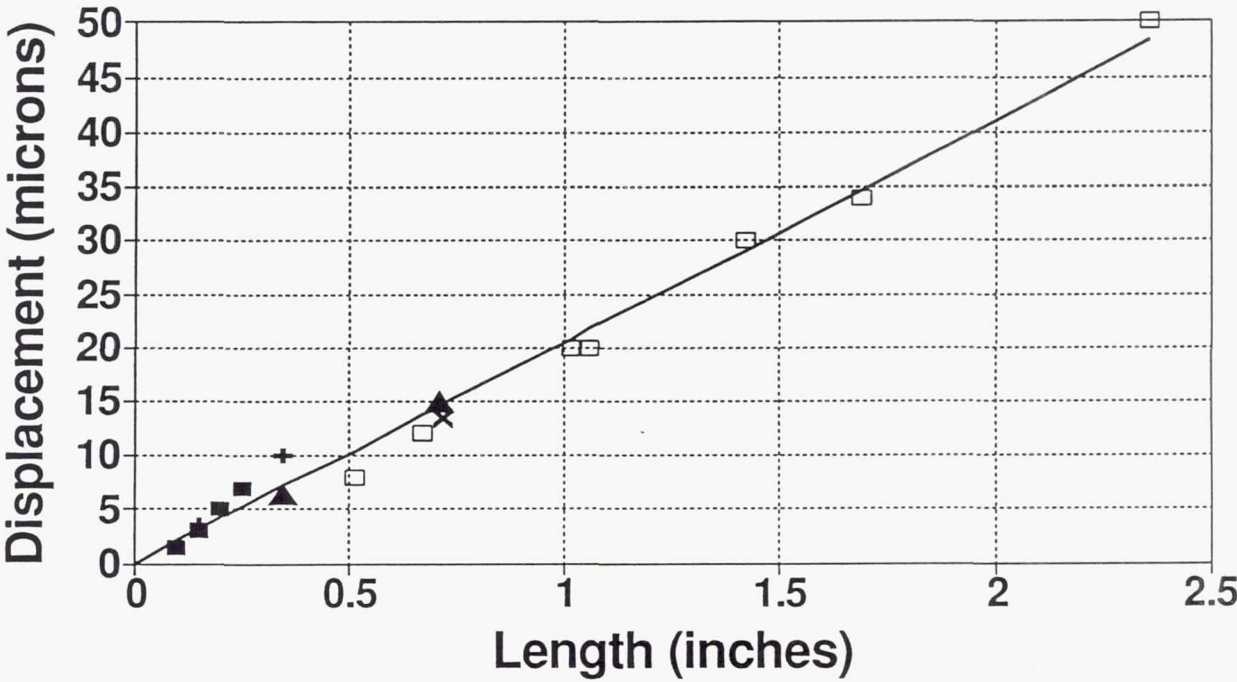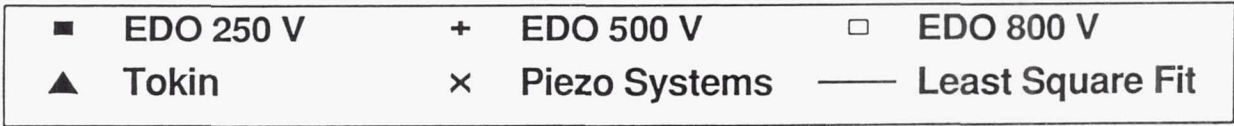
Figure 7 - Stacked Piezo Ceramic Actuator Displacement Performance
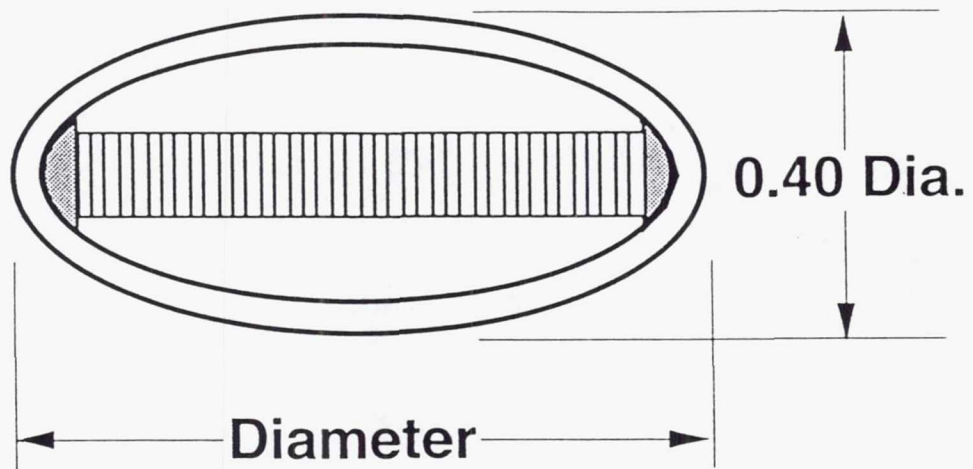
Figure 8 - Flextensional Actuator[73]
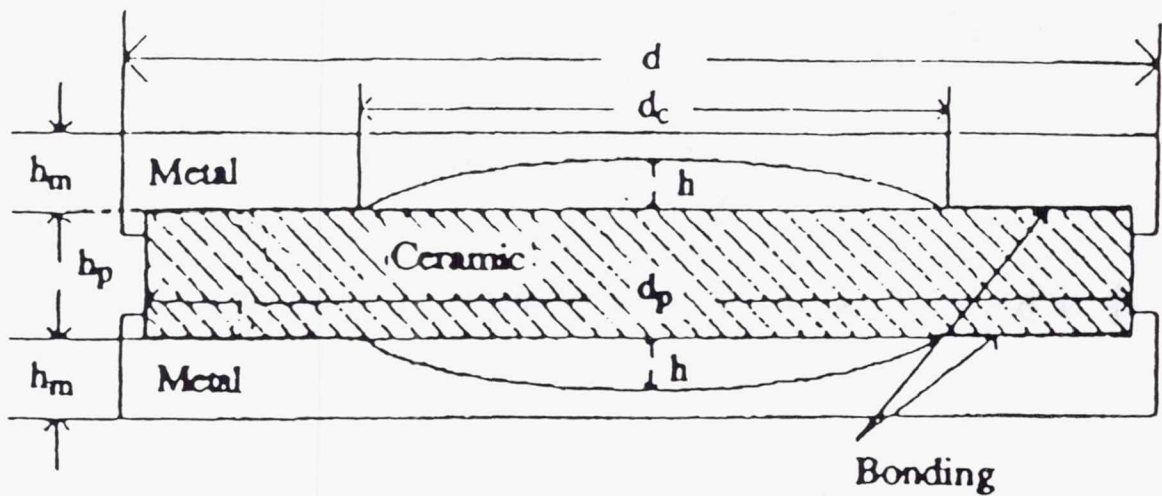
Figure 9 - "Moonie" Actuator [49]
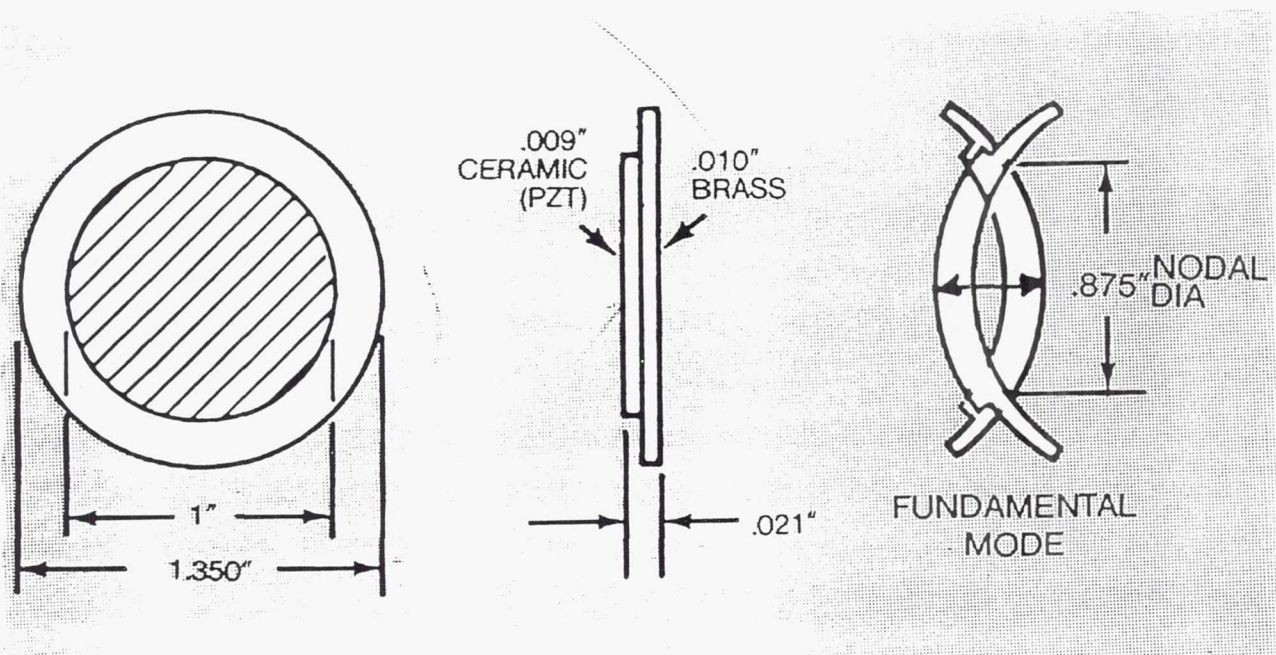
Figure 10 - Operating Principle of a Unimorph Actuator[21]

fo

(a) Node Support

$\approx fo/_2$
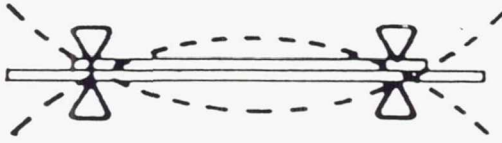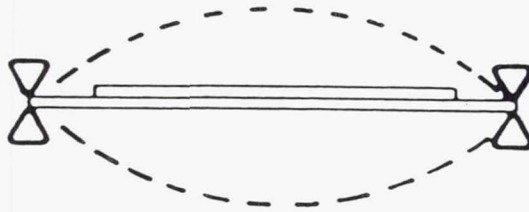
(b) Edge Support

$\approx fo/_2$
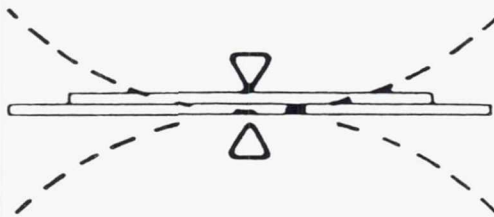
(c) Central Support

Figure 11 - Unimorph Mounting Schemes[74]

DRIVING FORCE OR
GENERATED MOTION
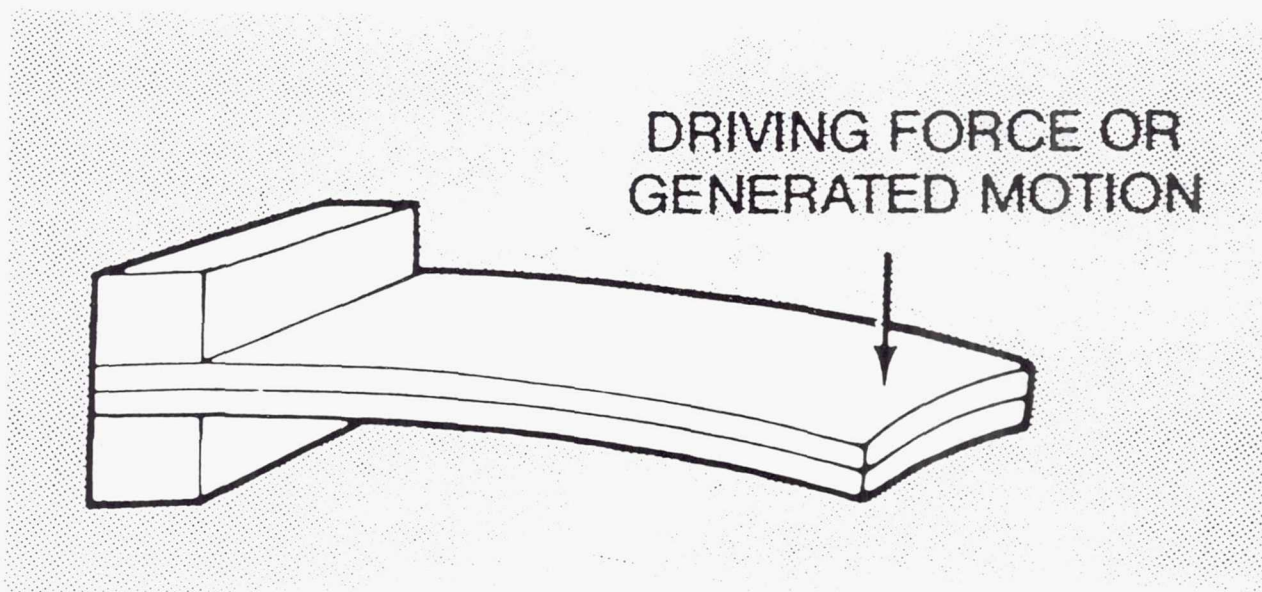
Figure 12 - Bimorph Actuator[21]

PIEZOFILM

FOAM

(a)
PVDF in Foam
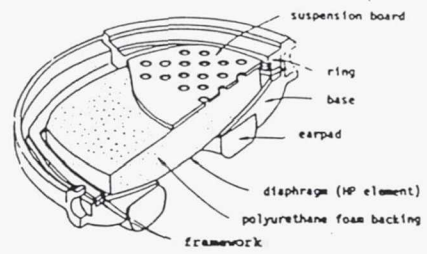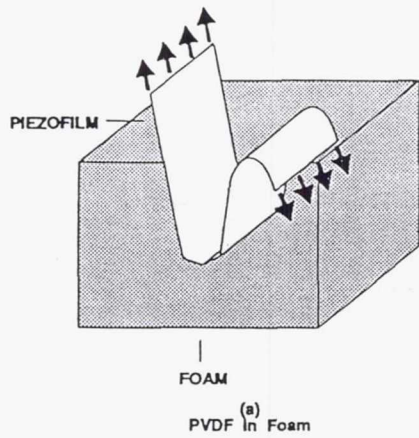
Fig. 9. Cross-sectional view of HP headphone.

suspension board
ring
base
earpad
diaphragm (HP element)
polyurethane foam backing
framework
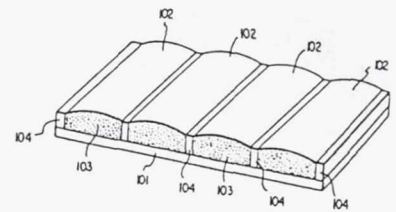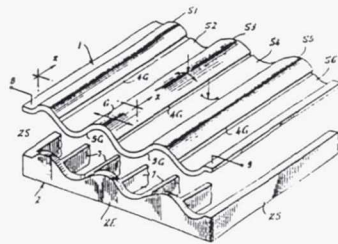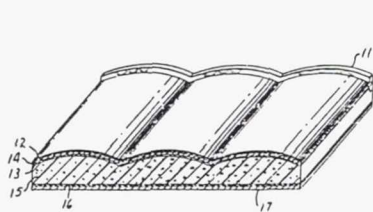
Figure 13 - High Polymer Film Actuators[9,22,75,76,77]
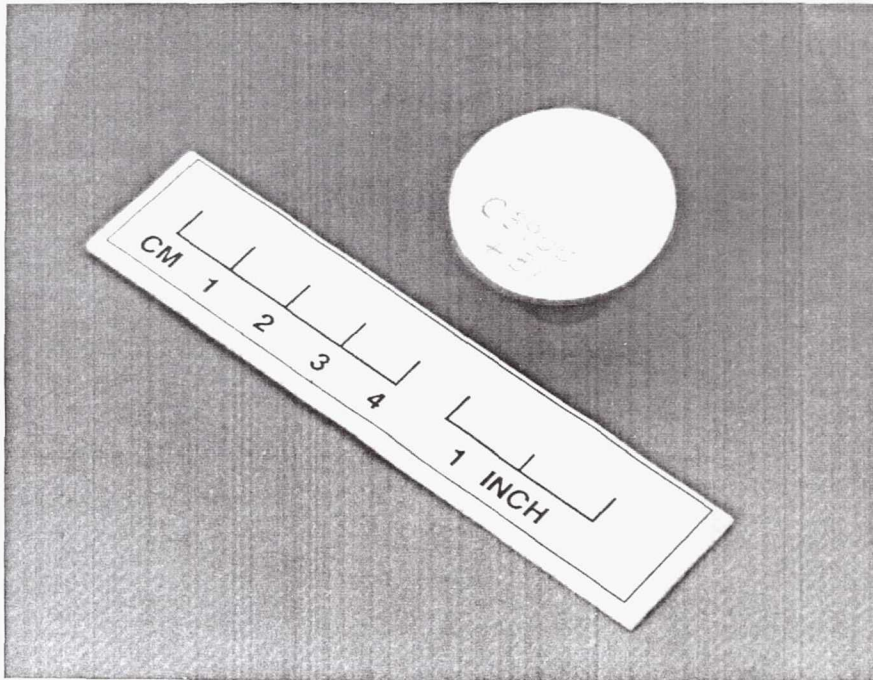
Figure 14 - Photograph of 1.25 inch Diameter Rainbow Wafer
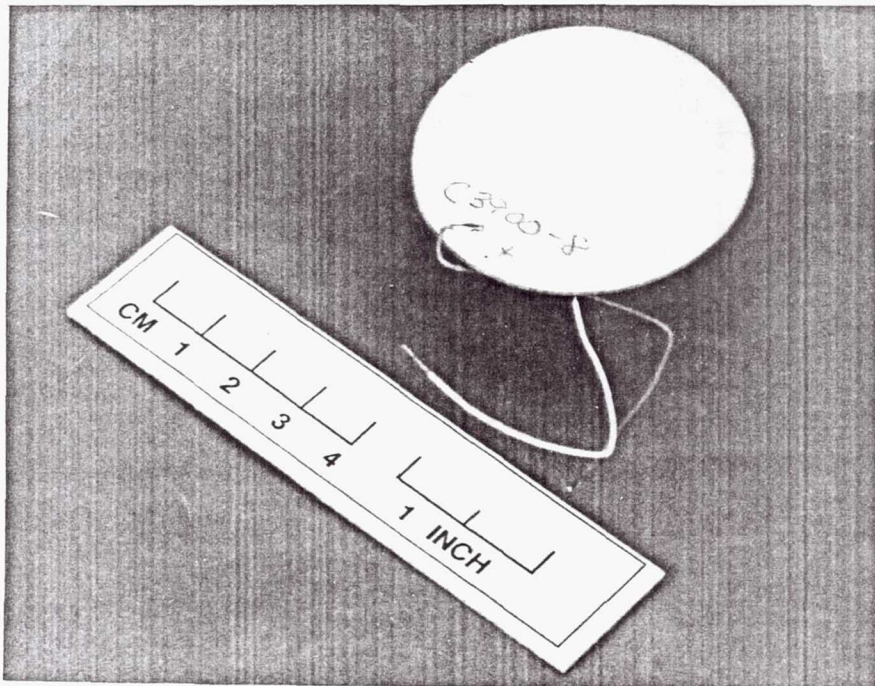
Figure 15 - Photograph of 2 inch Diameter Rainbow Wafer
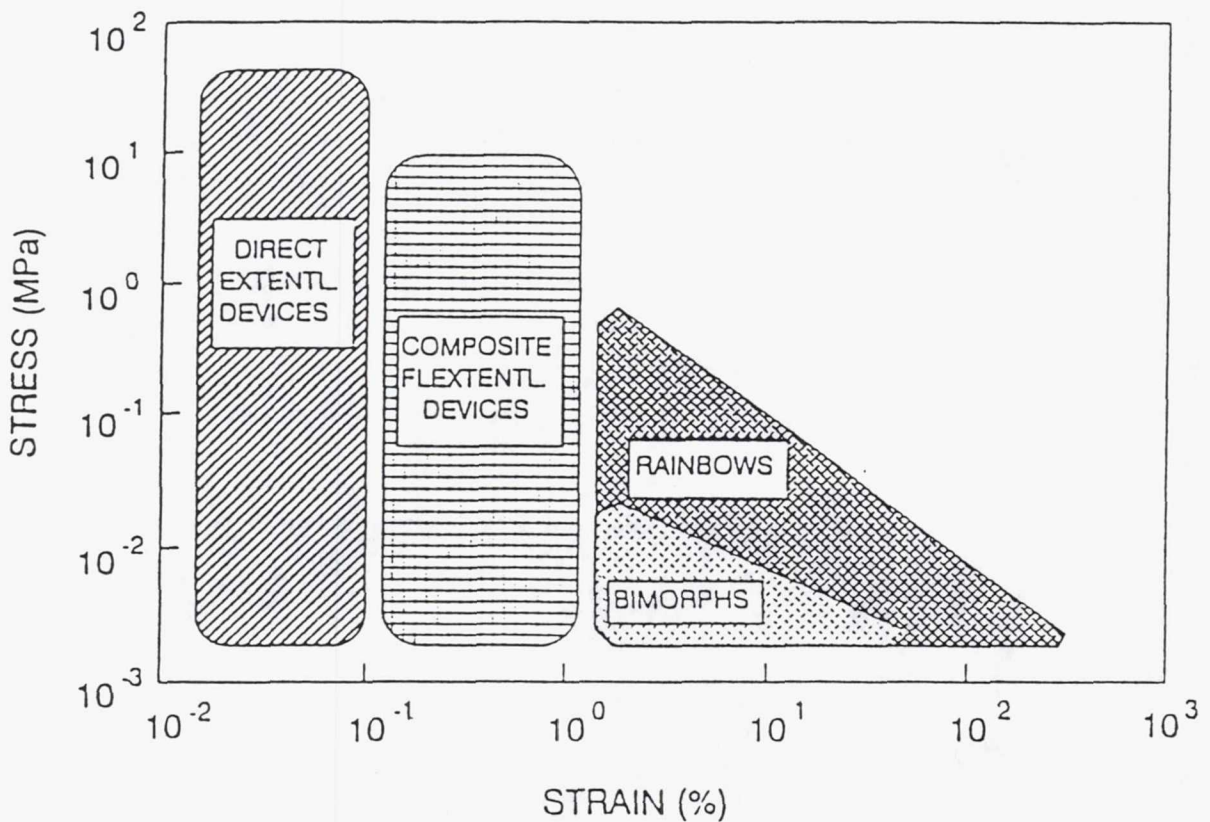
Figure 16 - Comparison of Ceramic Actuator Technology[35]
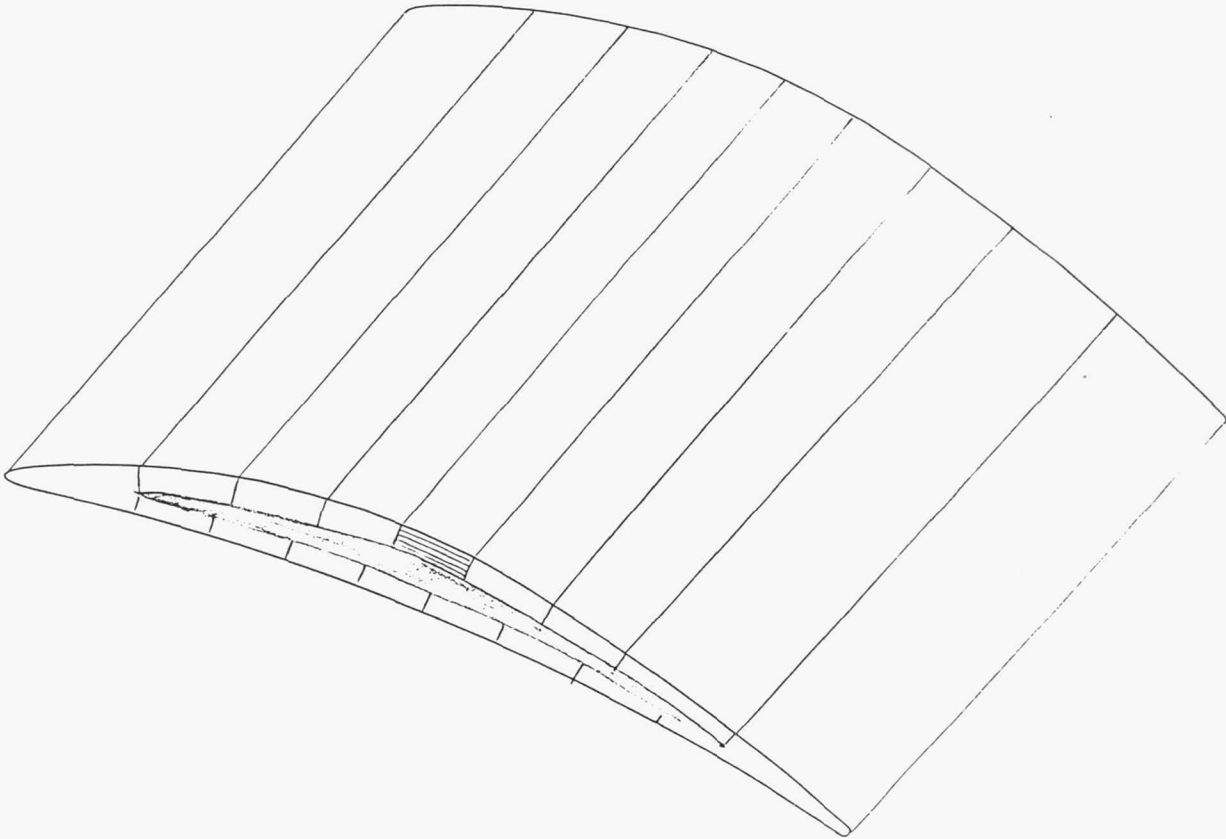
Figure 17 - Extensional Airfoil Concept
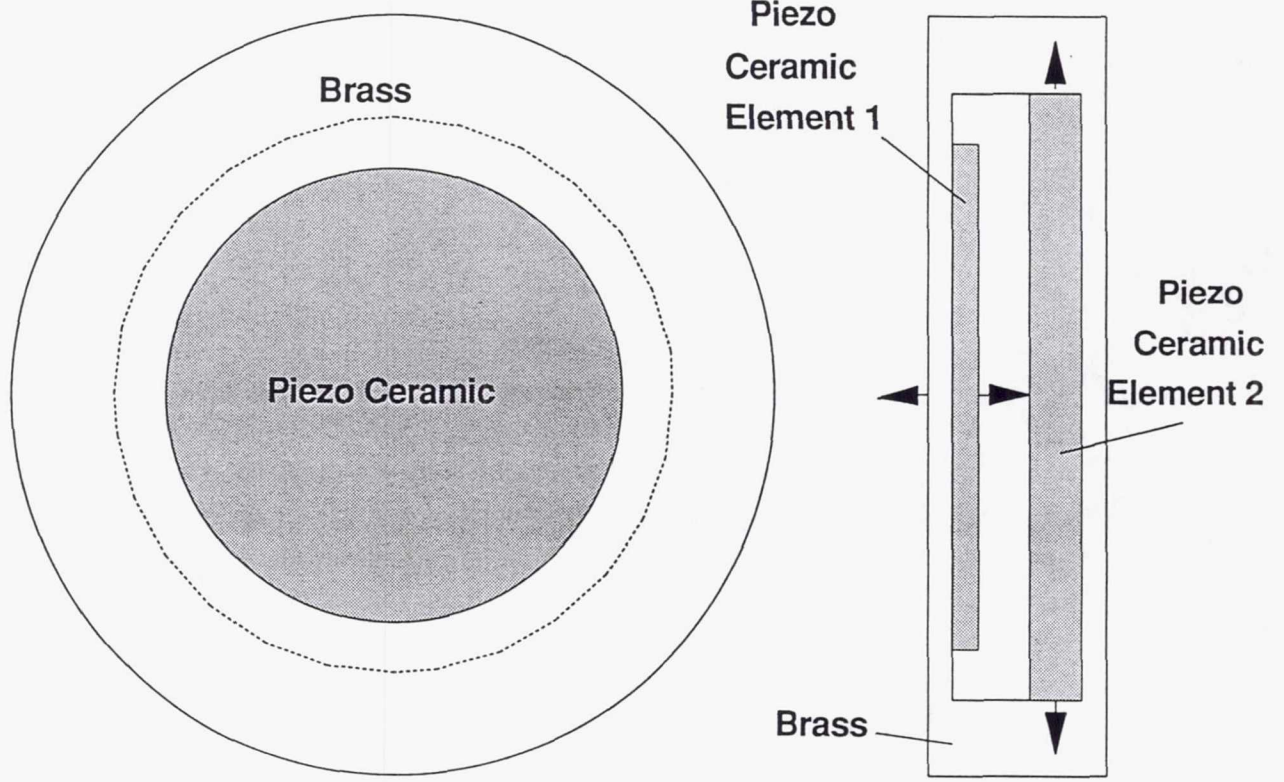
Figure 18 - Tunable Unimorph Actuator
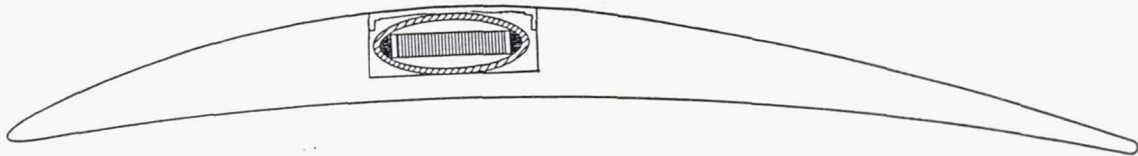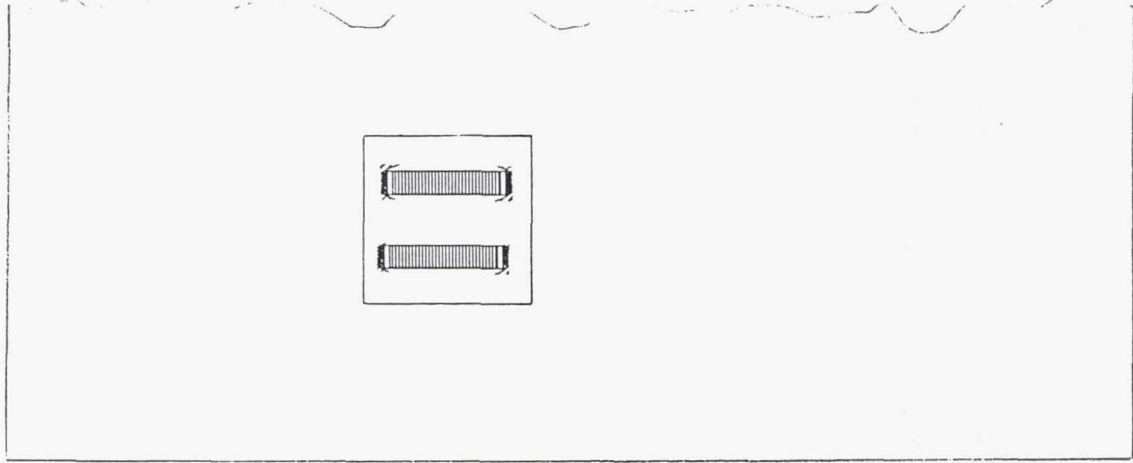
Figure 19 - Sketch of Miniature Flextensional Actuator Installed in Stator

SIDE VIEW

aerodynamic
surface

airflow →

end cap

bond

prestress shell

1.25"

0.5"

action/reaction
↔

airflow →

counter sink
for screw

terfenol rod

coil

gaps for expansion

TOP VIEW

1.25"
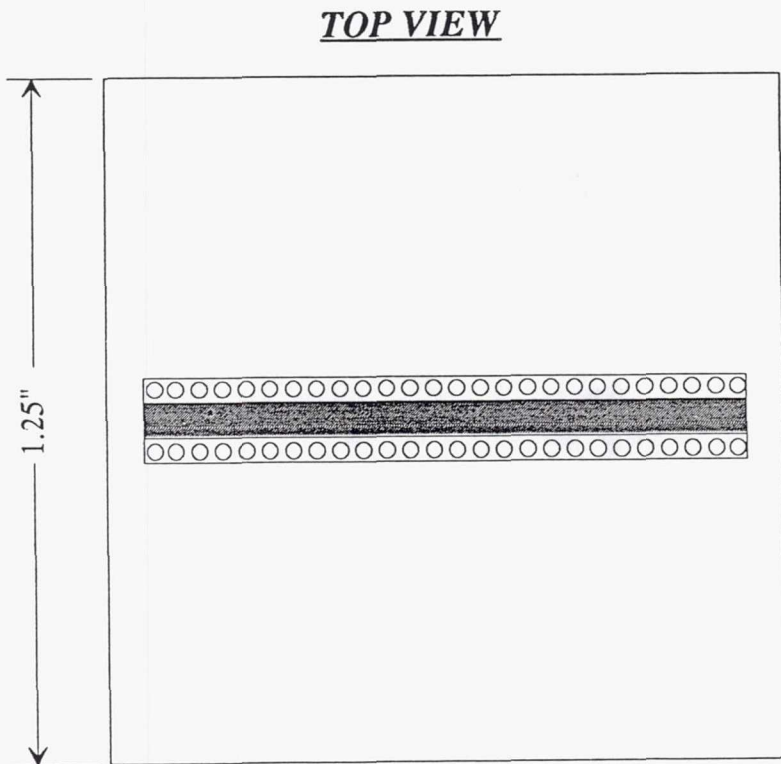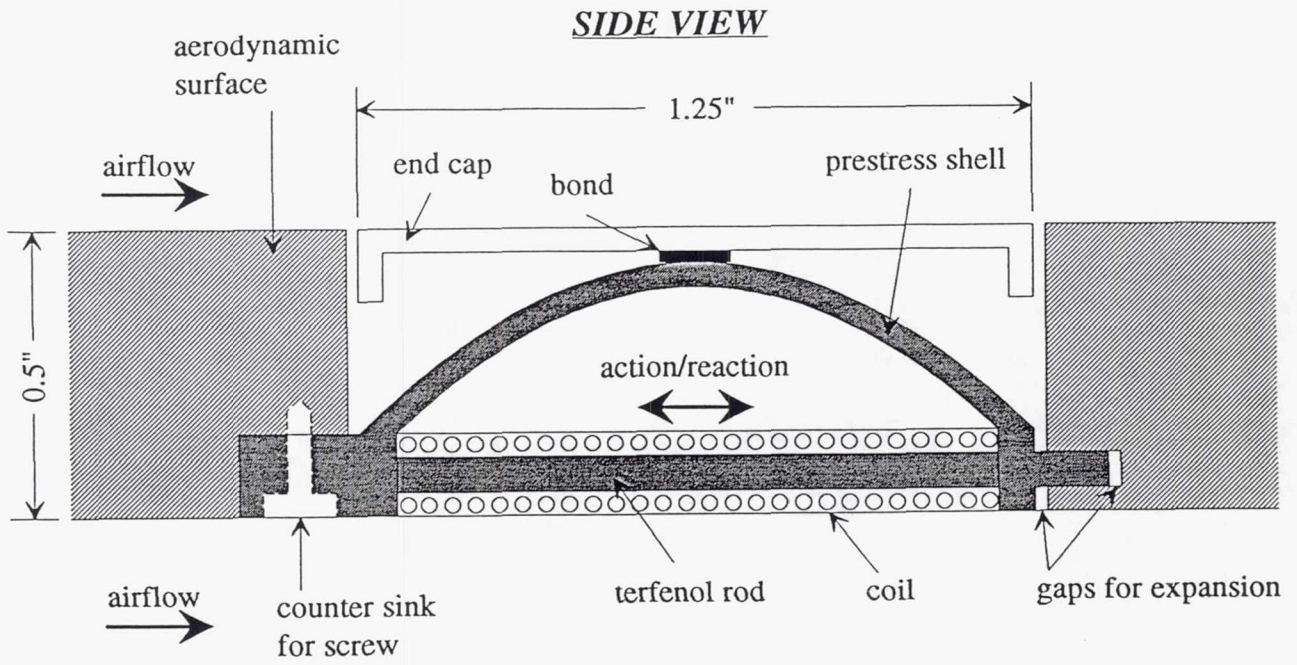
Figure 20 - Terfenol Moonie Actuator
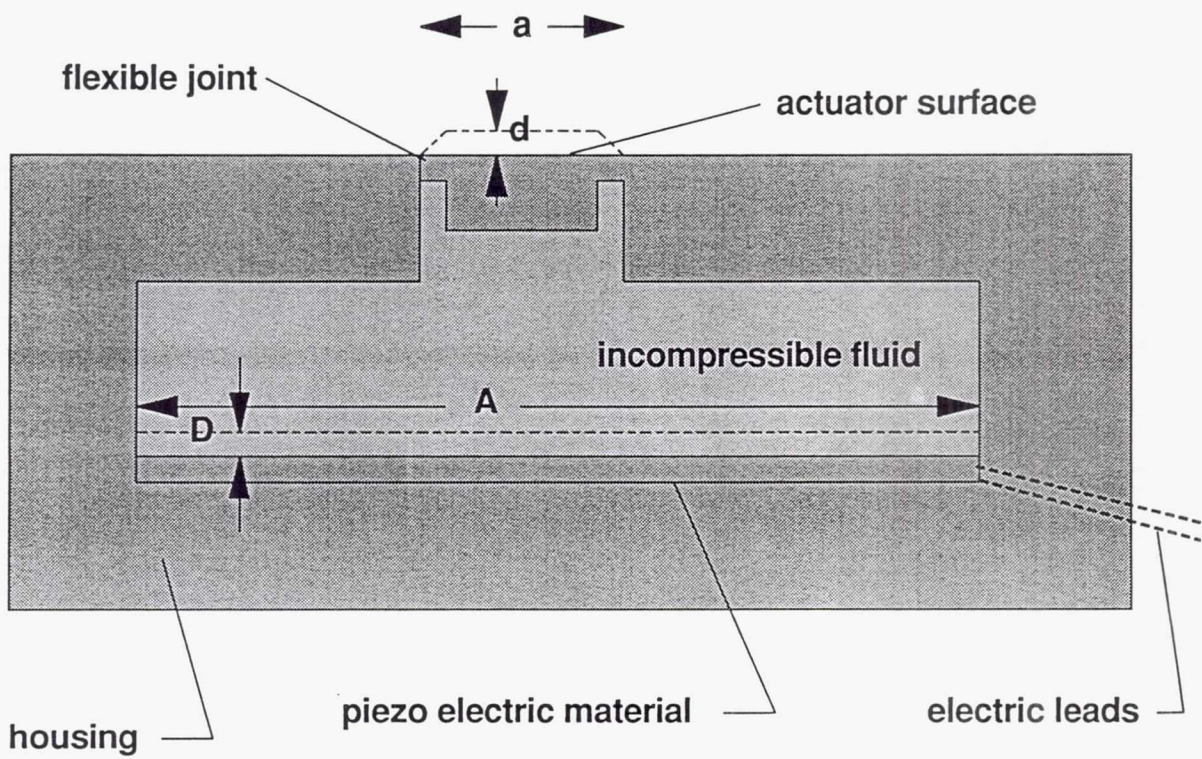
Figure 21 - Original Hybrid Actuator Concept

tape

fluid

diaphram

piezo stack
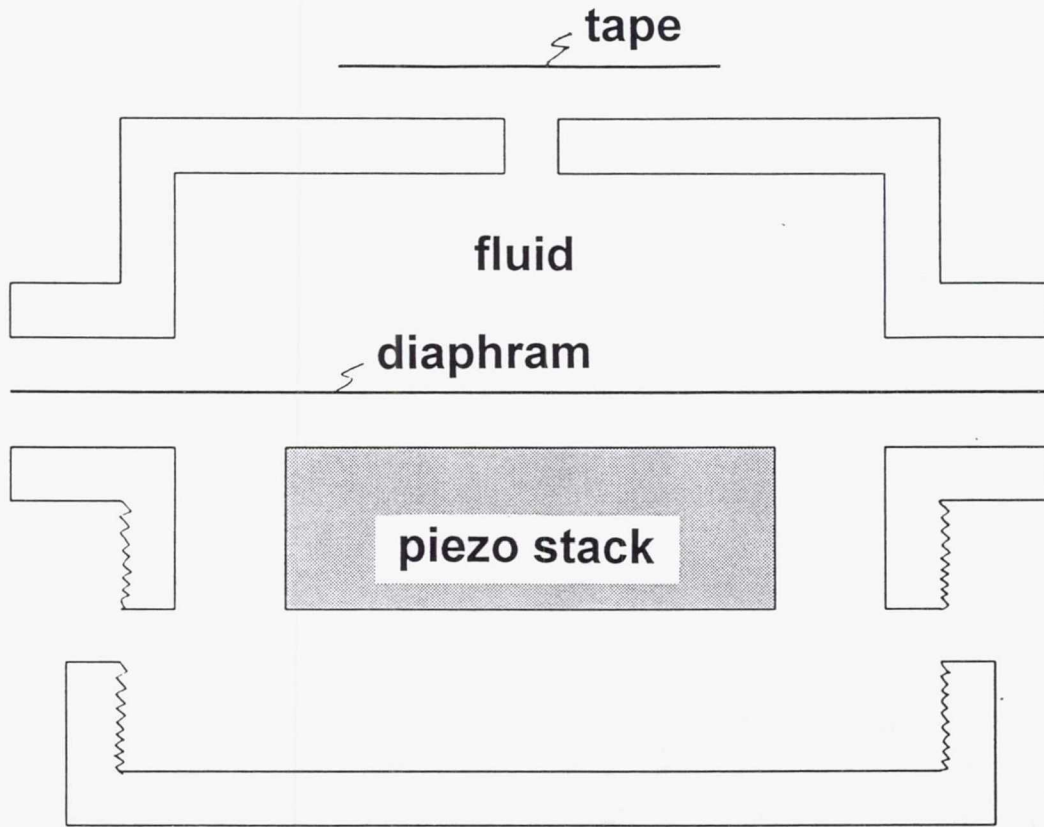
Figure 22 - Improved Hybrid Actuator Concept

tape

case

fluid
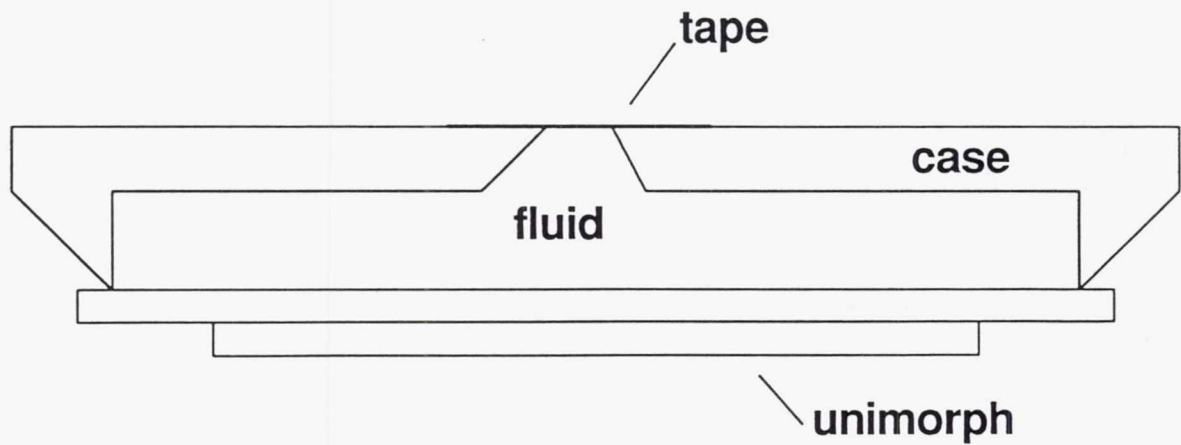
unimorph

Figure 23 - Hybrid Actuator Using Unimorph
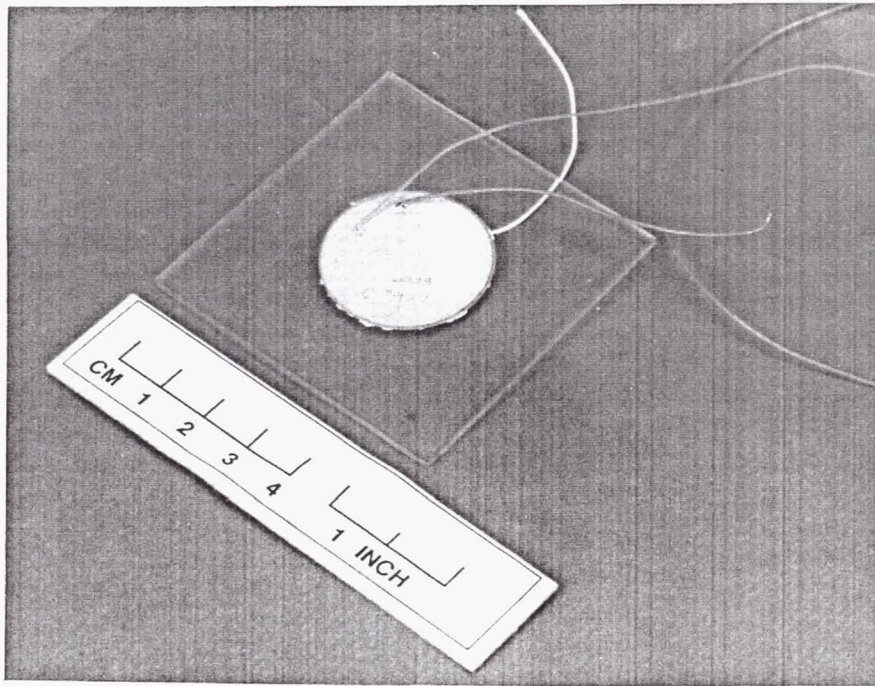
Figure 24 - Photograph of Rainbow Actuator Mounted to Plexiglas Holder
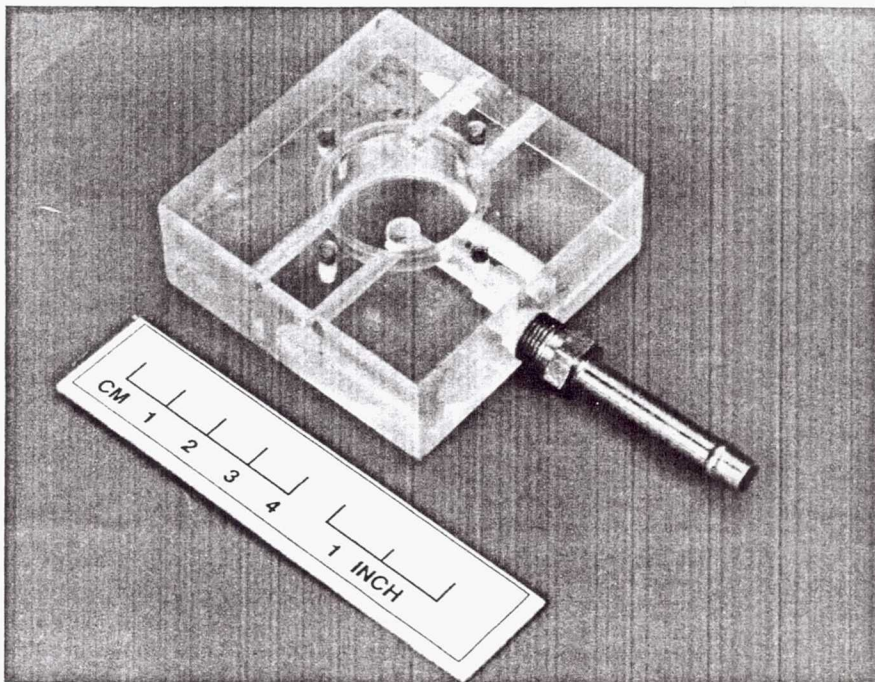
Figure 25 - Photograph of Rainbow Actuator Mount

87
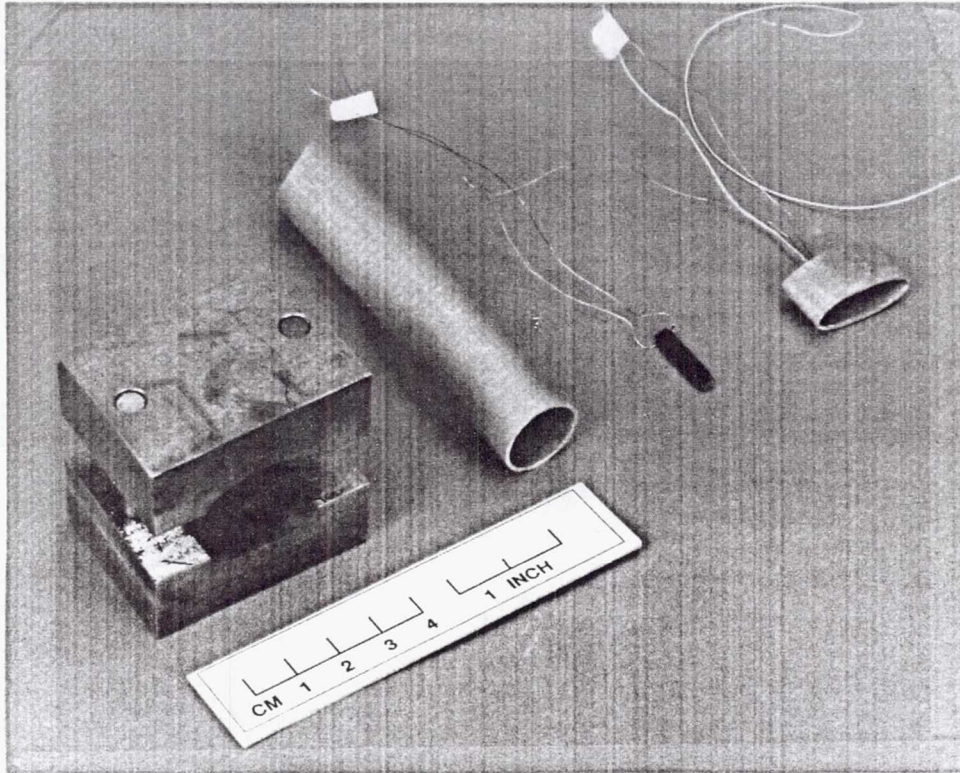
Figure 26 - Photograph of Fabrication of Miniature Flextensional Actuator
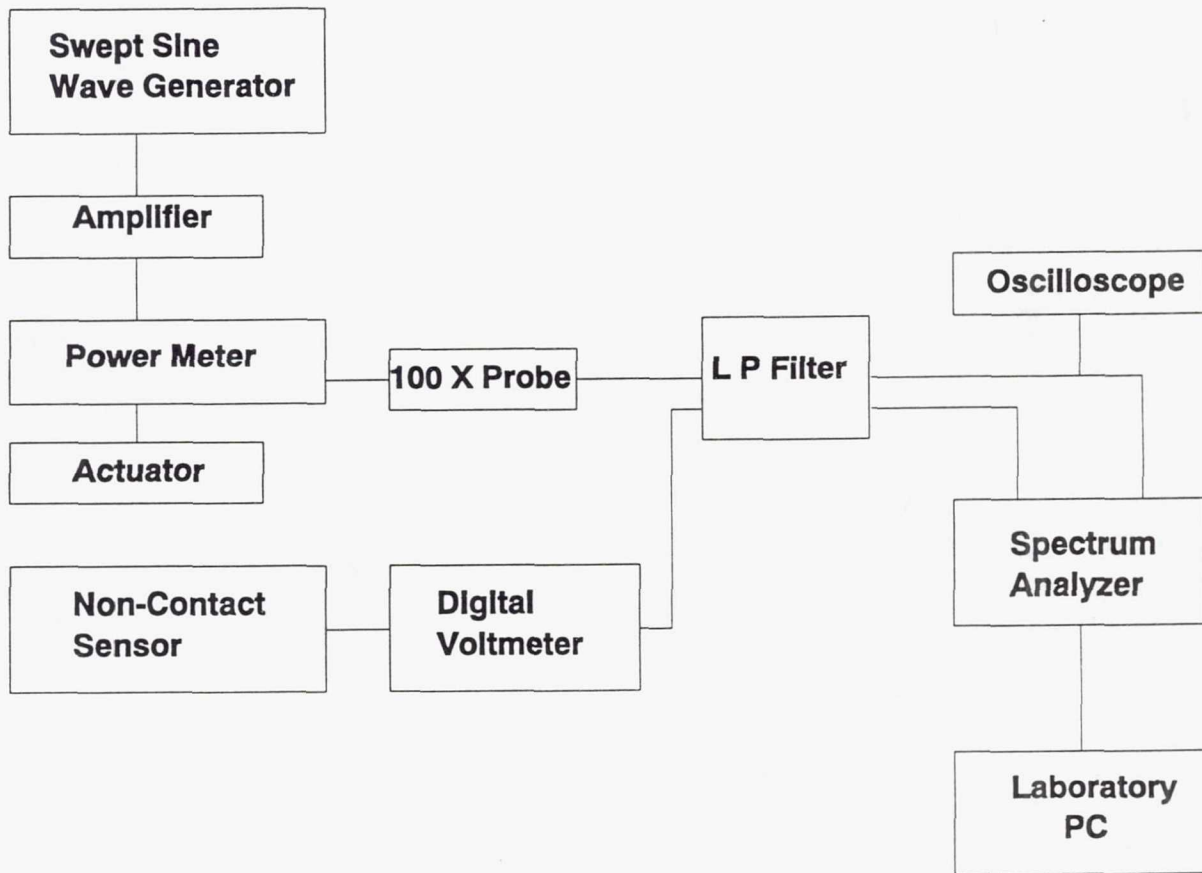
Figure 27 - Schematic Diagram of Laboratory Instrumentation

digital voltmeter

oscilloscope

high voltage
DC amplifier

power
meter

signal
generator

Op-amp

spectrum
analyzer

probe and traverse

flow meter
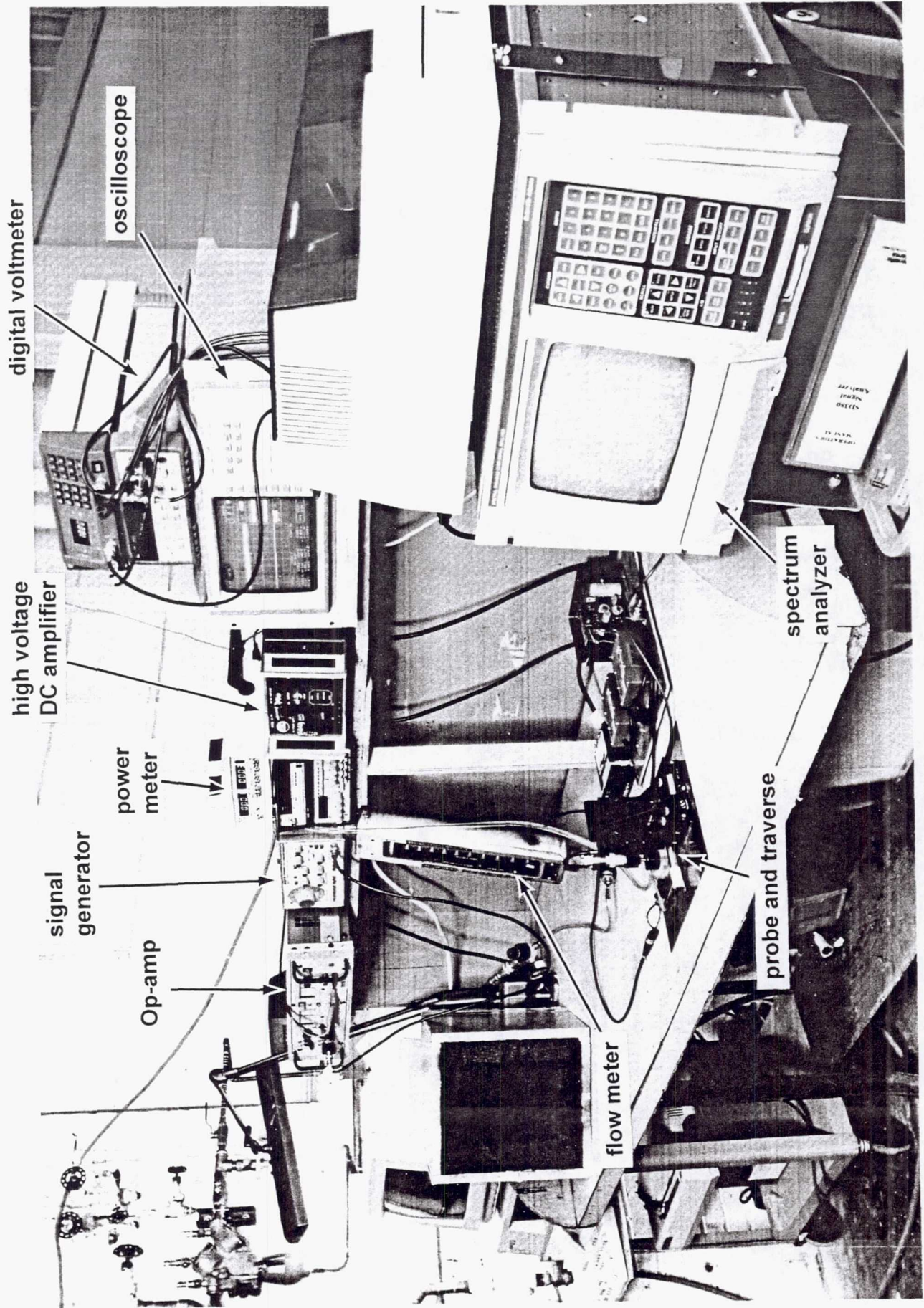
Figure 28 - Photograph of Experimental Arrangement

90
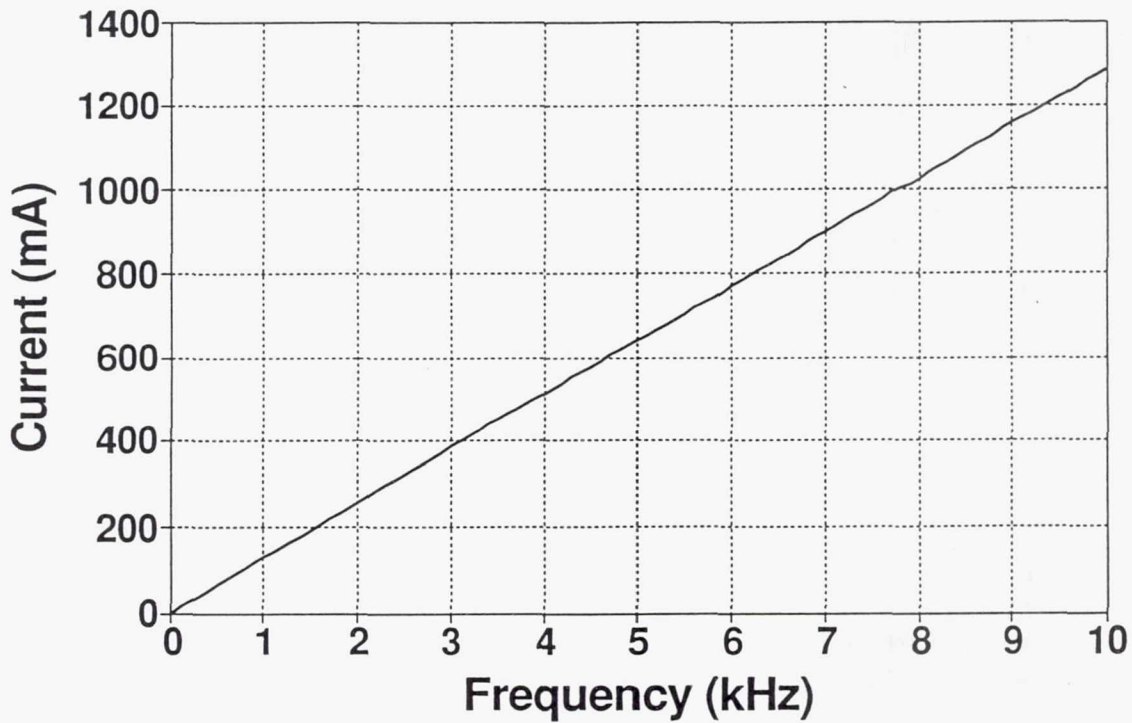
Figure 29 - Amplifier Current Requirements for 25 mil thick, 1.25 inch diameter Electrostrictive Rainbow Actuator, C = 45.5 nF, 450 V
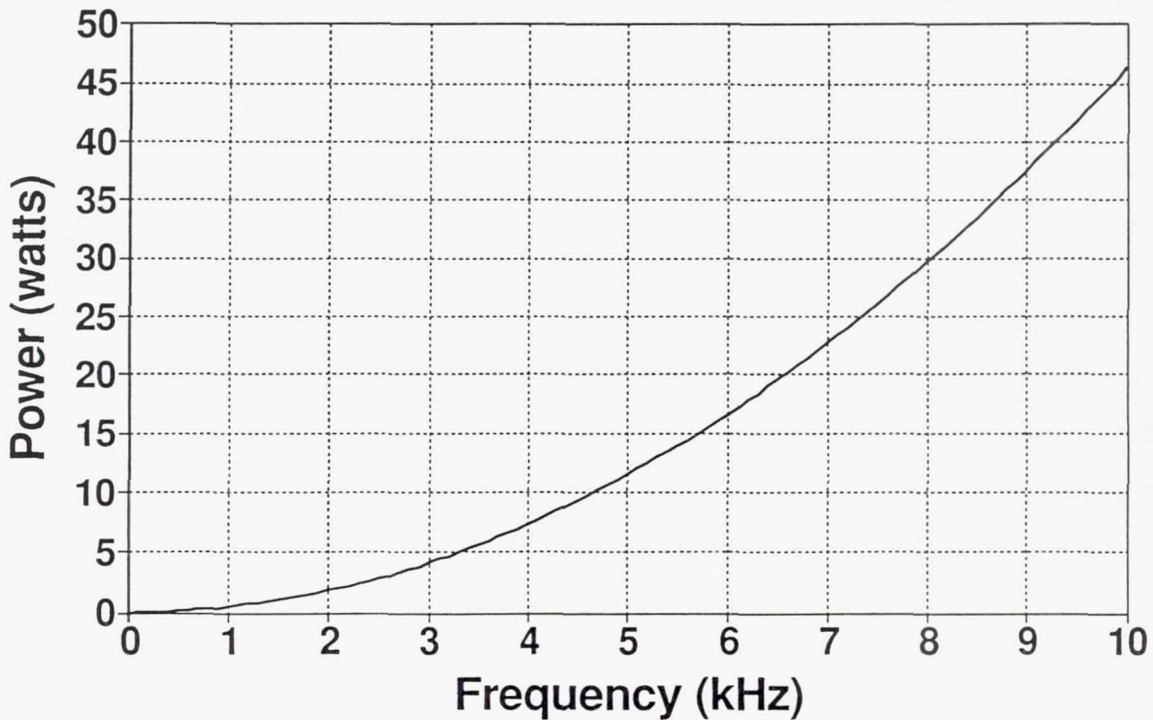
Figure 30 - Amplifier Power Requirements for 25 mil thick, 1.25 inch diameter Electrostrictive Rainbow Actuator, C = 45.5 nF, 450 V
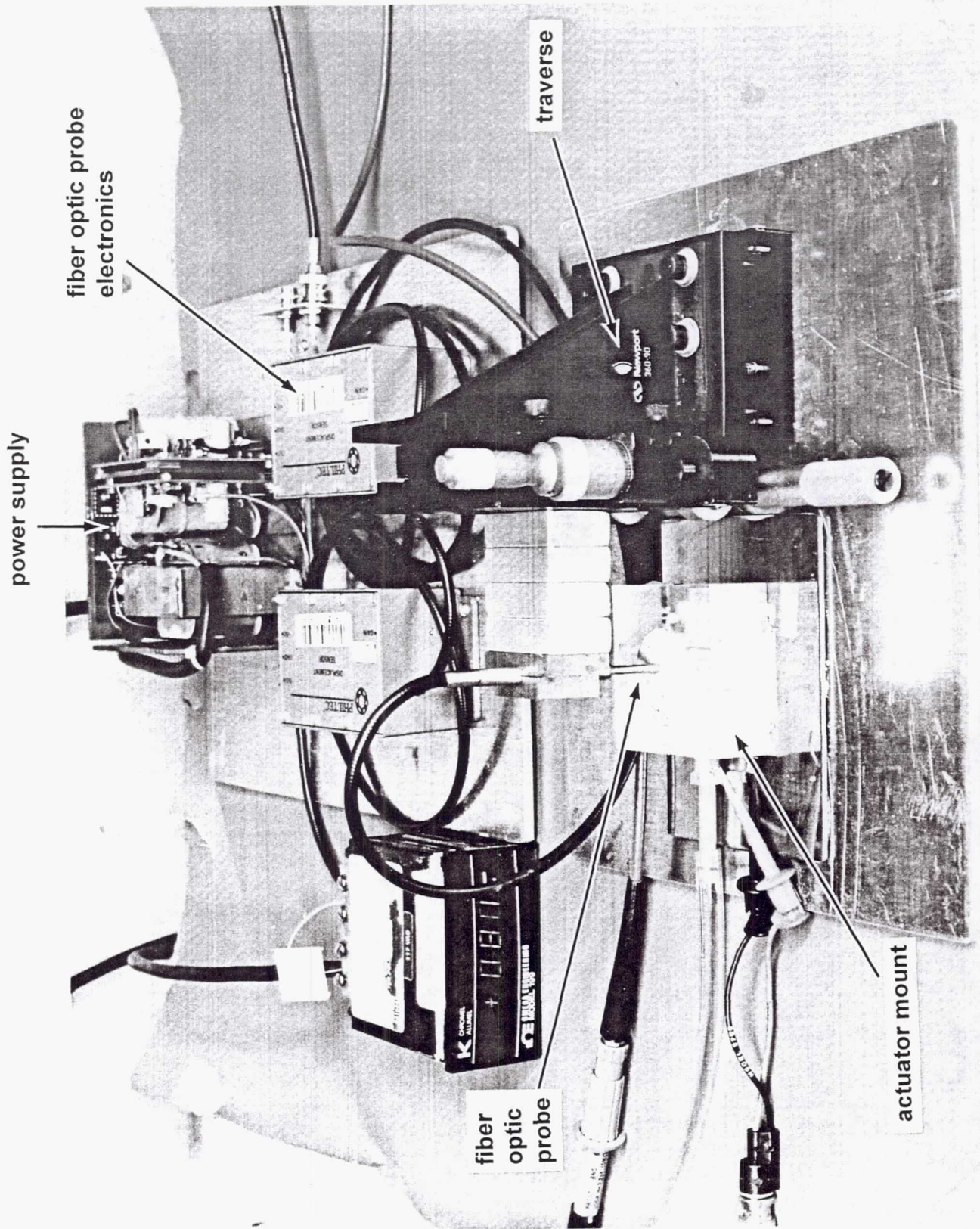
Figure 31 - Photograph of Probe Traverse
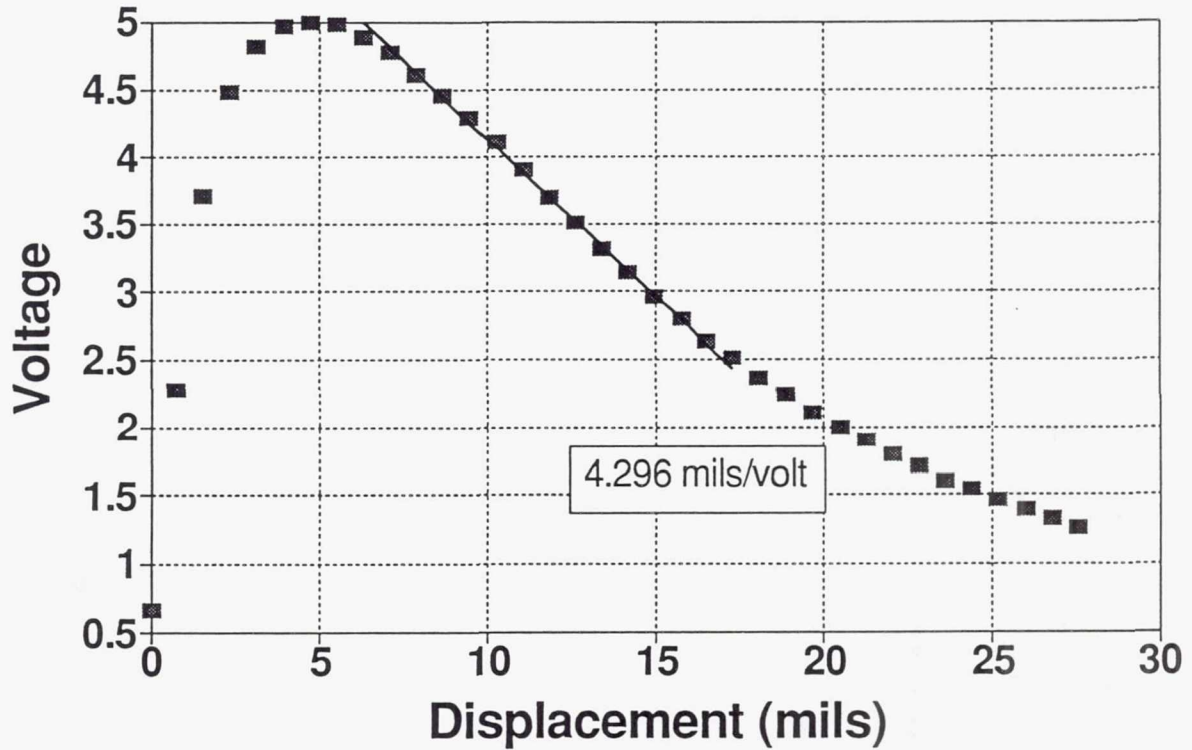
Figure 32 - Non-Contact Sensor Output Voltage vs Surface Displacement (Small Probe)
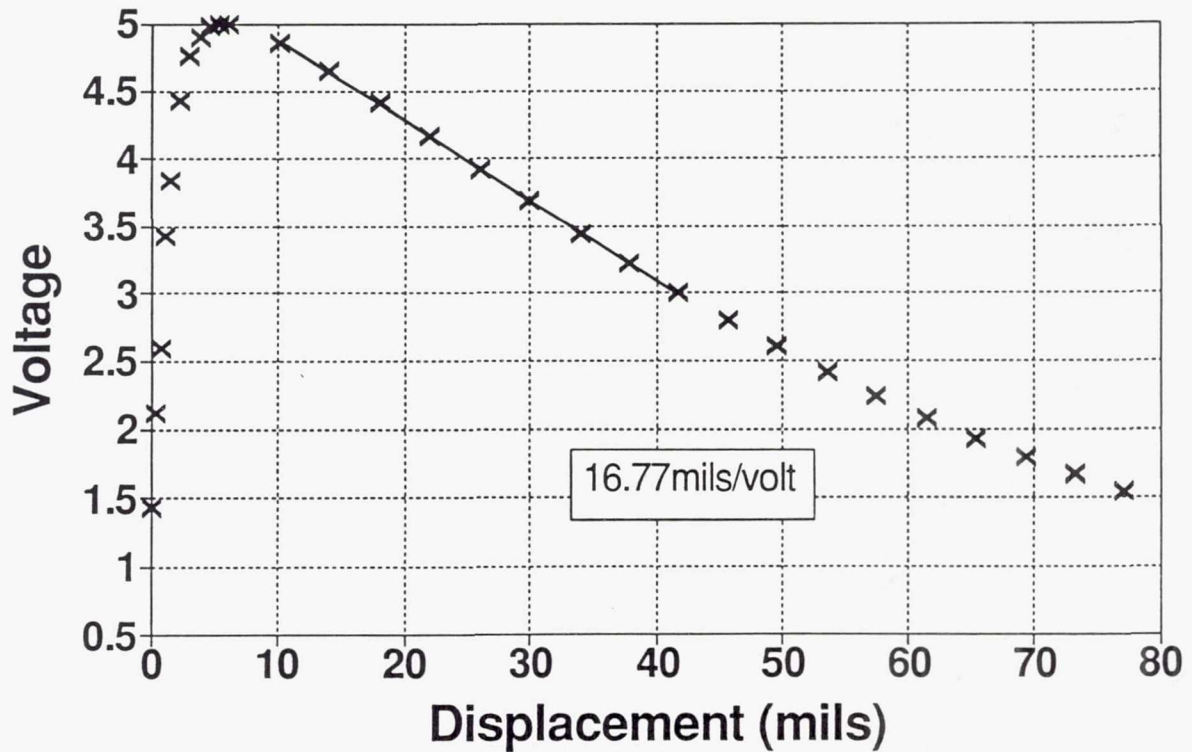
Figure 33 - Non-Contact Sensor Output Voltage vs Surface Displacement (Large Probe)

93
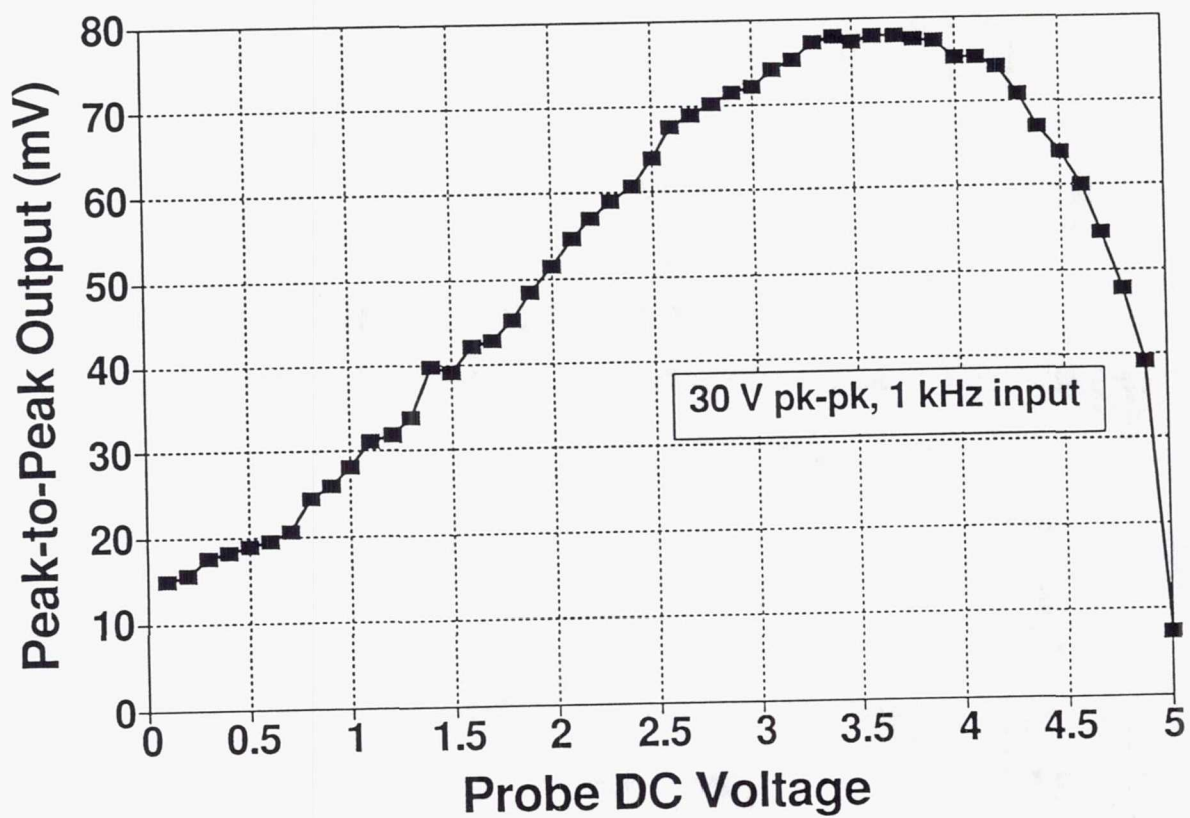
Figure 34 - Non-Contact Sensor RMS Output vs Standoff Distance
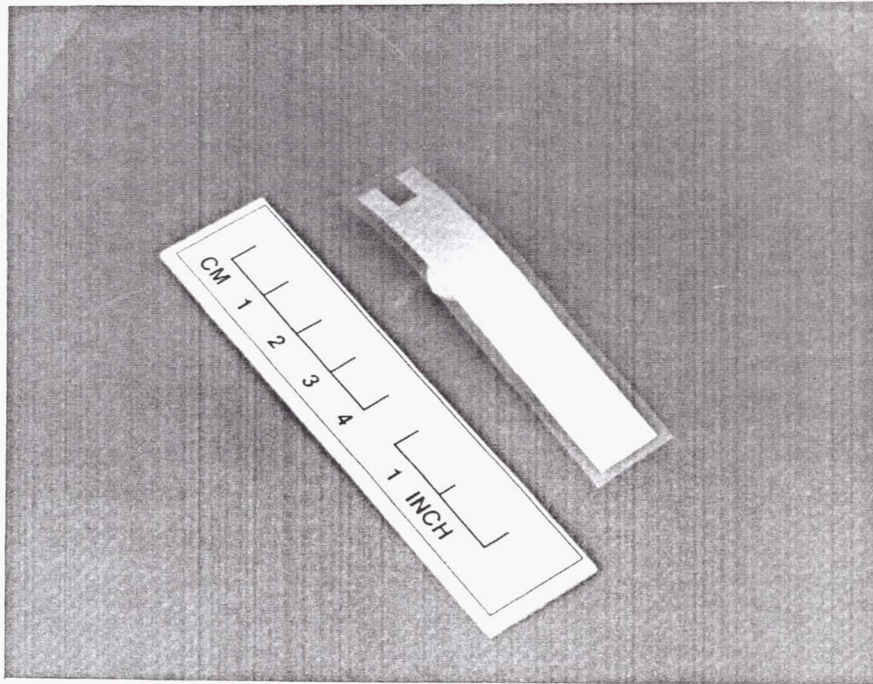
Figure 35 - Photograph of PVDF Actuator
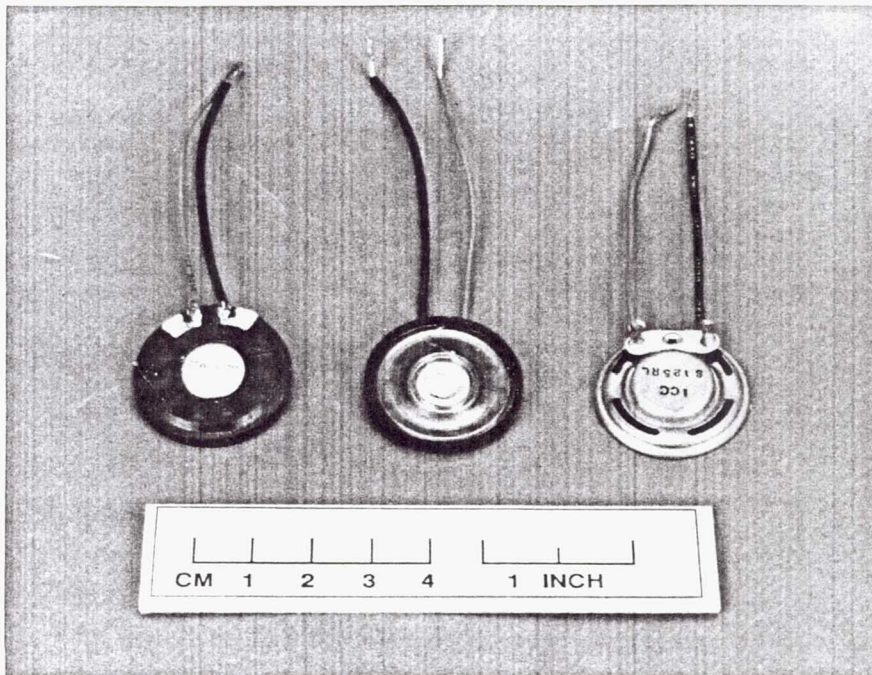
Figure 36 - Photograph of Miniature Speakers. (Left shows rear of plastic frame speaker, middle shows front of plastic frame speaker, right shows rear of metal frame speaker)
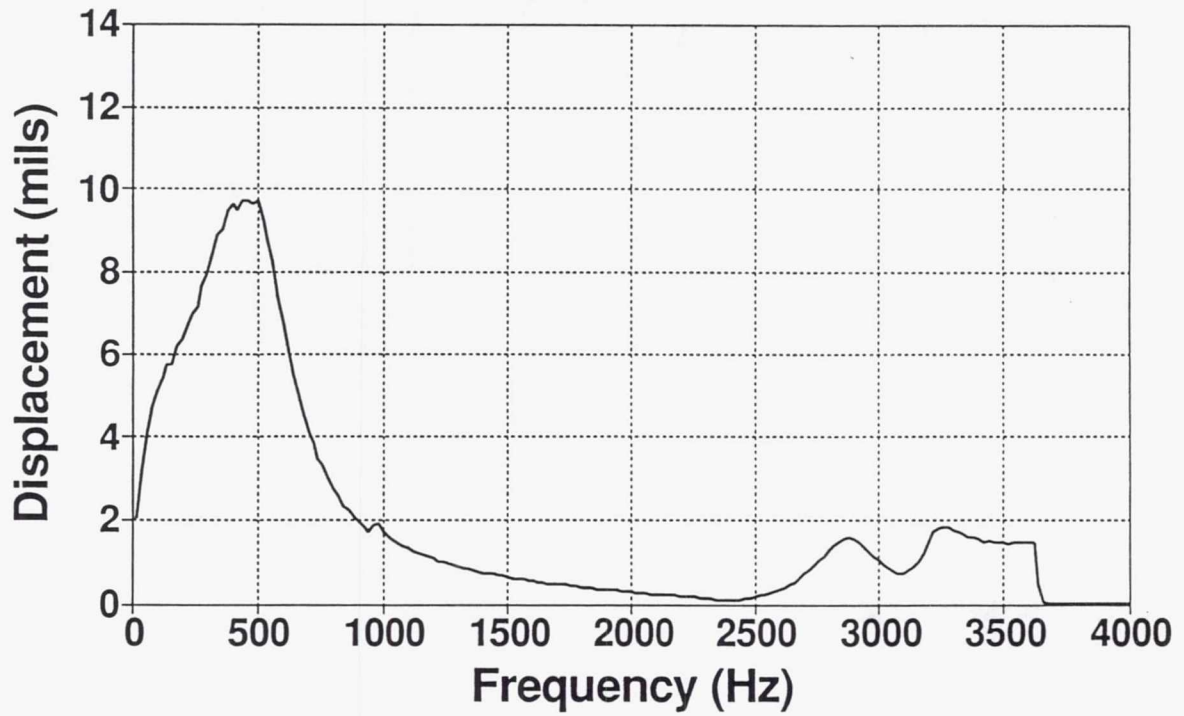
Figure 37 - Metal Frame Miniature Speaker (Intervox SR800RMF) Displacement vs Frequency
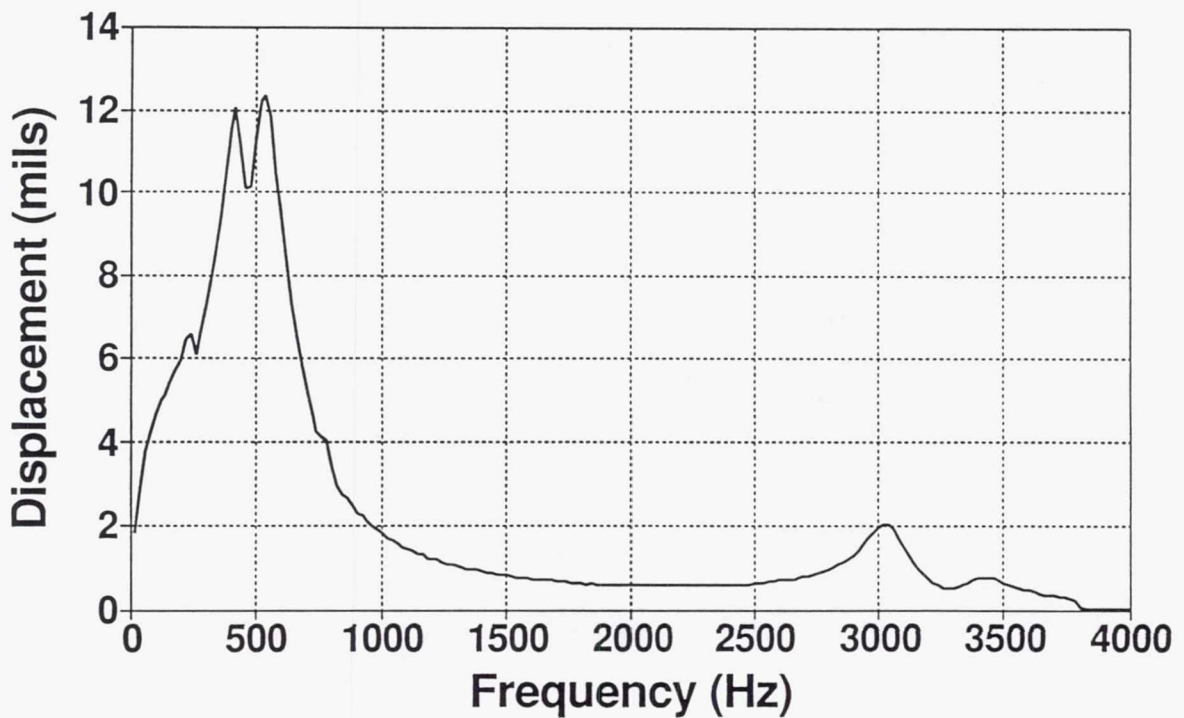
Figure 38 - Plastic Frame Miniature Speaker (Intervox S125RL) Displacement vs Frequency
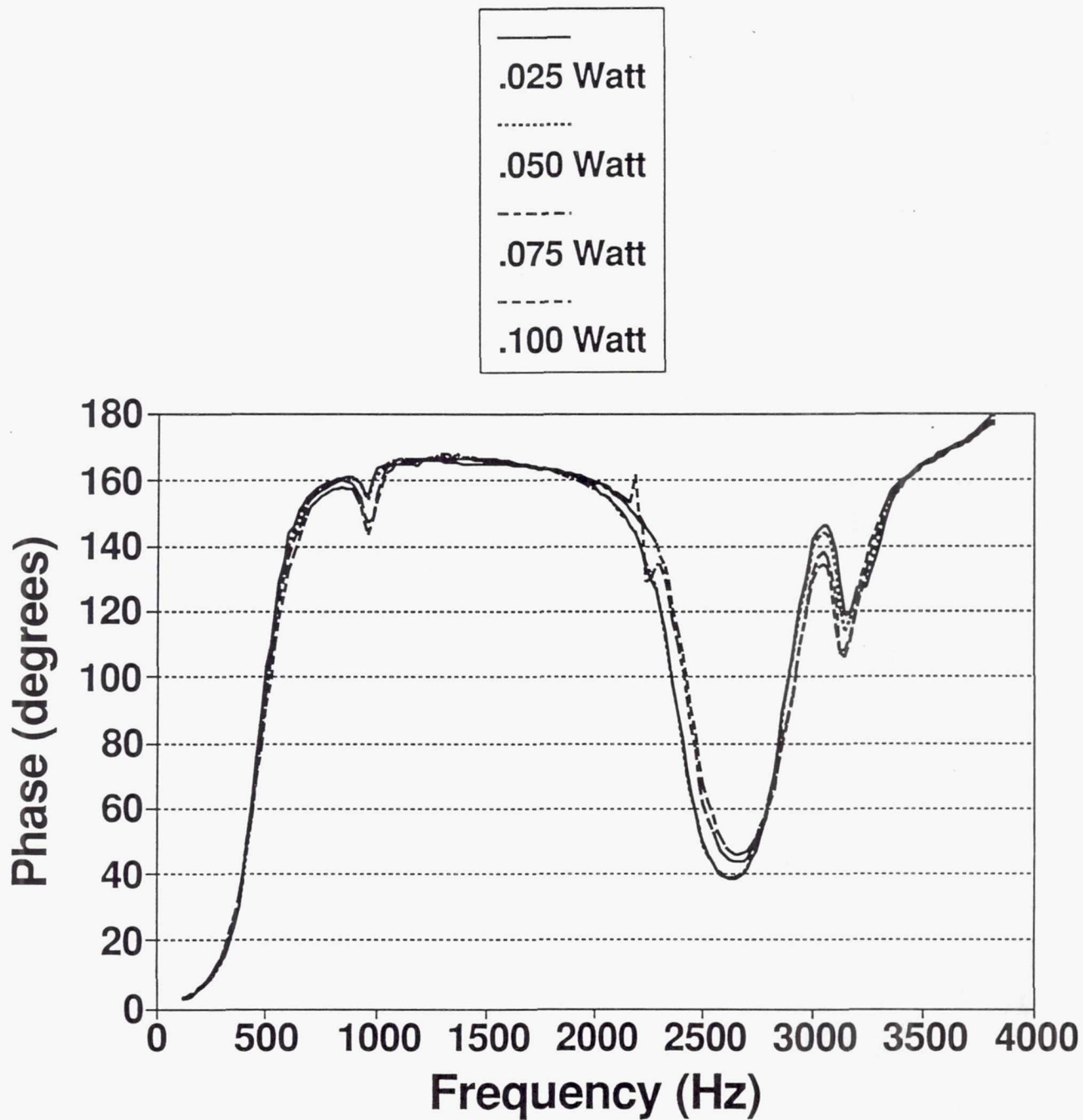
Figure 39 - Plastic Frame Miniature Speaker (Intervox S125RL) Phase Characteristics

97
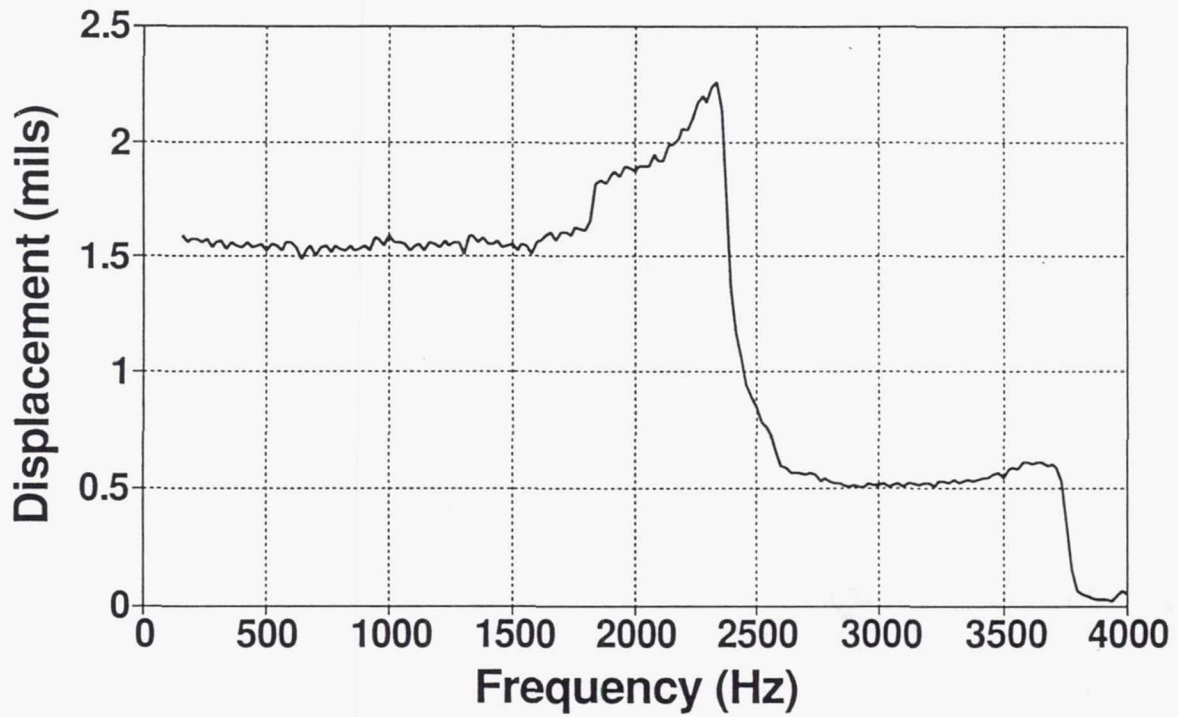
Figure 40 - Flextensional Actuator Displacement vs Frequency (±50 volt peak to peak sine wave, 50 V DC offset)
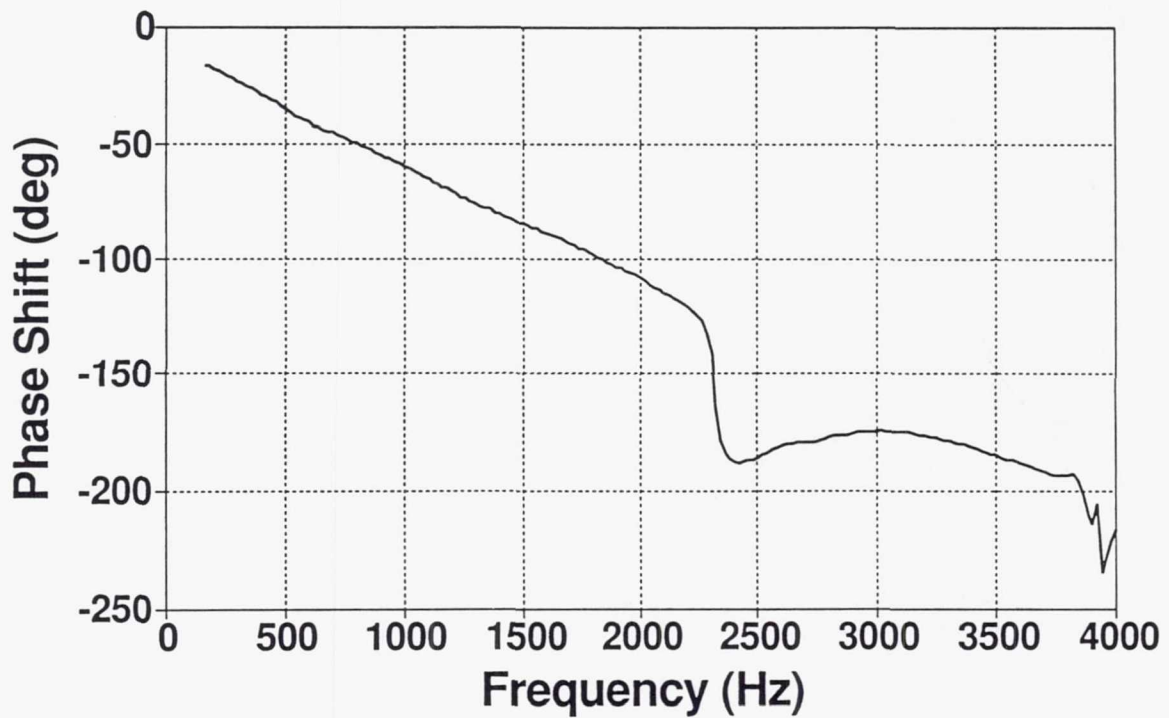
Figure 41 - Flextensional Actuator Phase Characteristics (±50 volt peak to peak sine wave, 50 V DC offset)
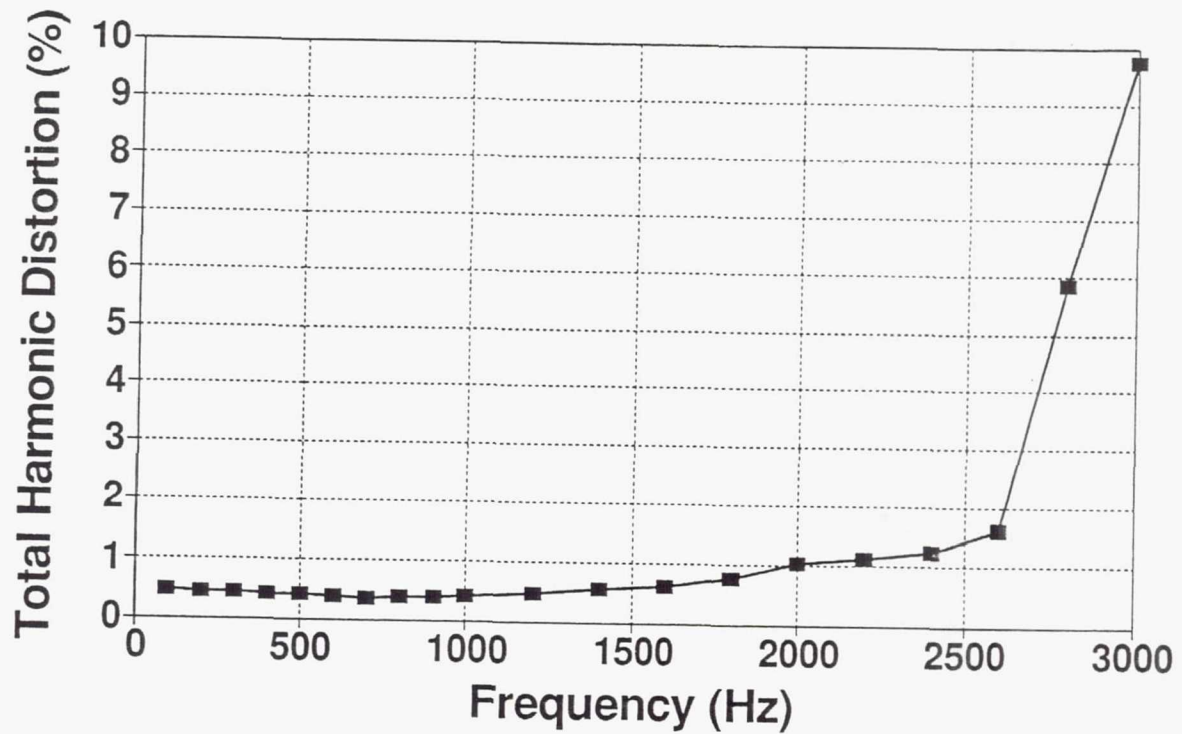
Figure 42 - Flextensional Actuator Total Harmonic Distortion Characteristics (±50 volt peak to peak sine wave, 50 V DC offset)
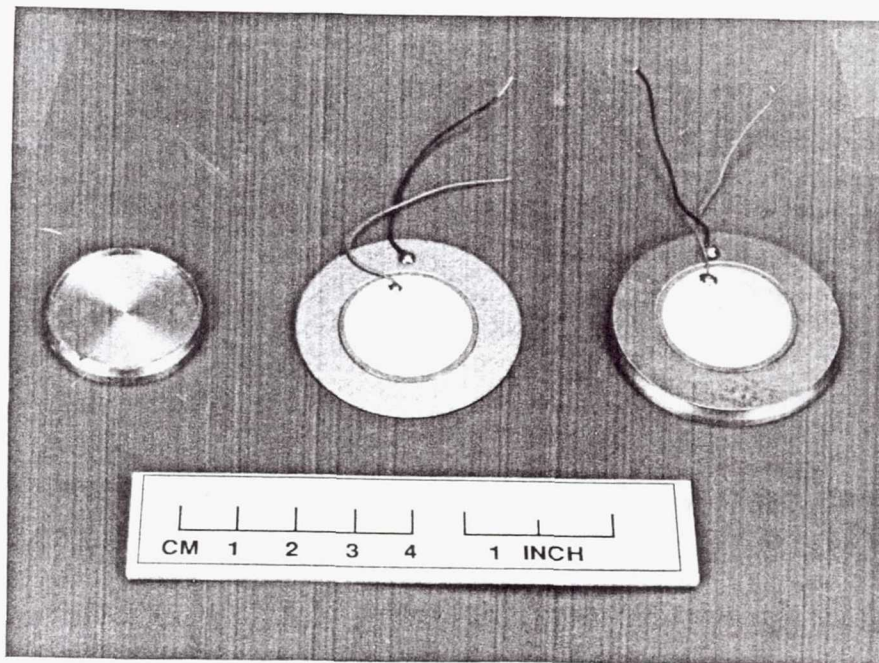
Figure 43 - Photograph of Basic Unimorph Actuator. (Node mount shown on left, actuator as received in the middle, right shows edge mounted actuator assembly)
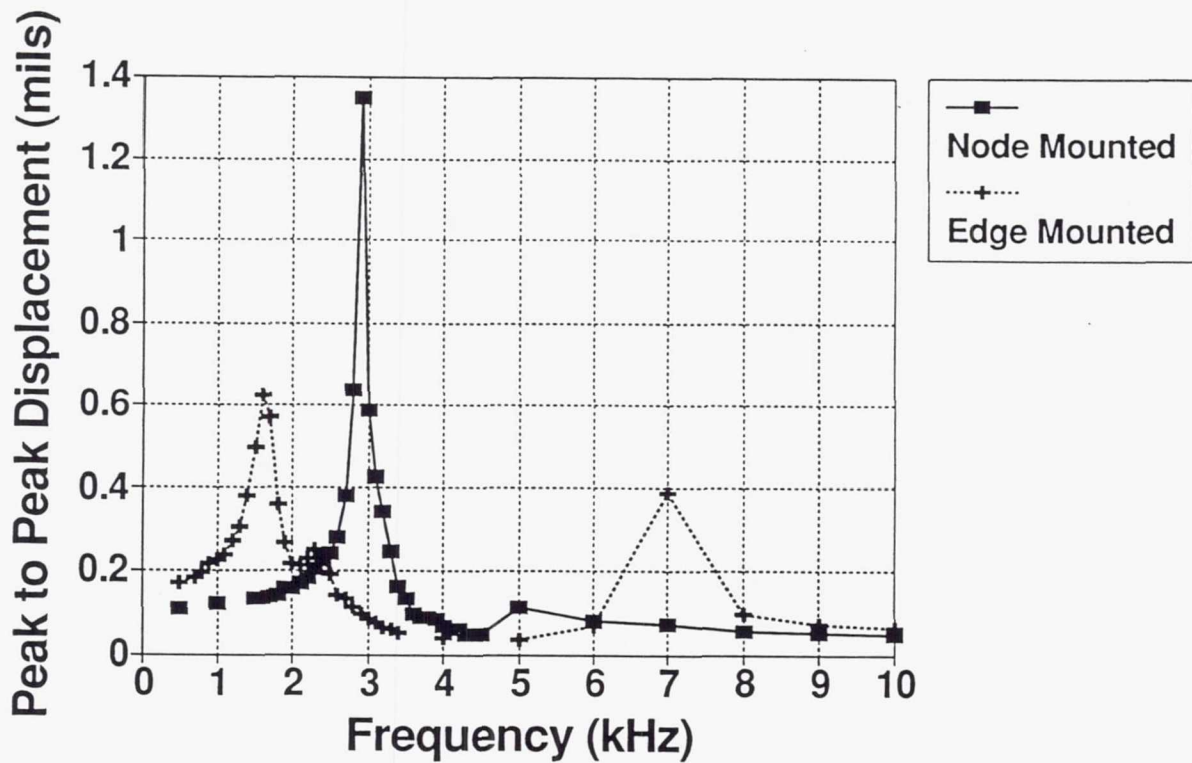
Figure 44 - Basic Unimorph Displacement vs Frequency (30 volt peak to peak sine wave)
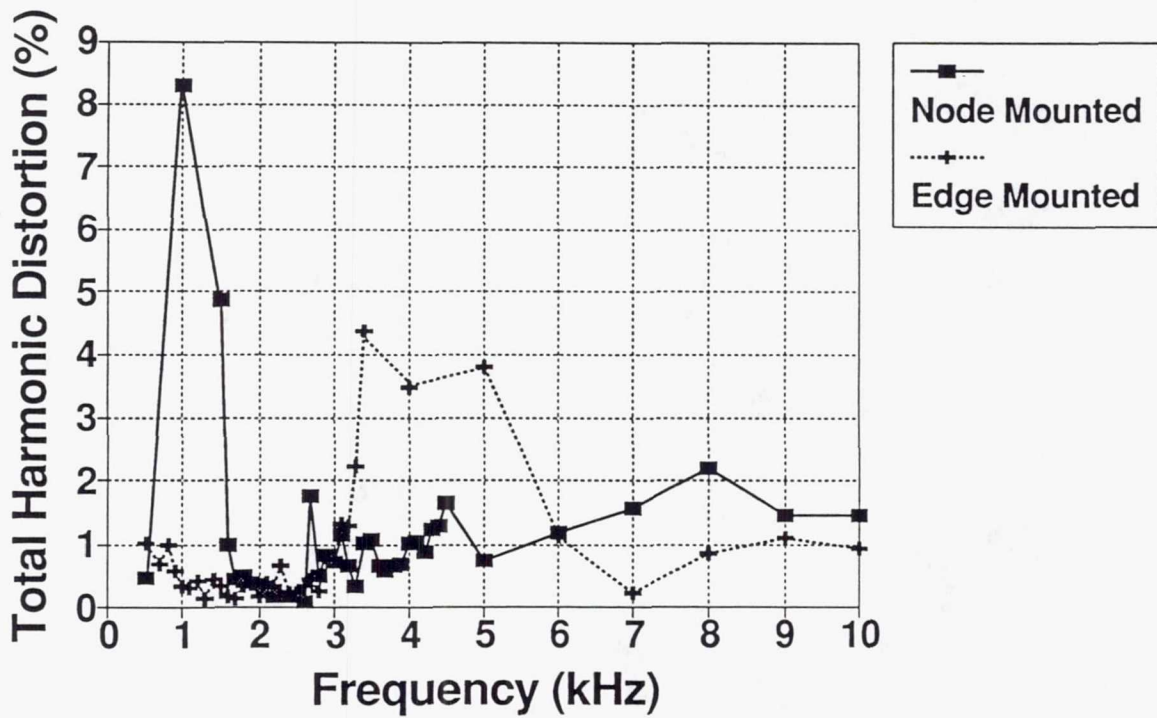
Figure 45 - Basic Unimorph Total Harmonic Distortion vs Frequency (30 volt peak to peak sine wave)
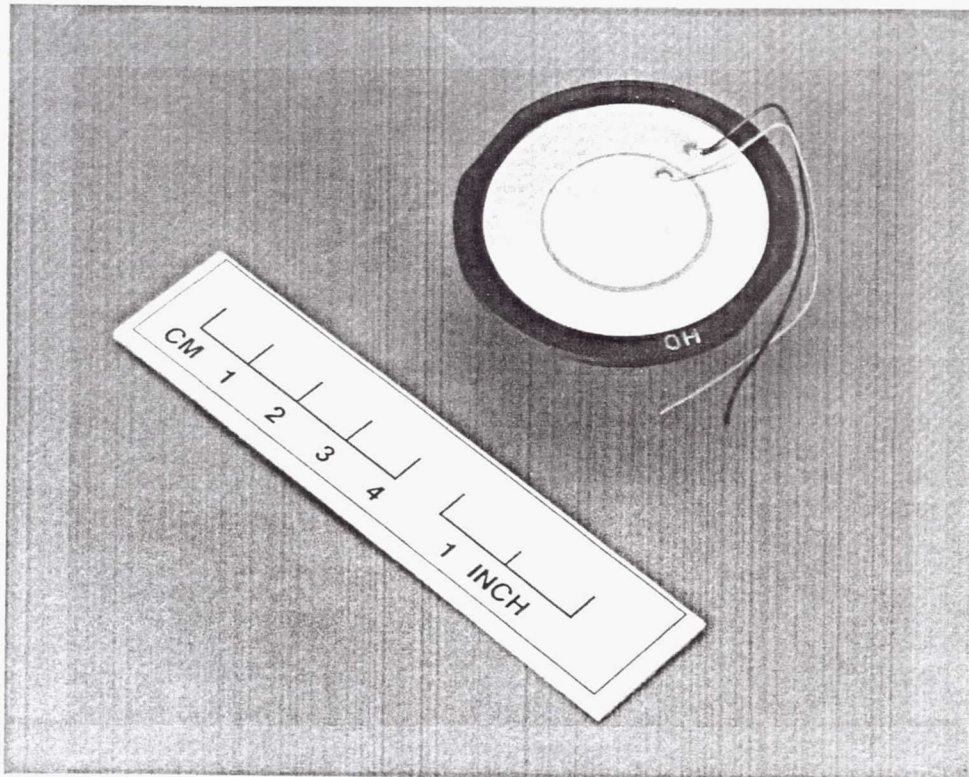
Figure 46 - Photograph of Telephone Unimorph
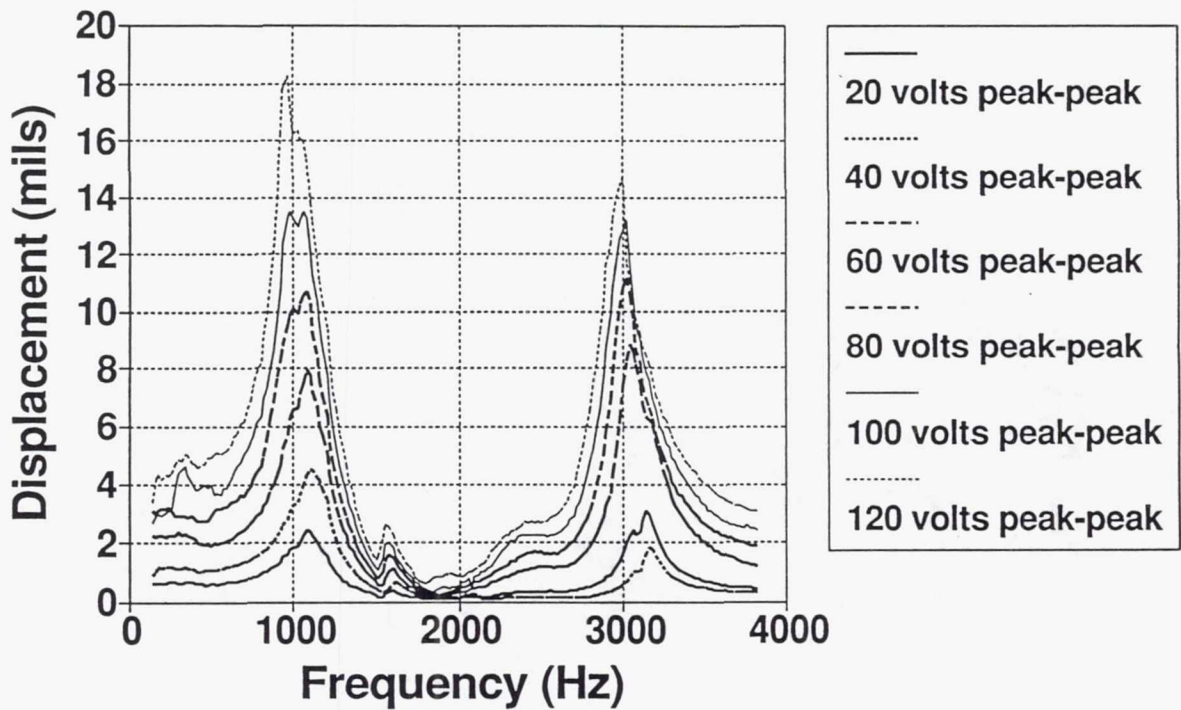
Figure 47 - Telephone Unimorph Displacement vs Frequency for Several Operating Voltages
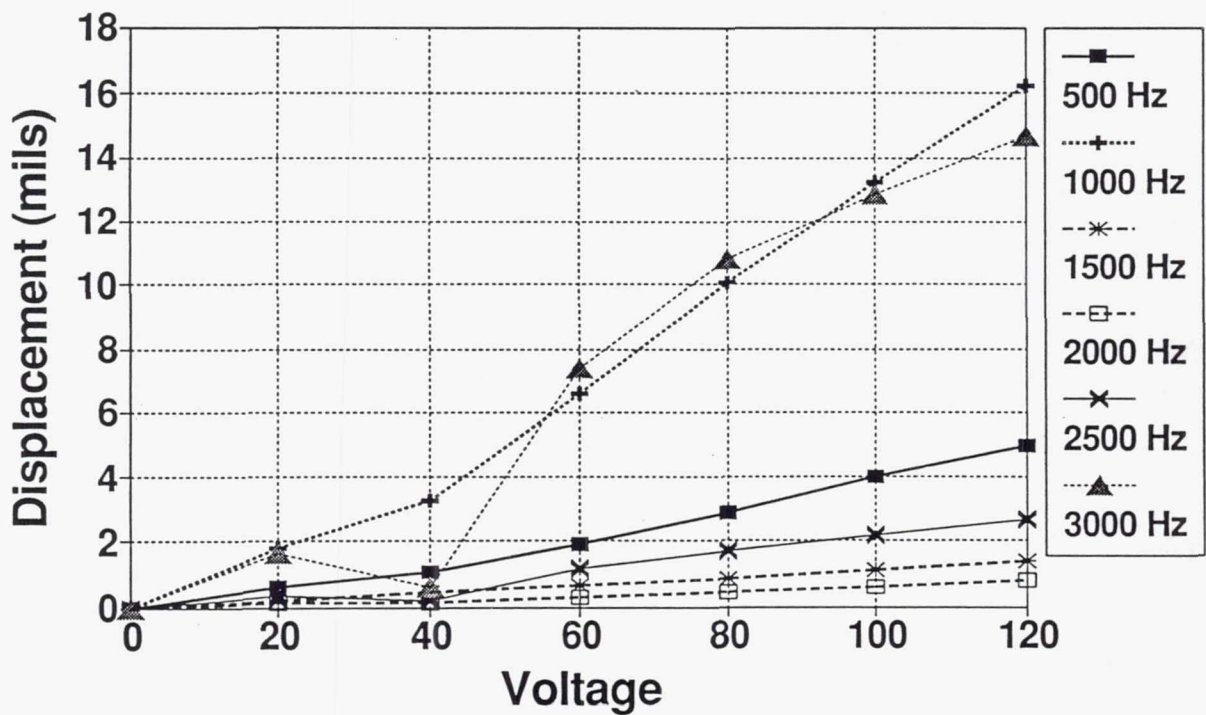
Figure 48 - Telephone Unimorph Displacement vs Input Voltage at Various Frequencies
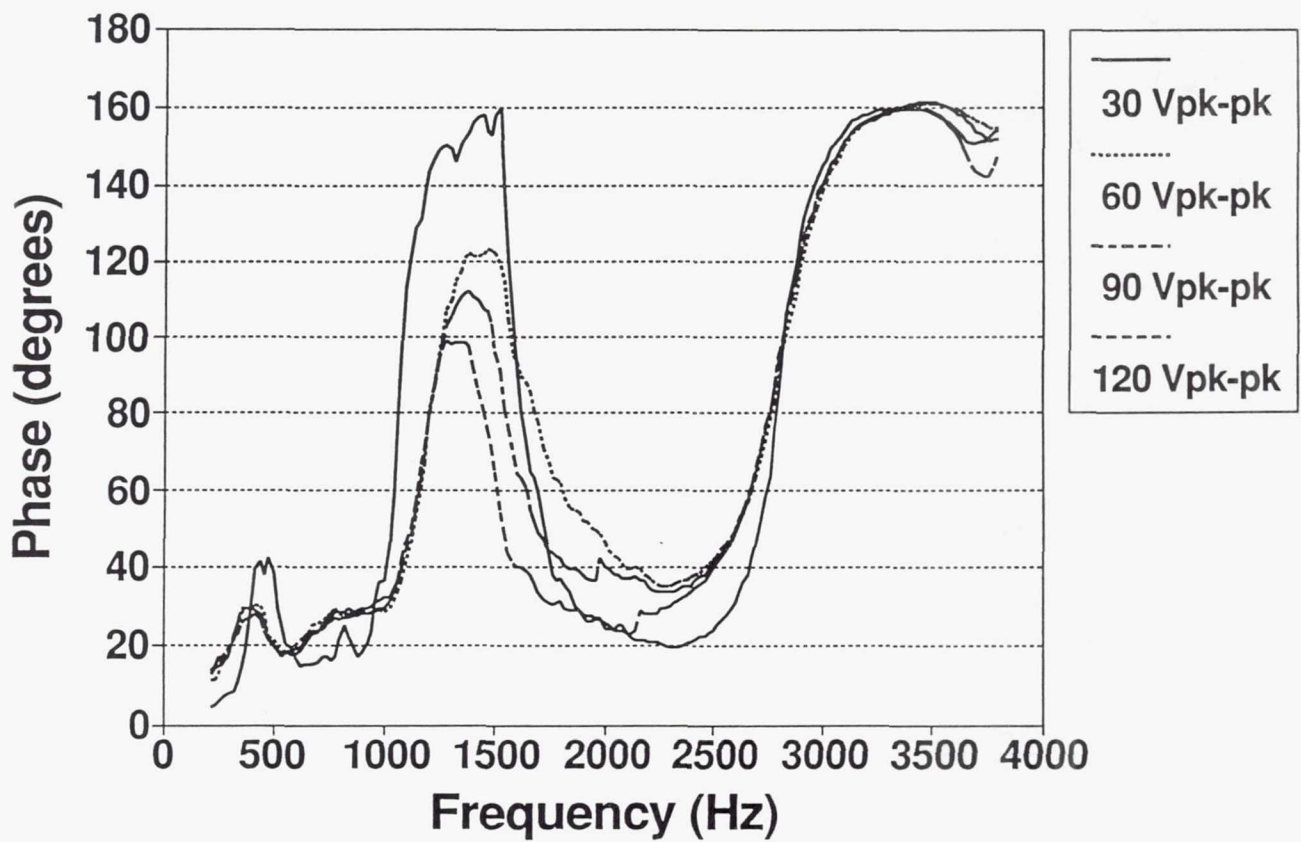
Figure 49 - Telephone Unimorph Phase Relationship vs Frequency for Various Voltage Levels
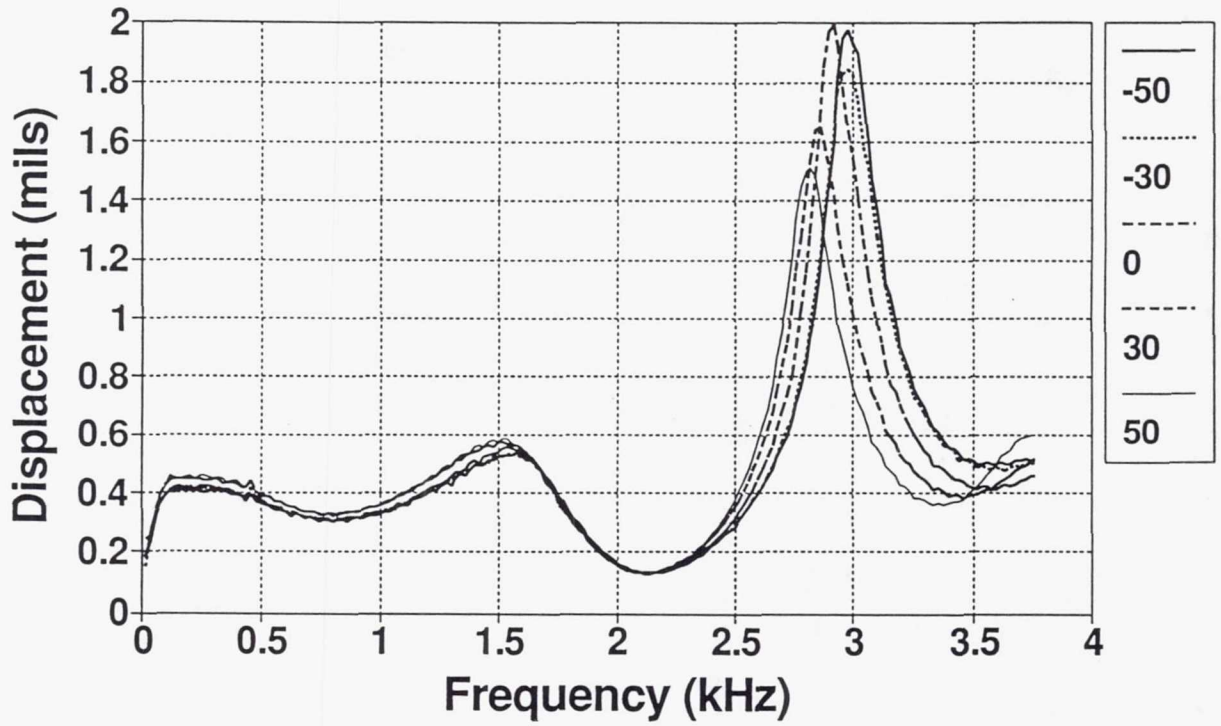
Figure 50 - Effect of DC Voltage on Displacement of Dual Bonded Unimorph
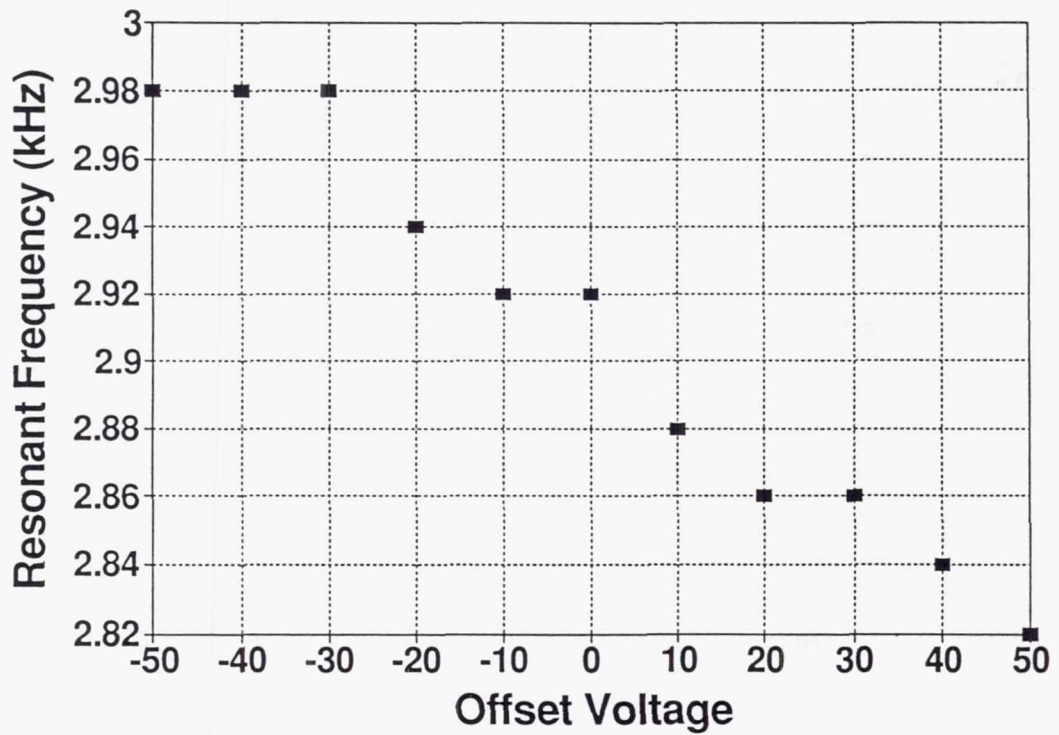
Figure 51 - Effect of DC Voltage on Resonant Frequency of Dual Bonded Unimorph
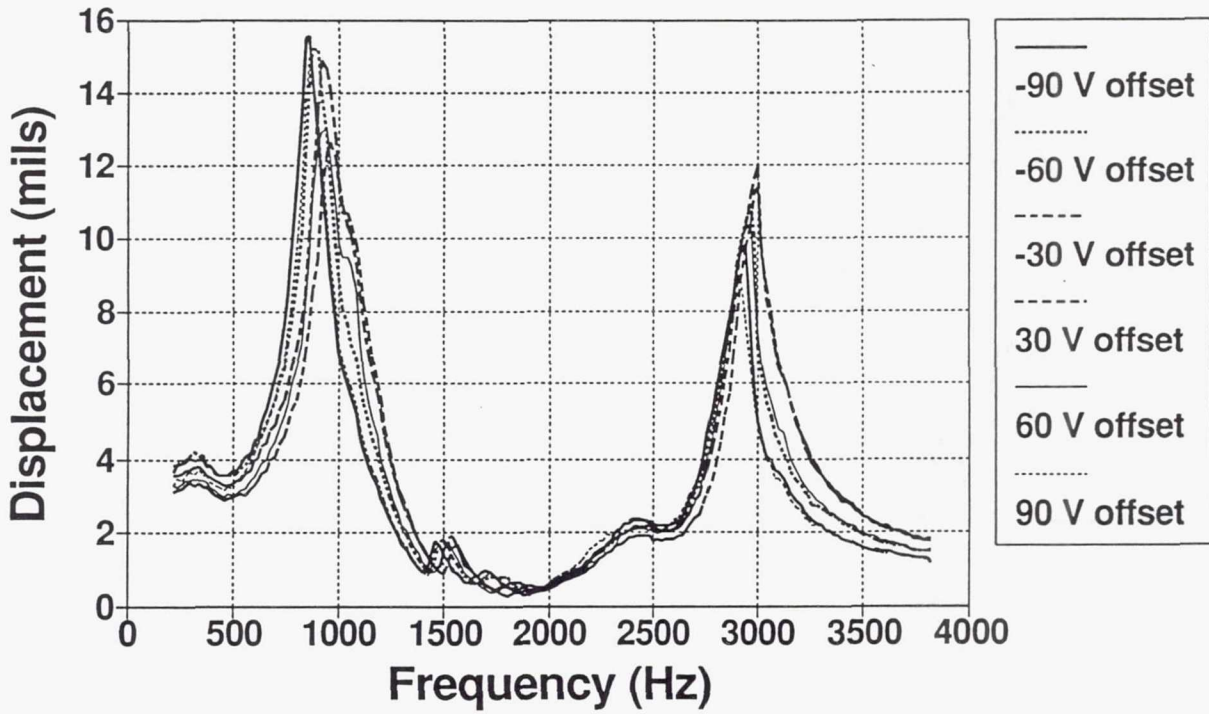
Figure 52 - Effect of DC Offset Voltage on Displacement of Telephone Unimorph
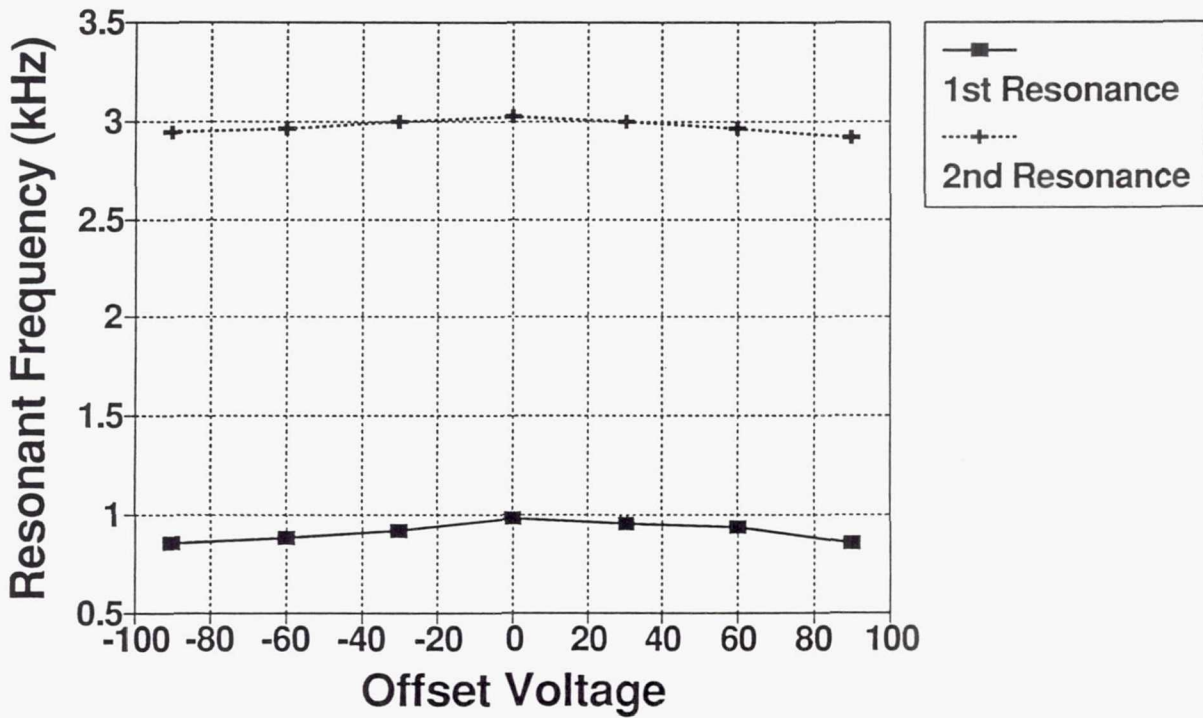
Figure 53 - Effect of DC Offset Voltage on Resonant Frequency of Telephone Unimorph
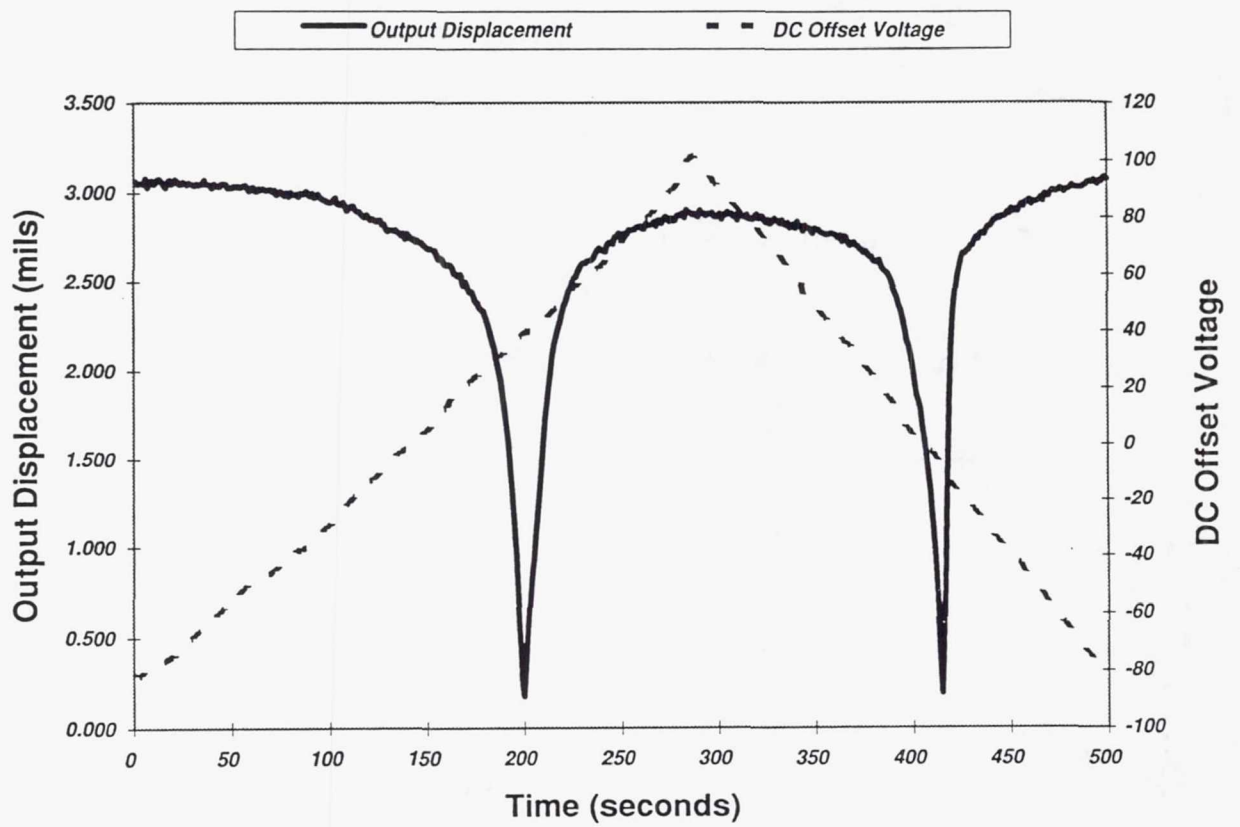
Figure 54 - Repoling Effect on Telephone Unimorph Displacement

106
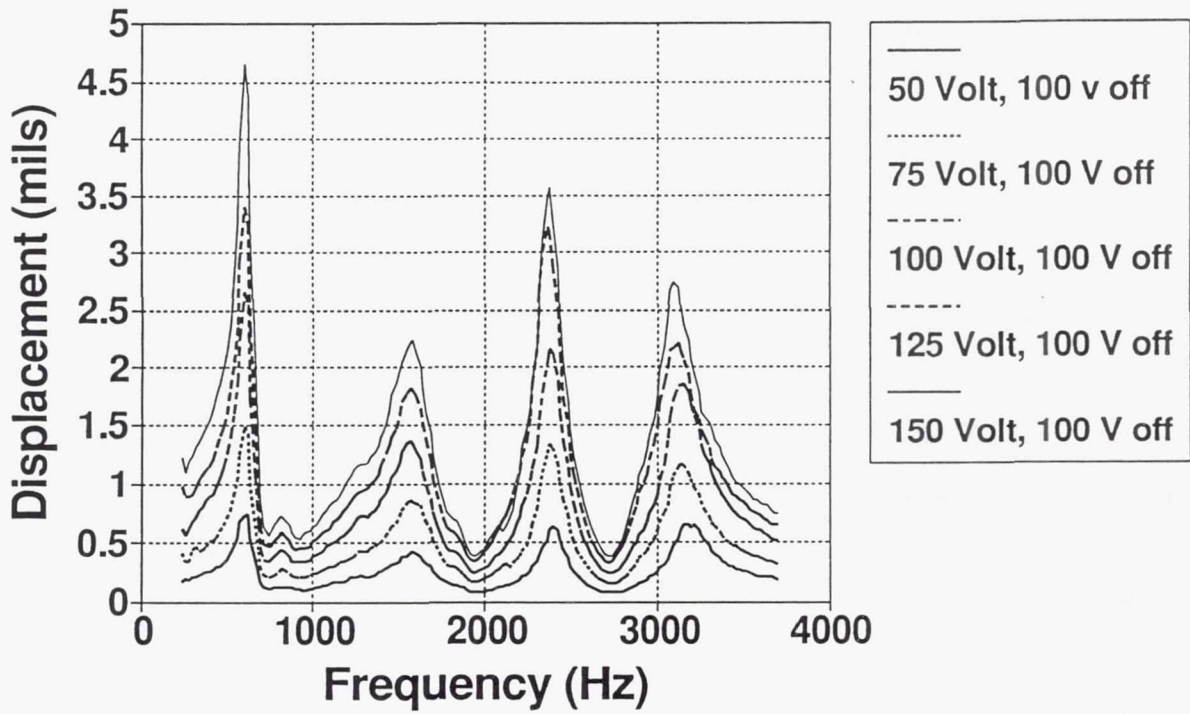
Figure 55 - Displacement vs Frequency of Electrostrictive Rainbow Actuator, 1.25 in dia., 0.015 in thick, PLZT
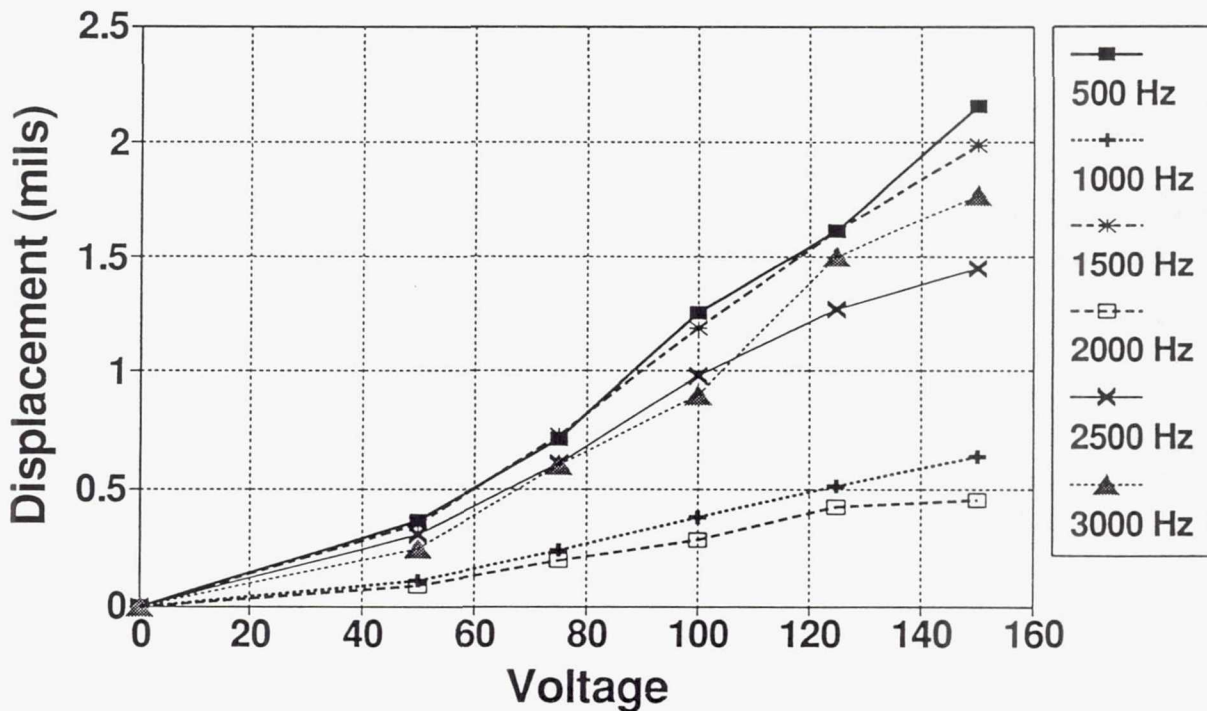
Figure 56 - Displacement vs Voltage of Electrostrictive Rainbow Actuator, 1.25 in dia., 0.015 inch thick, PLZT

107
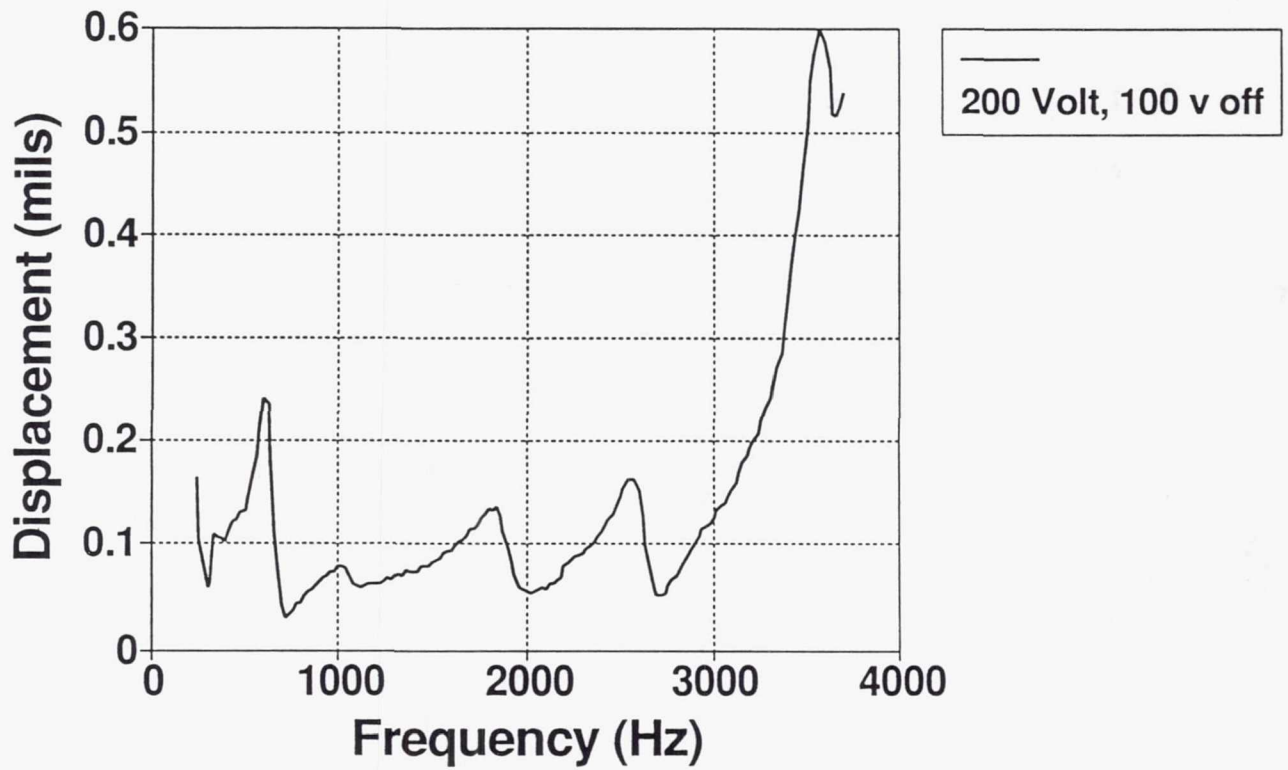
Figure 57 - Displacement vs Frequency of Electrostrictive Rainbow Actuator, 1.25 in dia., 0.030 inch thick, PLZT
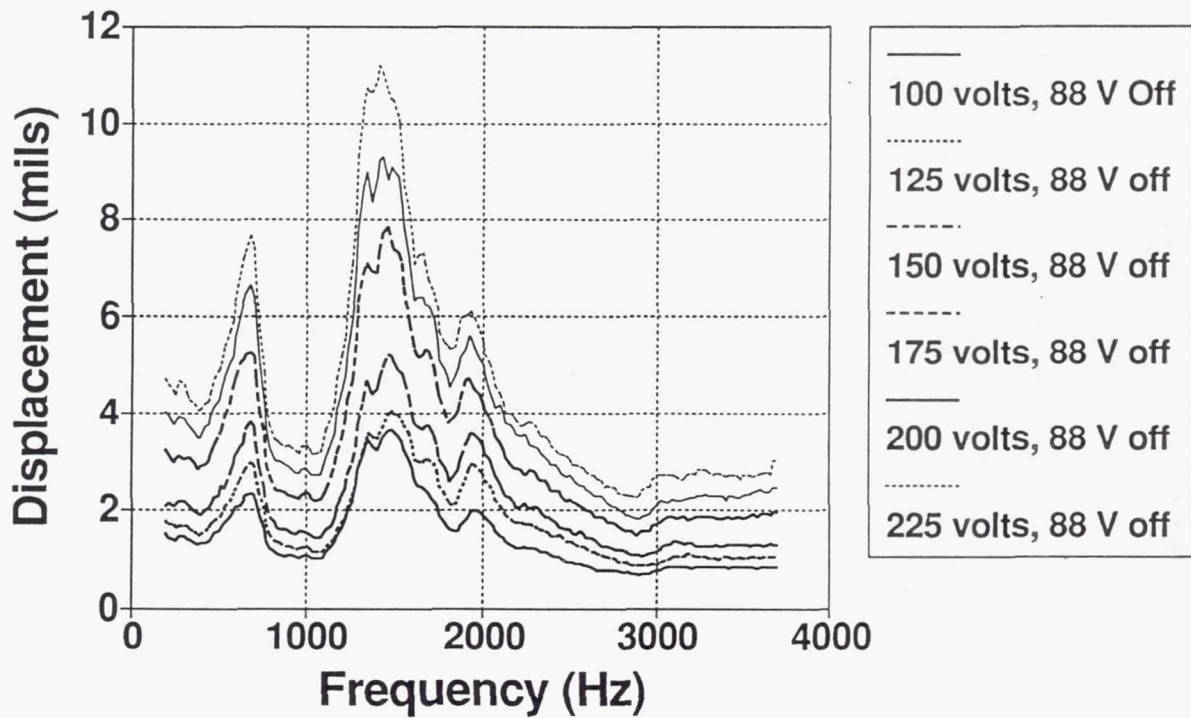
Figure 58 - Displacement vs Frequency of Piezoelectric Rainbow Actuator, 1.25 in dia., 0.008 inch thick, C3900
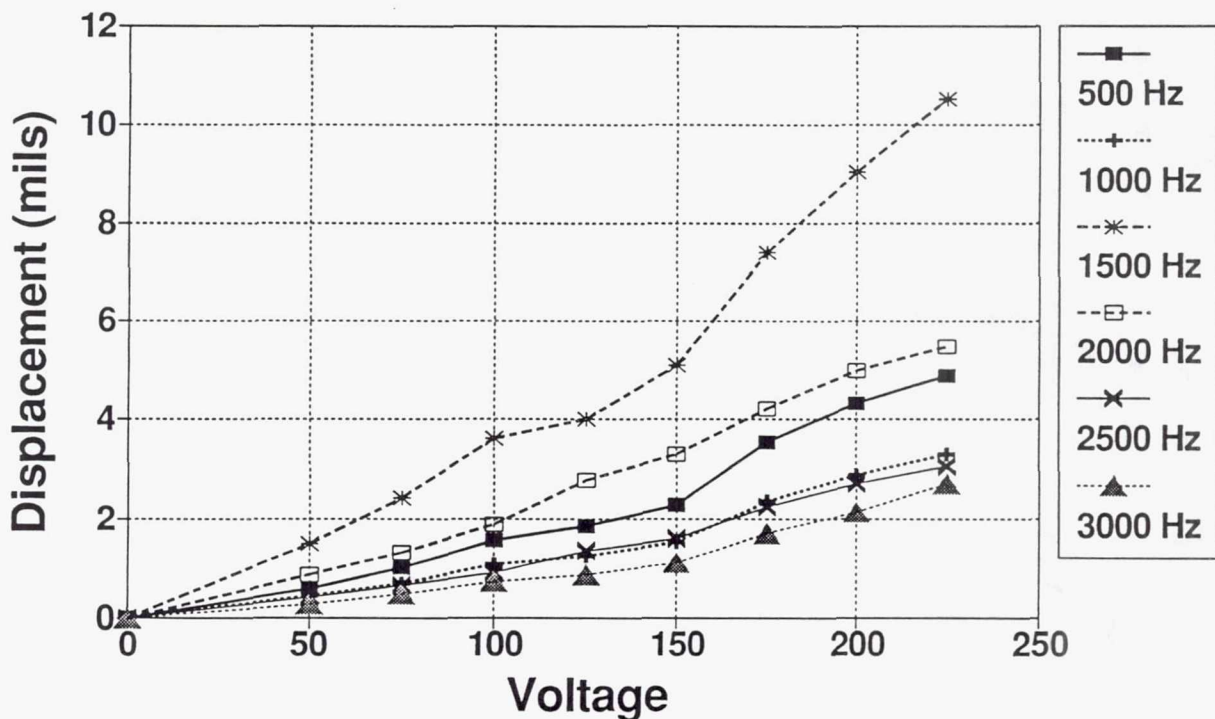
Figure 59 - Displacement vs Voltage of Piezoelectric Rainbow Actuator, 1.25 in dia., 0.008 inch thick, C3900
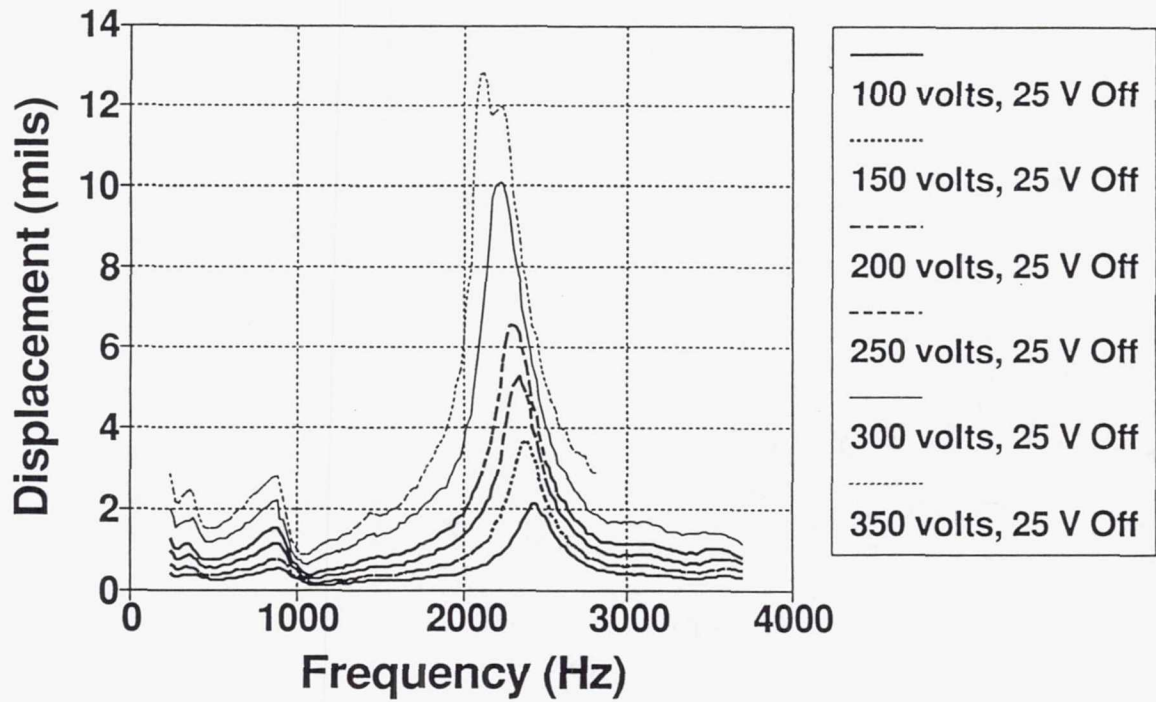
Figure 60 - Displacement vs Frequency of Piezoelectric Rainbow Actuator, 1.25 in dia., 0.015 inch thick, C3900
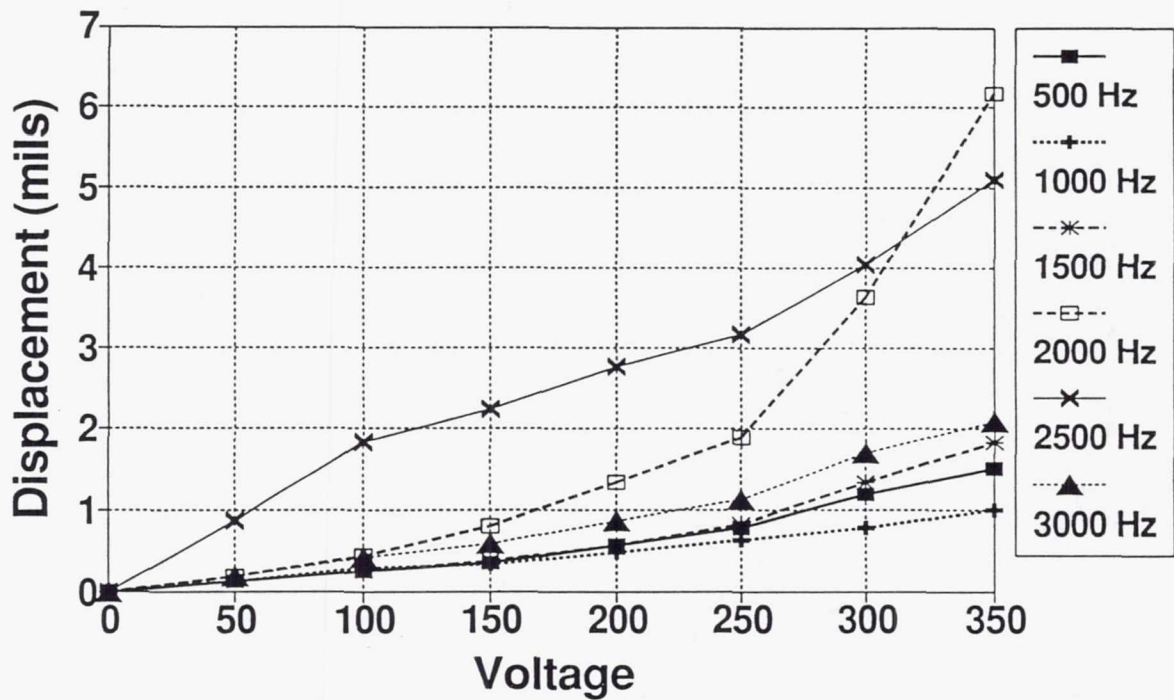
Figure 61 - Displacement vs Voltage of Piezoelectric Rainbow Actuator, 1.25 in dia., 0.015 inch thick, C3900

110
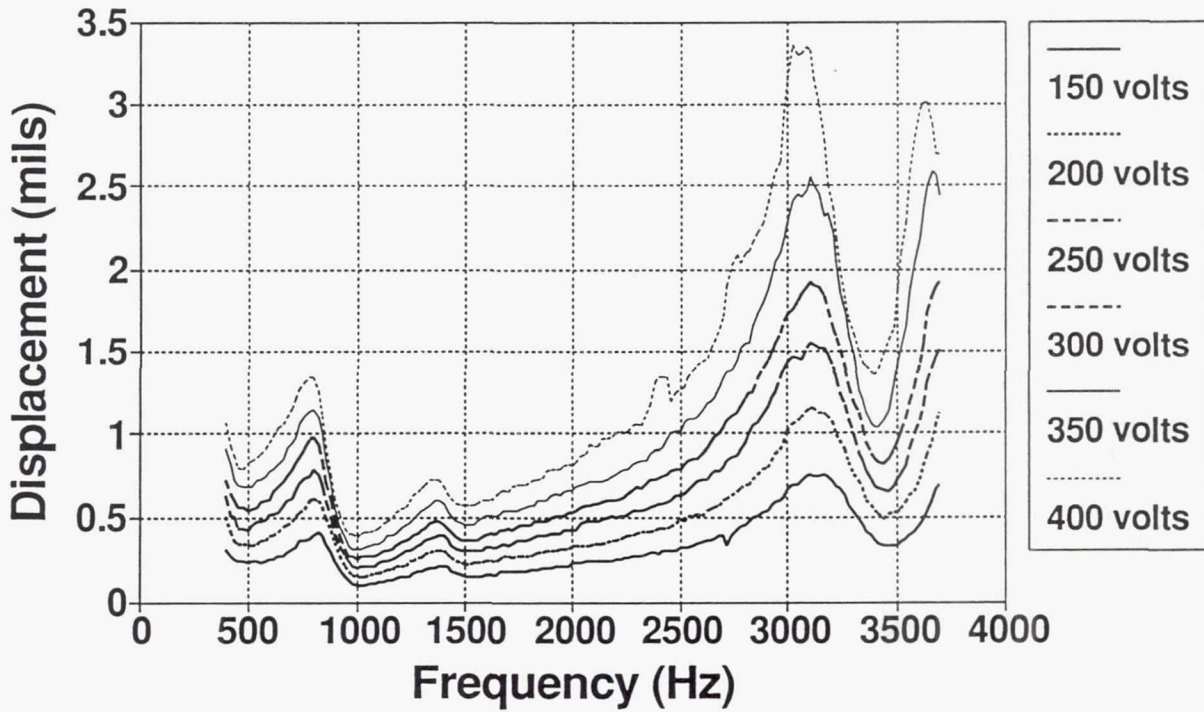
Figure 62 - Displacement vs Frequency of Piezoelectric Rainbow Actuator, 1.25 in dia., 0.030 inch thick, C3900
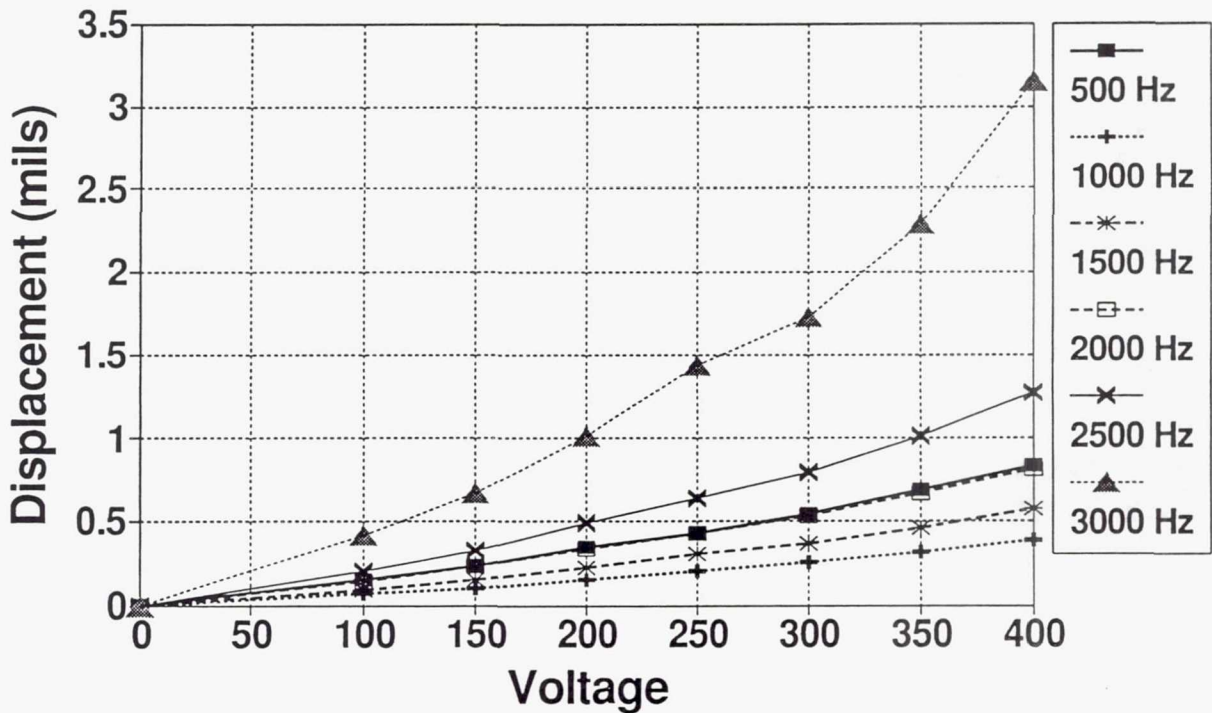
Figure 63 - Displacement vs Voltage of Piezoelectric Rainbow Actuator, 1.25 in dia., 0.030 inch thick, C3900
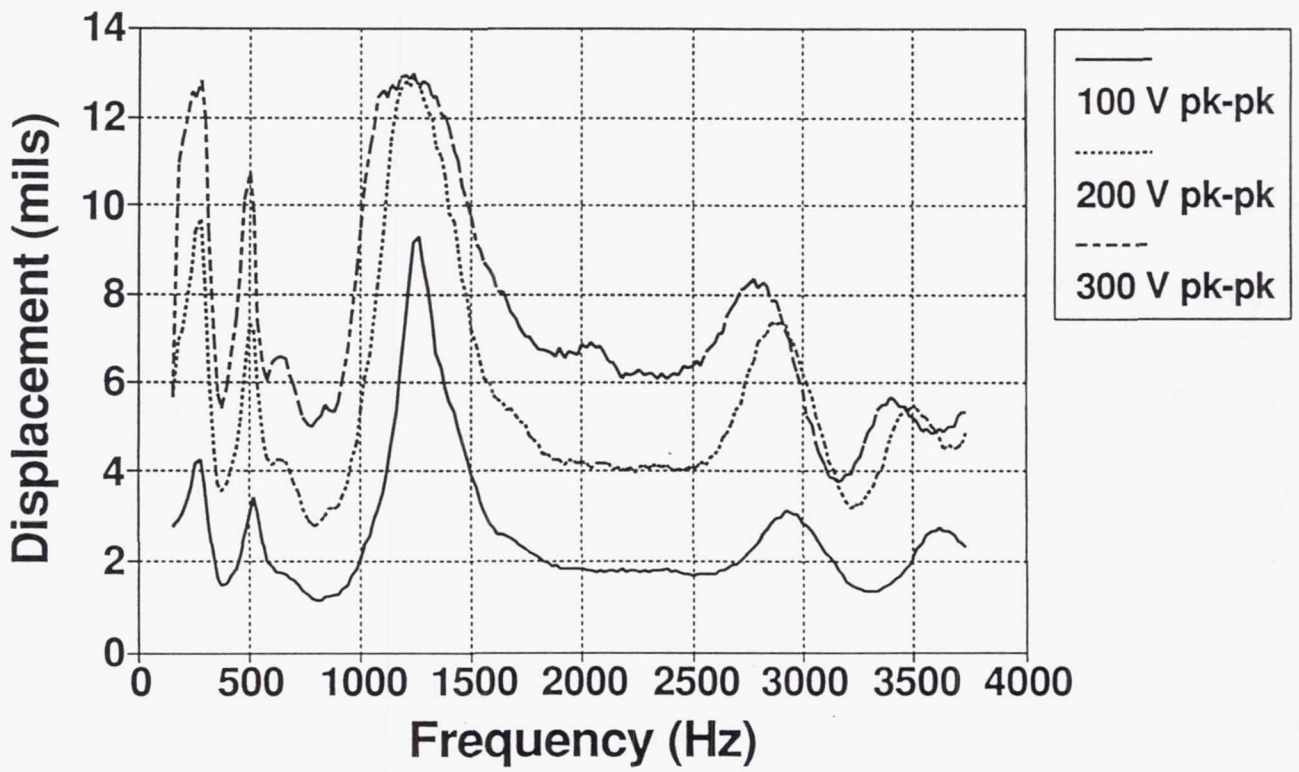
Figure 64 - Displacement vs Voltage of Piezoelectric Rainbow Actuator, 2 in dia., 0.015 inch thick, C3900
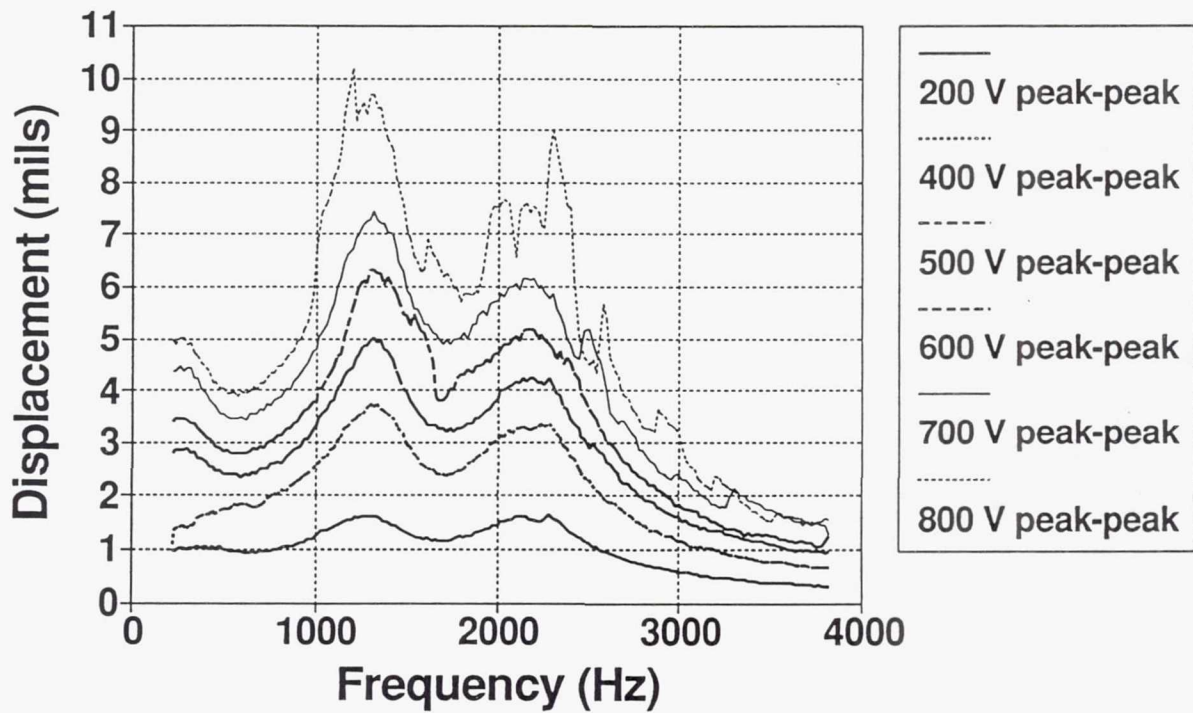
Figure 65 - Displacement vs Frequency of Hard Piezoelectric Rainbow Actuator, 1.25 in dia., 0.015 inch thick
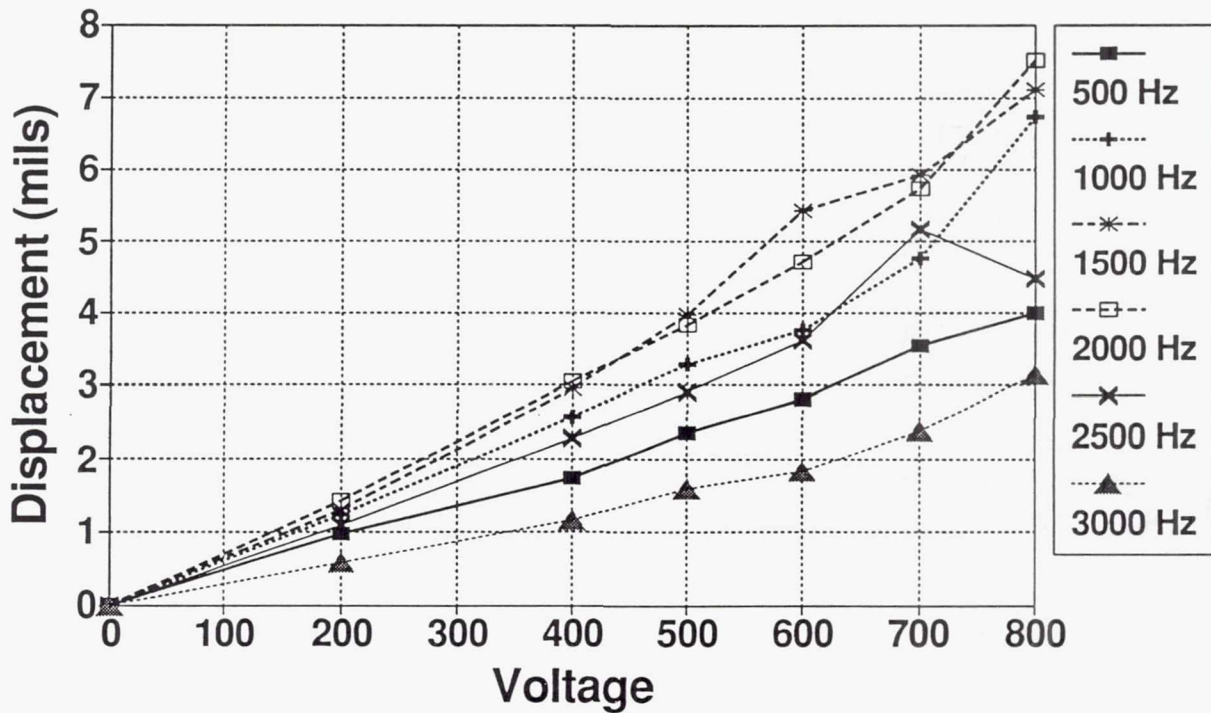
Figure 66 - Displacement vs Voltage Characteristic of Hard Piezoelectric Rainbow Actuator, 1.25 in dia., 0.015 inch thick

113
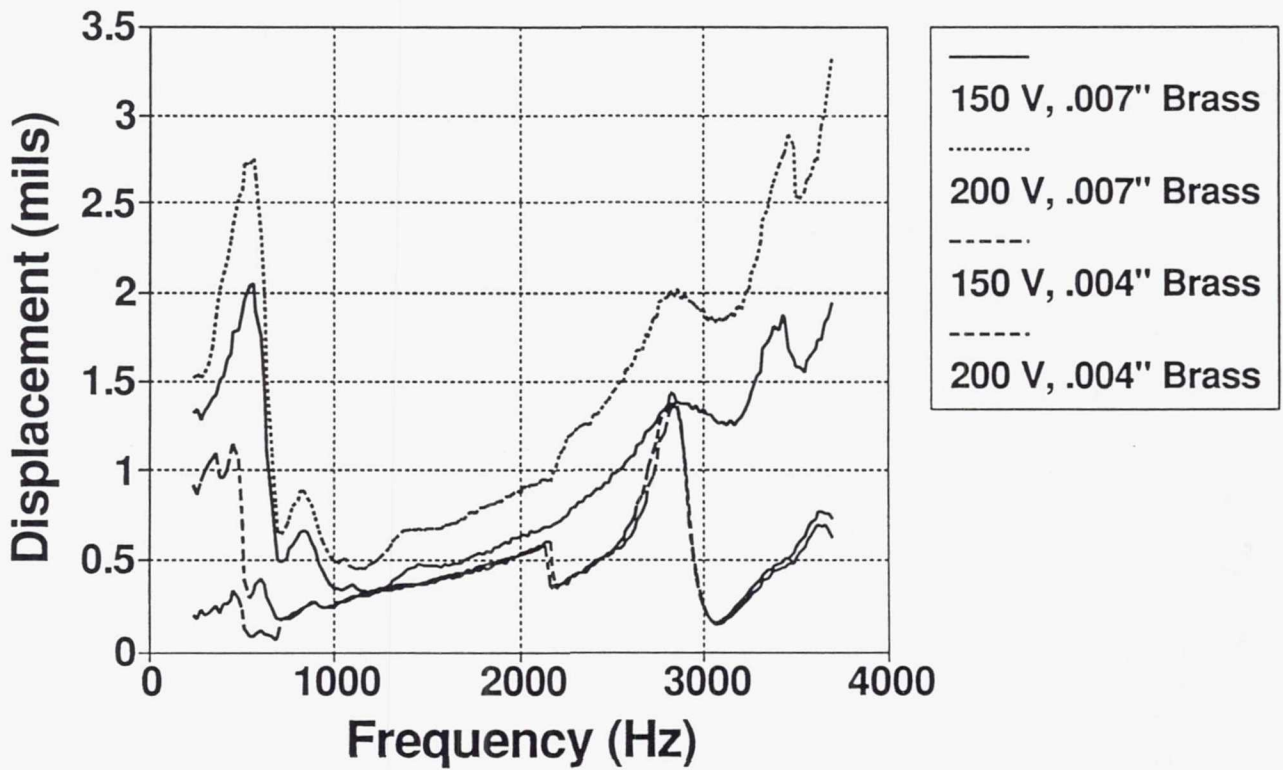
Figure 67 - Displacement vs Frequency Characteristic of Composite Rainbow Actuators, 0.004 and 0.007 inch Thick Brass

114
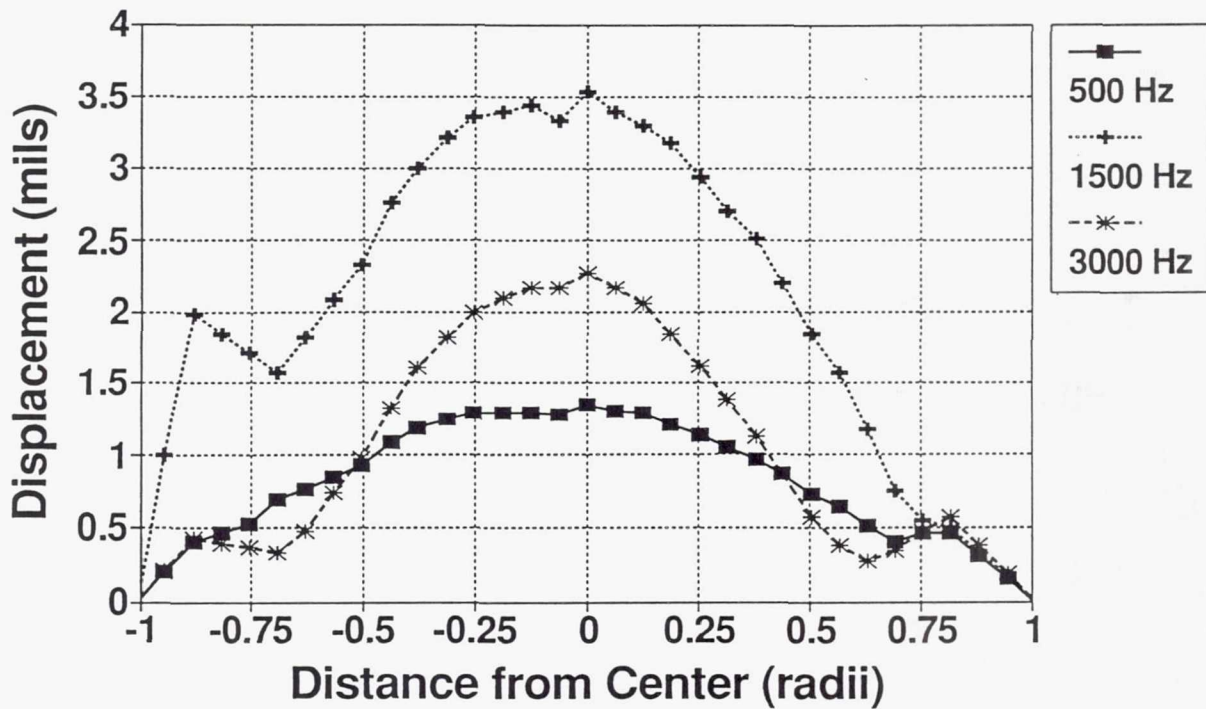
Figure 68 - Displacement vs Distance of Rainbow Actuator, 1.25 in dia., 0.015 inch thick, C3900
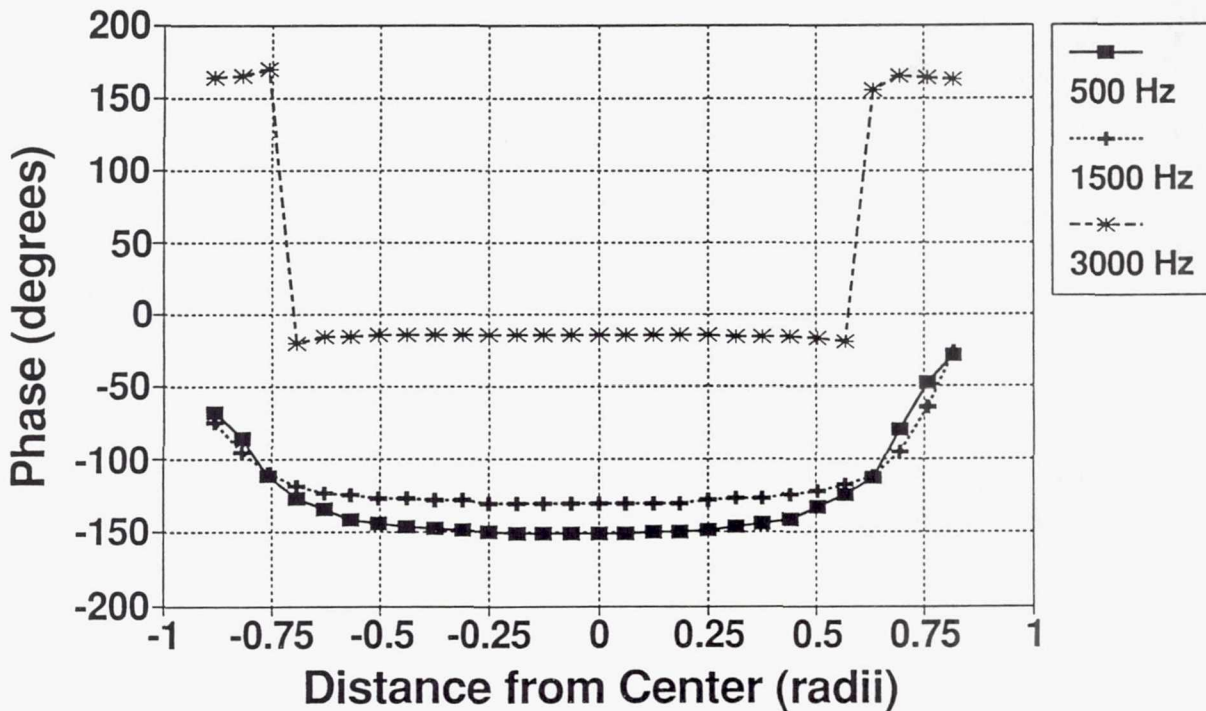
Figure 69 - Phase Between Input Signal and Displacement vs Distance for Rainbow Actuator, 1.25 in dia., 0.015 inch thick, C3900
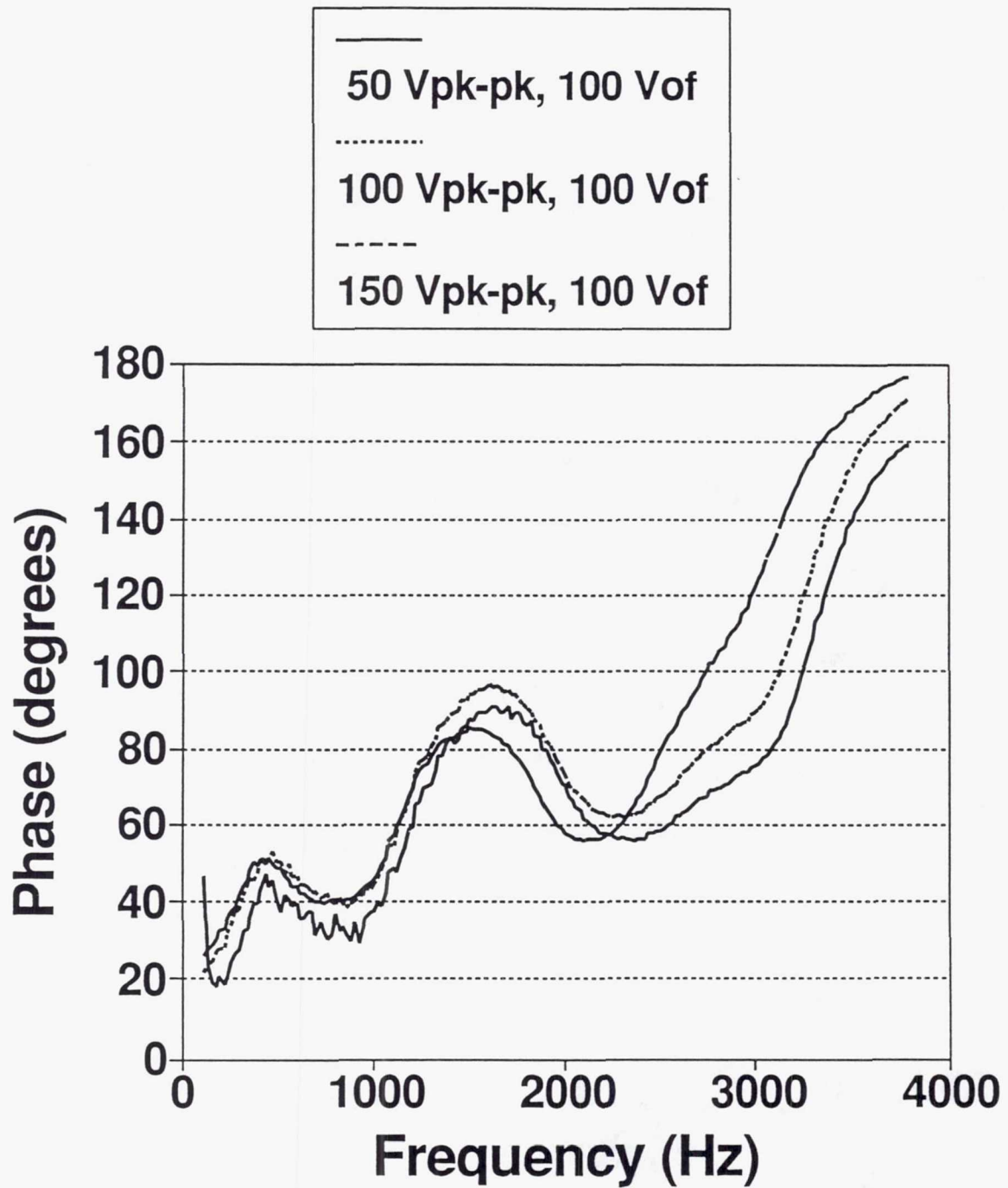
Figure 70 - Phase Between Input Signal and Output Displacement vs Frequency for Electrostrictive Rainbow Actuator, 1.25 in dia., 0.015 in thick, PLZT
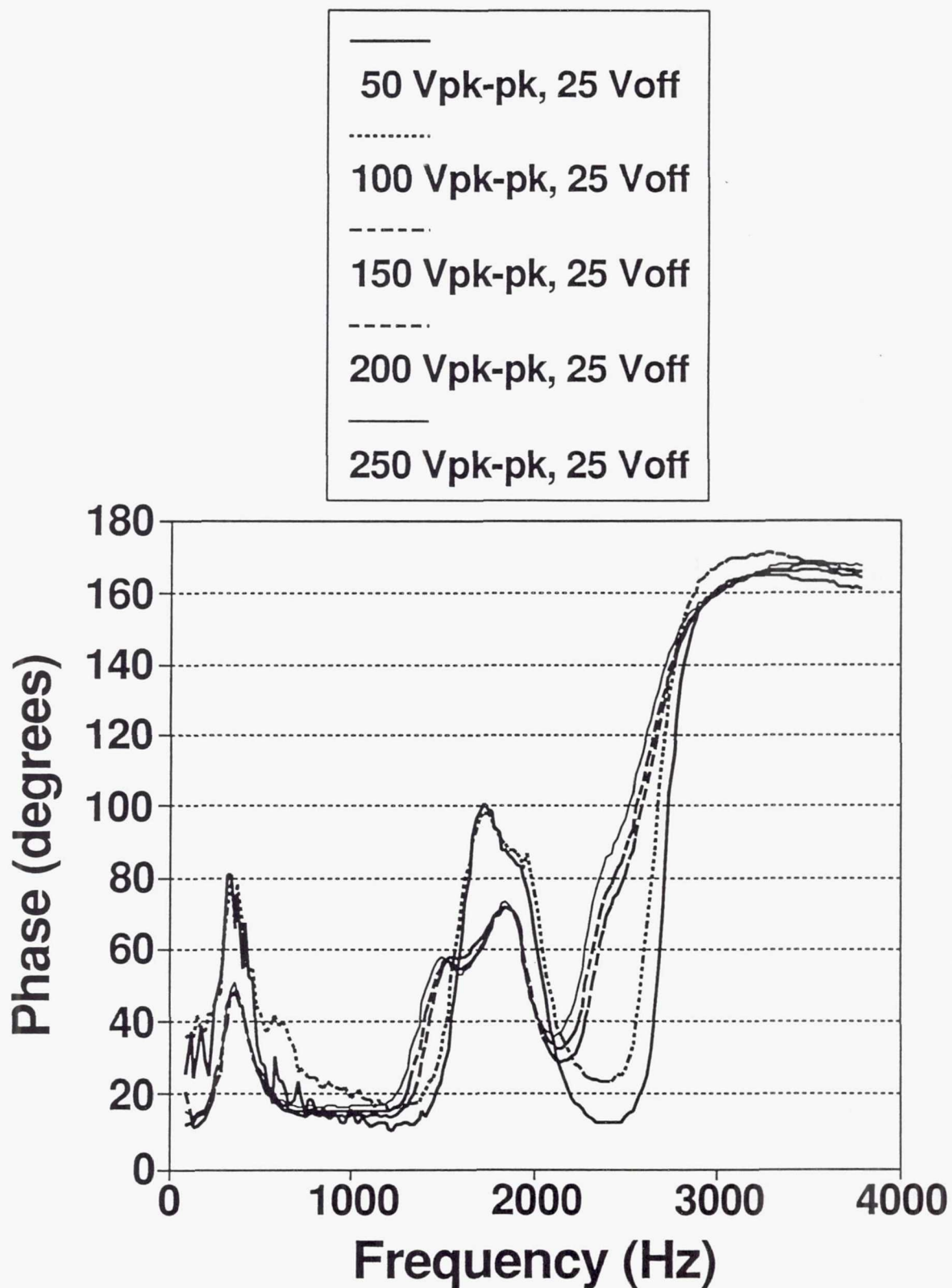
Figure 71 - Phase Between Input Signal and Output Displacement vs Frequency for Piezoelectric Rainbow Actuator, 1.25 in dia., 0.015 inch thick, C3900
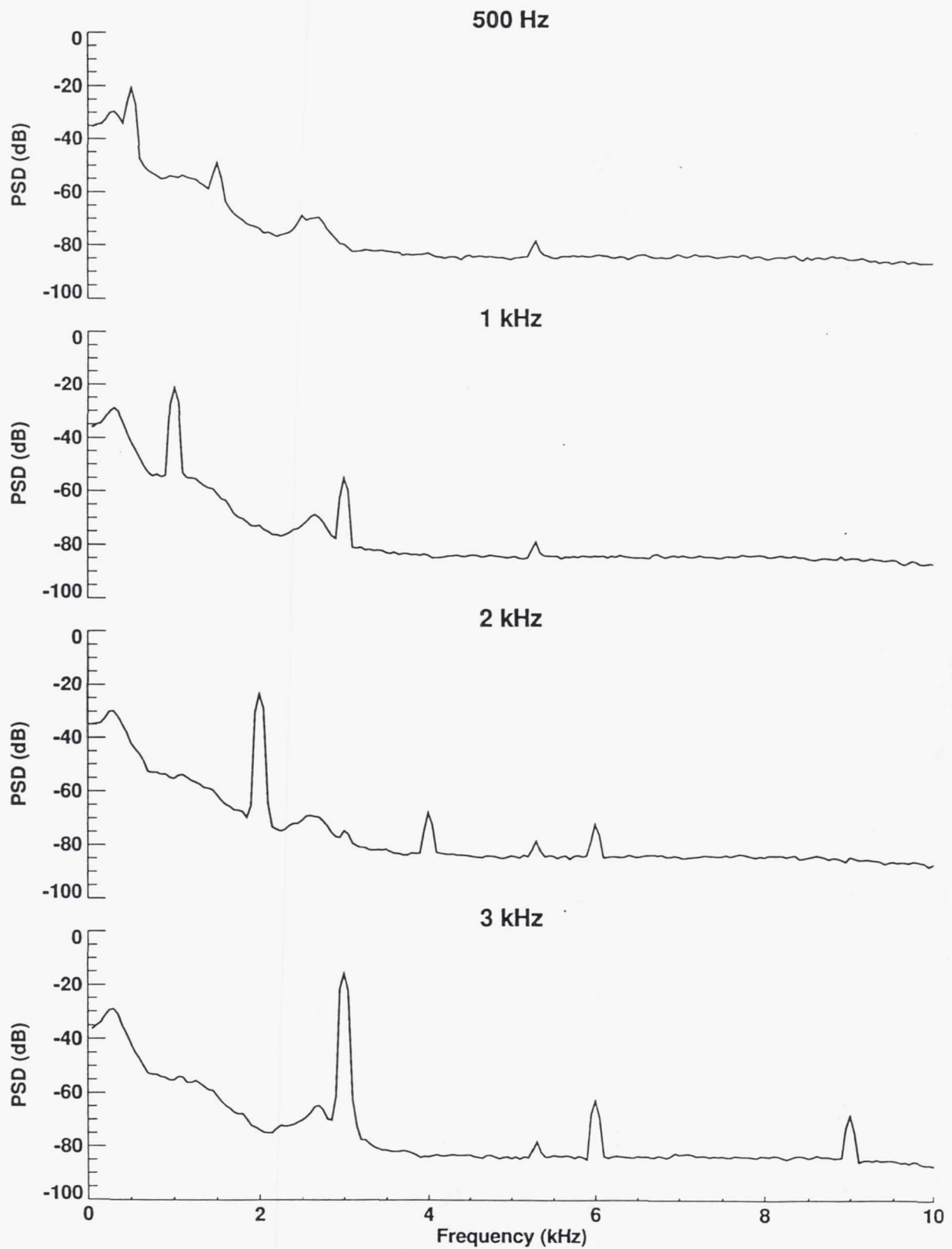
Figure 72 - Displacement Spectrum for Piezoelectric Rainbow Actuator, 100 Volts peak to peak, 1.25 in dia., 0.015 inch thick, C3900
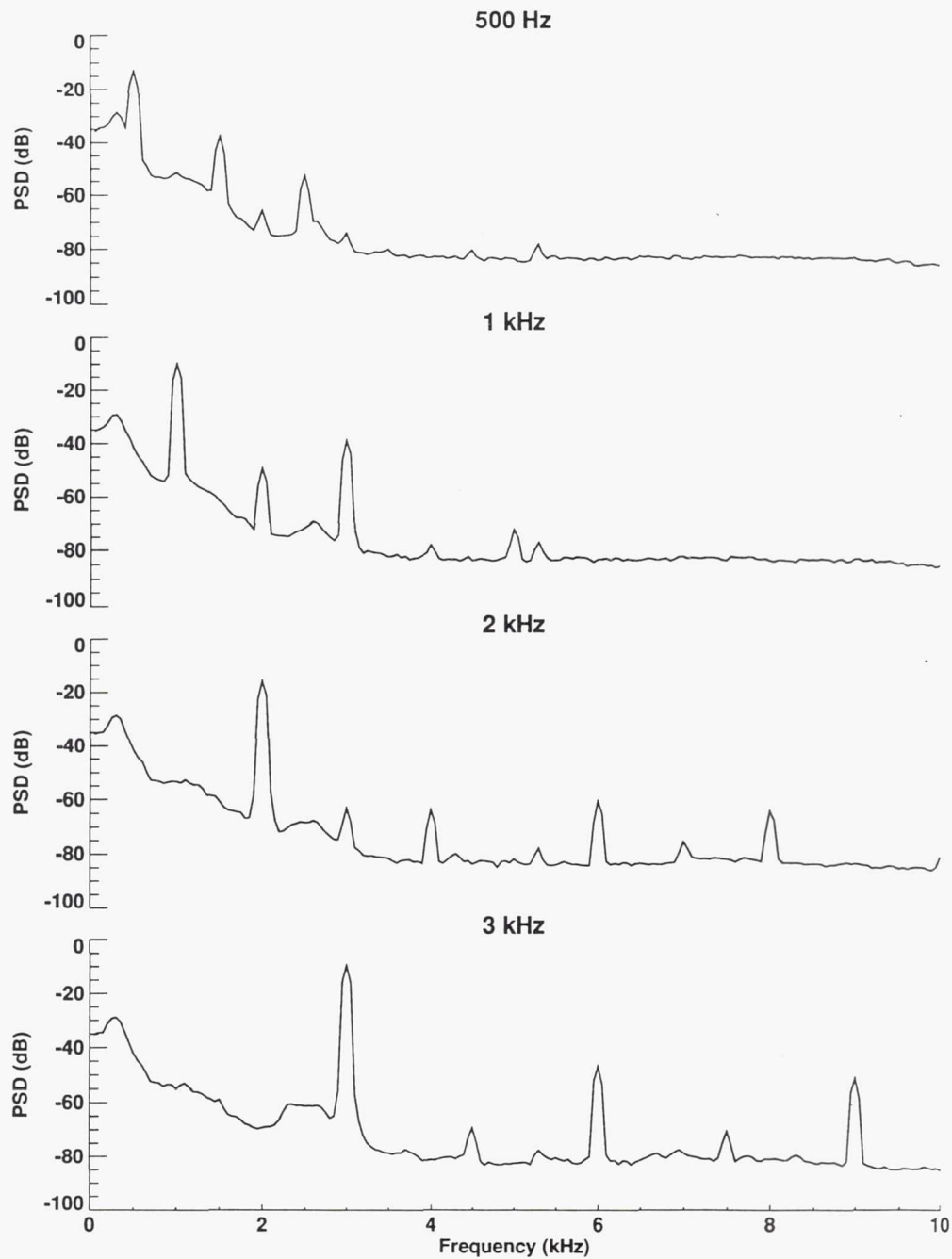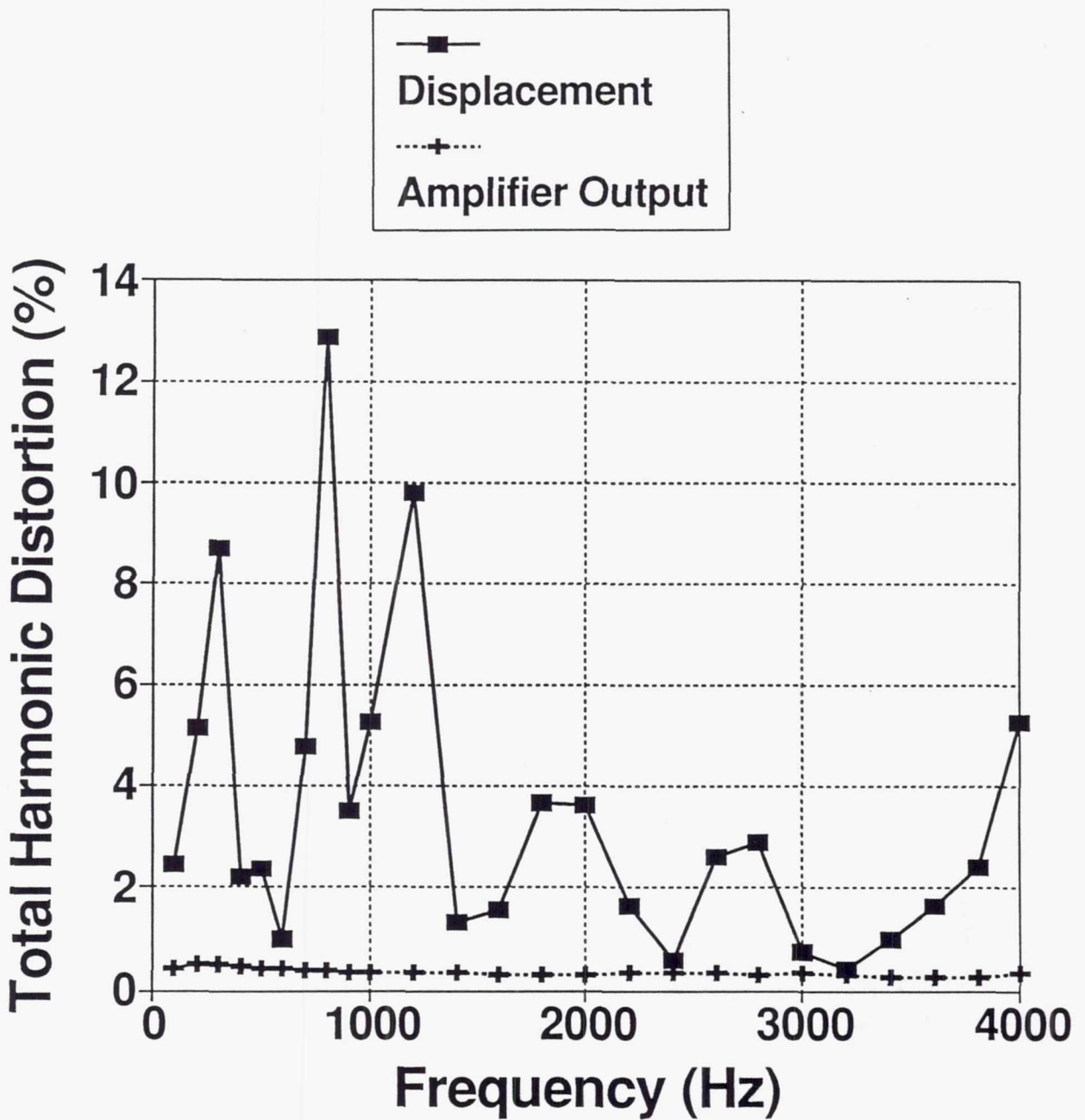
Figure 73 - Displacement Spectrum for Piezoelectric Rainbow Actuator, 200 Volts peak to peak, 1.25 in dia., 0.015 inch thick, C3900

Figure 74 - Total Harmonic Distortion of Electrostrictive Rainbow Actuator, 100 volts peak to peak, 1.25 in dia., 0.015 inch thick, PLZT
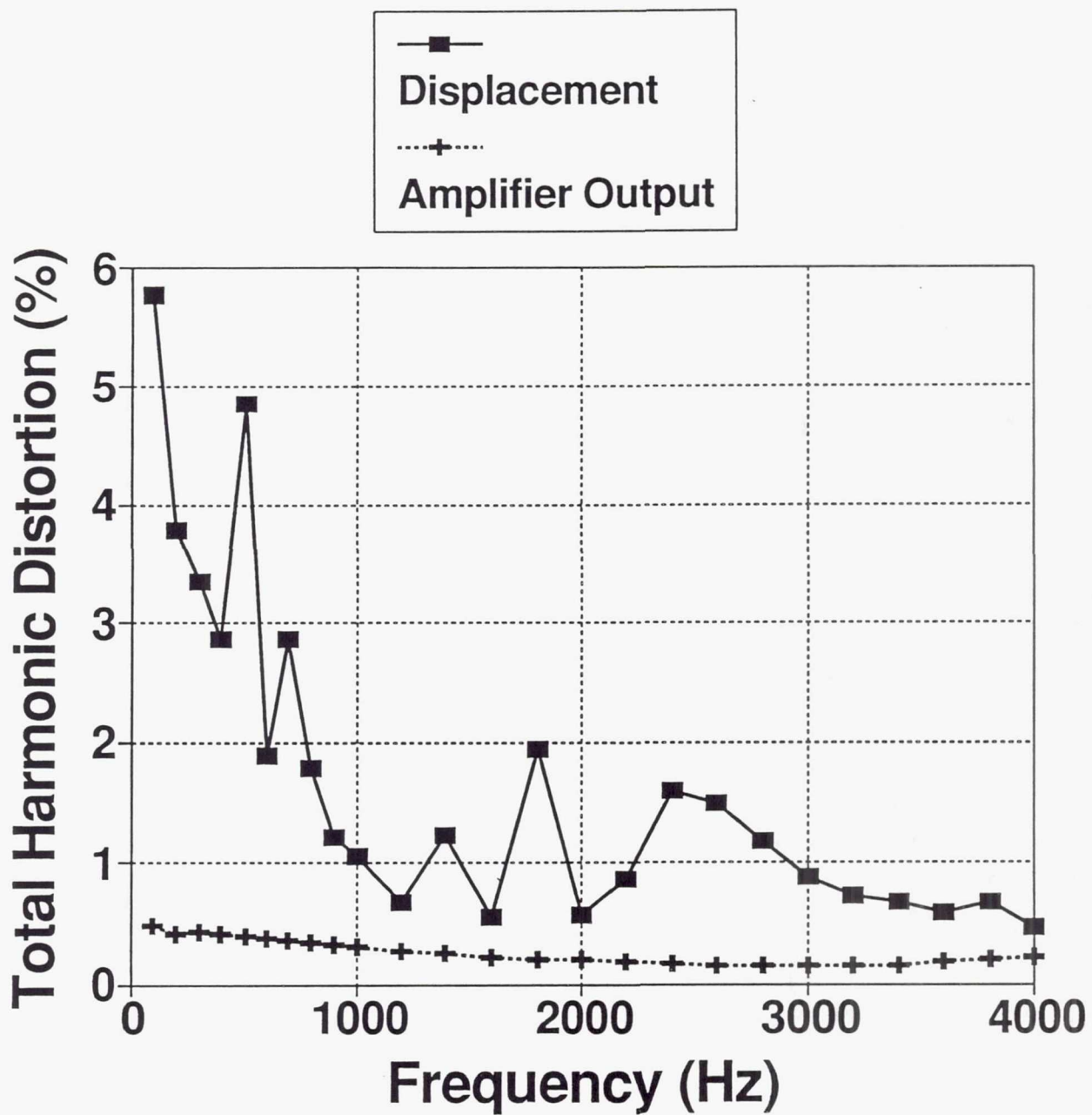
Figure 75 - Total Harmonic Distortion of Piezoelectric Rainbow Actuator, 175 volts peak to peak, 88 volts DC offset, 1.25 in. dia., 0.008 inch thick, C3900
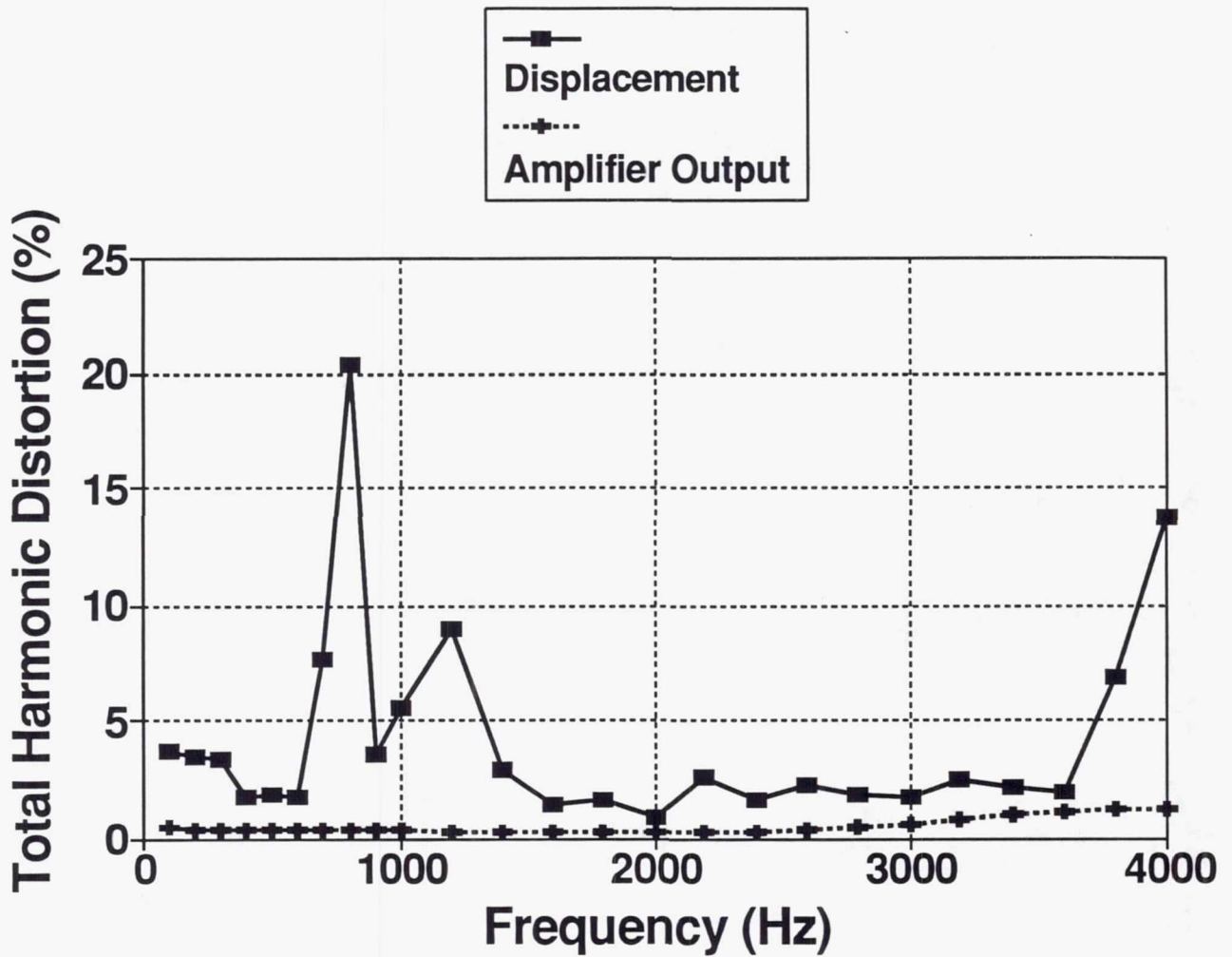
Figure 76 - Total Harmonic Distortion of Piezoelectric Rainbow Actuator, 250 volt peak to peak, 25 volt DC offset, 1.25 in. dia., 0.015 inch thick, C3900
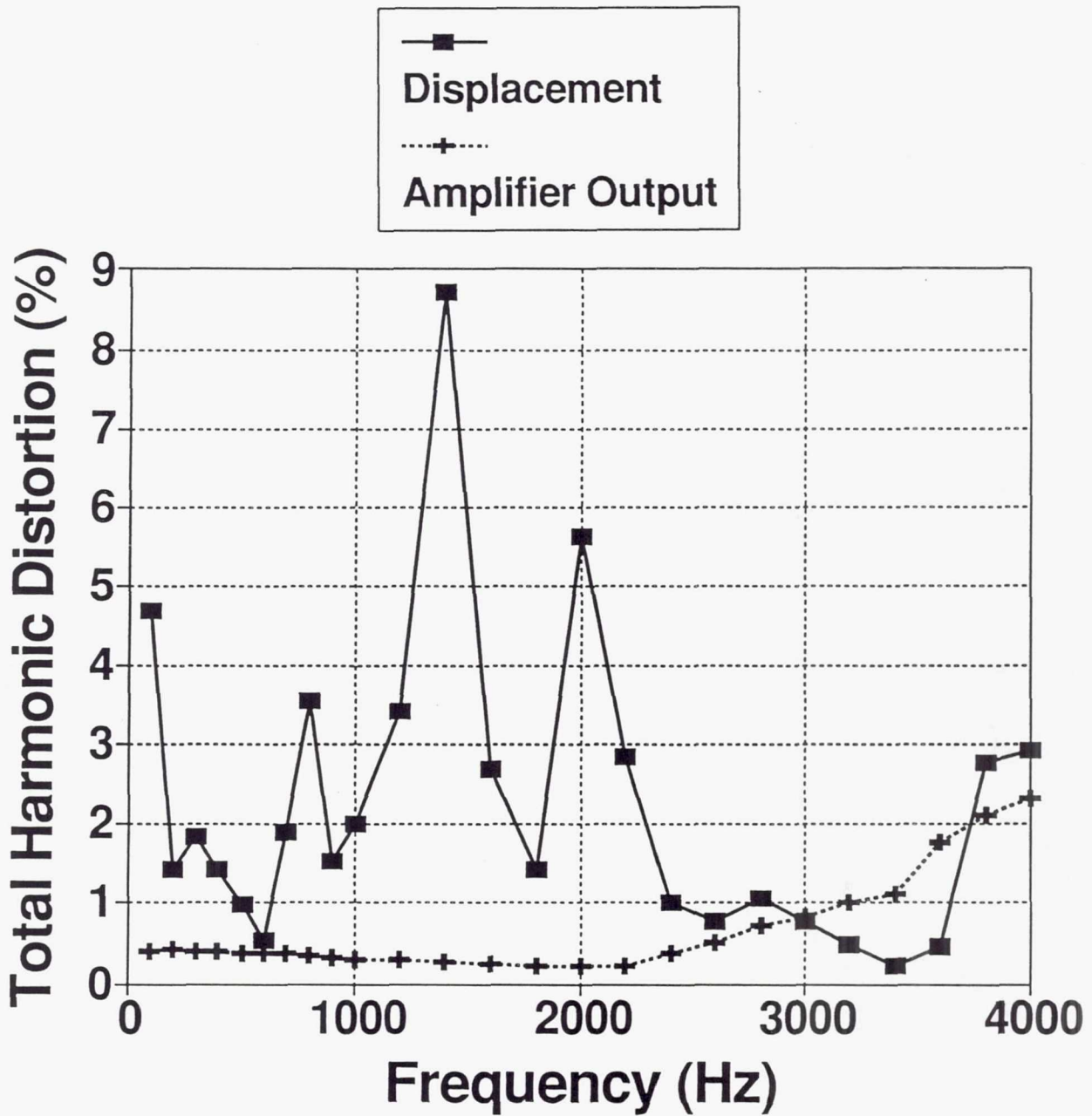
Figure 77 - Total Harmonic Distortion of Piezoelectric Rainbow Actuator, 300 volts peak to peak, 1.25 in. dia., 0.030 inch thick, C3900
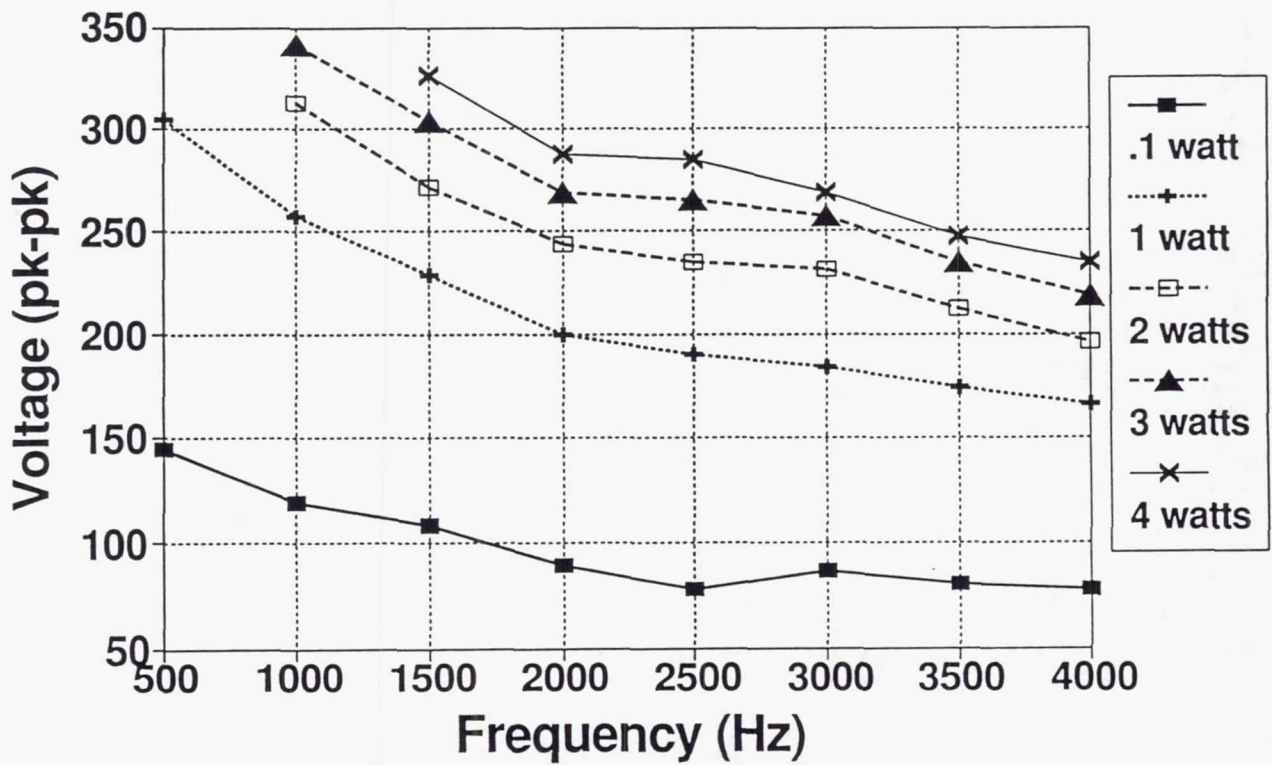
Figure 78 - Power Dissipation of Piezoelectric Rainbow Actuator, 3.1 SCFM cooling air rate, 1.25 in. dia., 0.015 inch thick, C3900

REPORT DOCUMENTATION PAGE

Form Approved
OMB No. 0704-0188

1. AGENCY USE ONLY (Leave blank)	2. REPORT DATE	3. REPORT TYPE AND DATES COVERED
	December 1994	Final Contractor Report

4. TITLE AND SUBTITLE

Actuator Feasibility Study for Active Control of Ducted Axial Fan Noise

5. FUNDING NUMBERS

WU–538–03–11
C–NAS3–26618

6. AUTHOR(S)

John C. Simonich

7. PERFORMING ORGANIZATION NAME(S) AND ADDRESS(ES)

United Technologies Research Center
400 Main Street, MS. 129–17
East Hartford, Connecticut 06108

8. PERFORMING ORGANIZATION REPORT NUMBER

E–9298

9. SPONSORING/MONITORING AGENCY NAME(S) AND ADDRESS(ES)

National Aeronautics and Space Administration
Lewis Research Center
Cleveland, Ohio 44135–3191

10. SPONSORING/MONITORING AGENCY REPORT NUMBER

NASA CR–195412

11. SUPPLEMENTARY NOTES

Project Manager, Laurence J. Heidelberg, Propulsion Systems Division, organization code 2770, NASA Lewis Research Center, (216) 433–3859.

12a. DISTRIBUTION/AVAILABILITY STATEMENT

Unclassified - Unlimited
Subject Categories 07 and 71

This publication is available from the NASA Center for Aerospace Information, (301) 621–0390.

12b. DISTRIBUTION CODE

13. ABSTRACT (Maximum 200 words)

A feasibility study was performed to investigate actuator technology which is relevant for a particular application of active noise control for gas turbine stator vanes. This study investigated many different classes of actuators and ranked them on the order of applicability. The most difficult requirements the actuators had to meet were high frequency response, large amplitude deflections and a thin profile. Based on this assessment, piezoelectric type actuators were selected as the most appropriate actuator class. Specifically, Rainbows (a new class of high performance piezoelectric actuators), and unimorphs (a ceramic/metal composite) appeared best suited to the requirements. A benchtop experimental study was conducted. The performance of a variety of different actuators was examined, including high polymer films, flextensional actuators, miniature speakers, unimorphs and Rainbows. The displacement/frequency response and phase characteristics of the actuators were measured. Physical limitations of actuator operation were also examined. This report includes the first known, high displacement, dynamic data obtained for Rainbow actuators. A new "hard" ceramic Rainbow actuator which does not appear to be limited in operation by self heating as are "soft" ceramic Rainbows was designed, constructed and tested. The study concludes that a suitable actuator for active noise control in gas turbine engines can be achieved with state of the art materials and processing.

14. SUBJECT TERMS

Active noise control; High speed actuators; Noise cancellation; Piezoceramic actuators; Rainbow actuators

15. NUMBER OF PAGES

131

16. PRICE CODE

A07

17. SECURITY CLASSIFICATION OF REPORT	18. SECURITY CLASSIFICATION OF THIS PAGE	19. SECURITY CLASSIFICATION OF ABSTRACT	20. LIMITATION OF ABSTRACT
Unclassified	Unclassified	Unclassified	